Molecular Endocrinology Laboratory
Departament of Cellular and Molecular Neurobiology
Current Opportunities at Lab

We are requesting graduate students (M.Sc. and Ph.D.) and postdoctoral fellows interested in investigating the regulation of the proteases cleaving prolactin into its metabolites, vasoinhibins, and the effect of both, full-length prolactin and vasoinhibins on inflammatory, vascular, proliferative, apoptotic, and metabolic processes underlying the physiopathology of inflammatory arthritis, liver injury, diabetic retinopathy and neuropathy. Please read five of our recent related publications.

Dra. Carmen Clapp
Instituto de Neurobiología
Universidad Nacional Autónoma de México (UNAM)
Campus UNAM-Juriquilla
Querétaro, México, 76230
Tel: 442-238-1028 o 55 5623-4028
clapp@unam.mx

Prolactin promotes cartilage survival and attenuates inflammation in inflammatory arthritis

Norma Adán,[1] Jessica Guzmán-Morales,[1] Maria G. Ledesma-Colunga,[1] Sonia I. Perales-Canales,[1] Andrés Quintanar-Stéphano,[2] Fernando López-Barrera,[1] Isabel Méndez,[1] Bibiana Moreno-Carranza,[1] Jakob Triebel,[1] Nadine Binart,[3] Gonzalo Martínez de la Escalera,[1] Stéphanie Thebault,[1] and Carmen Clapp[1]

[1]Instituto de Neurobiología, Universidad Nacional Autónoma de México (UNAM), Campus UNAM-Juriquilla, Querétaro, México. [2]Centro de Ciencias Básicas, Universidad Autónoma de Aguascalientes, Aguascalientes, México. [3]INSERM U693, Université Paris-Sud, Faculté de Médecine Paris-Sud, Le Kremlin-Bicêtre, France.

Chondrocytes are the only cells in cartilage, and their death by apoptosis contributes to cartilage loss in inflammatory joint diseases, such as rheumatoid arthritis (RA). A putative therapeutic intervention for RA is the inhibition of apoptosis-mediated cartilage degradation. The hormone prolactin (PRL) frequently increases in the circulation of patients with RA, but the role of hyperprolactinemia in disease activity is unclear. Here, we demonstrate that PRL inhibits the apoptosis of cultured chondrocytes in response to a mixture of proinflammatory cytokines (TNF-α, IL-1β, and IFN-γ) by preventing the induction of p53 and decreasing the BAX/BCL-2 ratio through a NO-independent, JAK2/STAT3–dependent pathway. Local treatment with PRL or increasing PRL circulating levels also prevented chondrocyte apoptosis evoked by injecting cytokines into the knee joints of rats, whereas the proapoptotic effect of cytokines was enhanced in PRL receptor–null (*Prlr*$^{-/-}$) mice. Moreover, eliciting hyperprolactinemia in rats before or after inducing the adjuvant model of inflammatory arthritis reduced chondrocyte apoptosis, proinflammatory cytokine expression, pannus formation, bone erosion, joint swelling, and pain. These results reveal the protective effect of PRL against inflammation-induced chondrocyte apoptosis and the therapeutic potential of hyperprolactinemia to reduce permanent joint damage and inflammation in RA.

Introduction

Rheumatoid arthritis (RA) is a chronic, autoimmune inflammatory disease with a worldwide prevalence of 1% to 2%. Autoimmunity followed by the articular infiltration of leukocytes and hyperplasia of synovial cells lead to the development of an invasive inflammatory pannus that destroys the adjacent cartilage and bone. Locally produced cytokines are crucial for initiating the inflammatory process and destroying articular tissue (1). Among these cytokines, TNF-α, IL-1β, and IFN-γ stimulate both chondrocyte apoptosis and cartilage extracellular matrix degradation, and their inhibition ameliorates joint destruction (1–4). Transgenic mice expressing TNF-α, a model of polyarthritis (5), display chondrocyte apoptosis before the onset of full arthritis, suggesting that cytokine-induced chondrocyte apoptosis is a primary cause of, rather than an event secondary to, cartilage matrix breakdown (6). Thus, factors able to counteract chondrocyte apoptosis under inflammatory conditions are relevant for the treatment of RA (7–11). One such factor is prolactin (PRL).

PRL acts both as a circulating hormone and a cytokine to regulate the function of a wide variety of tissues, including cartilage. PRL and the PRL receptor are expressed in chondrocytes (12, 13), where this hormone can promote differentiation and survival. PRL stimulates the synthesis of proteoglycans and type II collagen by bone marrow–derived chondrocytic mesenchymal cells (14), and it inhibits the apoptosis of articular chondrocytes induced by serum deprivation (13). The action of PRL on chondrocyte survival may be relevant in RA. PRL is present in RA synovial fluid (14, 15), is produced by RA synovial cells (16), and can influence cartilage survival by exerting immunoregulatory effects. The PRL receptor is a member of the hematopoietin/cytokine receptor superfamily and is expressed in a variety of immune cells, in which this hormone can be proinflammatory or antiinflammatory by regulating proliferation, survival, and the release of inflammatory mediators (17).

Given that cytokine-induced chondrocyte apoptosis contributes to cartilage destruction in RA (1, 2, 6, 9), we investigated the survival effect of PRL on chondrocytes treated in vitro or in vivo with a mixture of TNF-α, IL-1β, and IFN-γ (Cyt) and whether this effect protects against cartilage destruction in the adjuvant-induced model of inflammatory arthritis in rats. We demonstrate that PRL treatment inhibits, and PRL receptor deficiency enhances, Cyt-induced cartilage apoptosis and that the PRL effect on survival occurs in chondrocytes via a NO-independent, JAK2/STAT3–dependent pathway. We also show that hyperprolactinemia promotes the survival of arthritic cartilage by blocking the expression of proinflammatory cytokines and their proapoptotic effect on chondrocytes and that PRL delays the onset and ameliorates the severity of inflammatory arthritis. We conclude that current medications able to increase prolactinemia constitute novel potential therapies to control inflammation-driven cartilage degradation and joint damage in RA.

Authorship note: Norma Adán, Jessica Guzmán-Morales, and Maria G. Ledesma-Colunga contributed equally to this work. Sonia I. Perales-Canales is deceased.

Conflict of interest: The authors have declared that no conflict of interest exists.

Citation for this article: *J Clin Invest.* 2013;123(9):3902–3913. doi:10.1172/JCI69485.

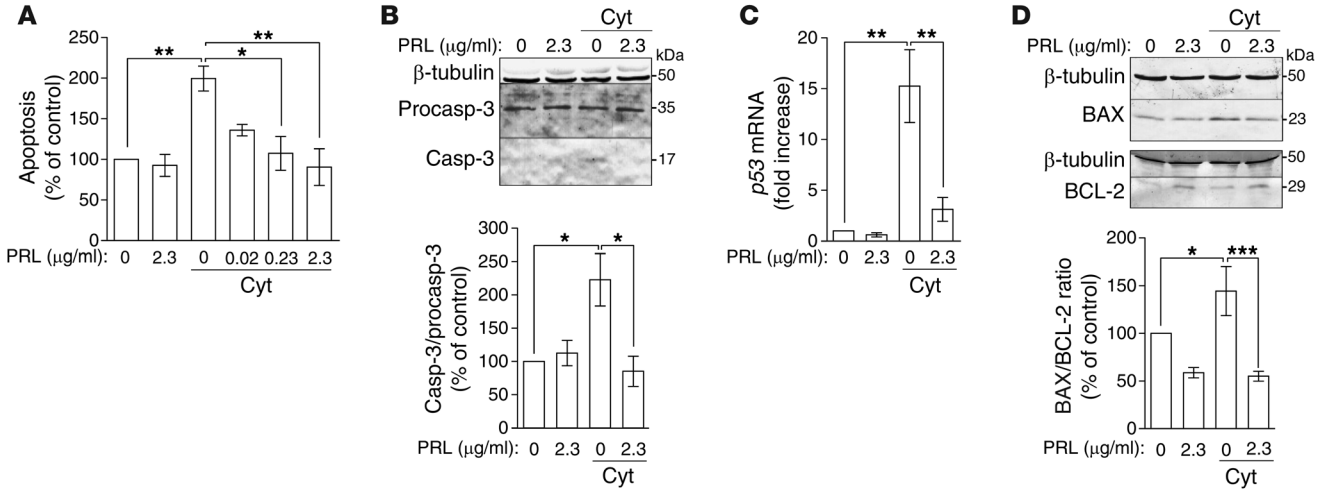

Figure 1

PRL inhibits Cyt-induced apoptosis of chondrocytes in culture. (**A**) Primary cultures of rat chondrocytes were challenged with Cyt, combined or not with different concentrations of PRL, and apoptosis was evaluated at 24 hours by ELISA (n = 3–6). (**B**) Representative Western blot of procaspase-3 and active caspase-3 (Procasp-3 and Casp-3, respectively) in lysates of chondrocytes incubated or not with Cyt in the absence or presence of PRL for 6 hours. The graph shows the quantification of active caspase-3 by densitometry after normalization to procaspase-3 (n = 3). (**C**) qRT-PCR–based quantification of *p53* mRNA levels (n = 3) in chondrocytes incubated or not with Cyt in the absence or presence of PRL for 24 hours. (**D**) Representative Western blot of BAX and BCL-2 in chondrocytes incubated or not with Cyt in the absence or presence of PRL for 4 hours. The graph shows the quantification of BAX/BCL-2 by densitometry (n = 3). Values are mean ± SEM. $^*P < 0.05$, $^{**}P < 0.01$, $^{***}P < 0.001$.

Results

PRL blocks Cyt-induced apoptosis of chondrocytes in culture by a NO-independent, JAK2/STAT3–dependent pathway. We first studied whether PRL can act on chondrocytes to inhibit the proapoptotic effect of Cyt using primary cultures of rat articular chondrocytes. Cyt induced a 2-fold increase in chondrocyte apoptosis, as determined by chondrocyte internucleosomal DNA fragmentation measured by ELISA, and this increase was blocked in a dose-dependent manner by the coadministration of PRL (Figure 1A). The antiapoptotic effect of PRL was confirmed by Western blot analysis of procaspase-3 cleavage to the caspase-3 active form (Figure 1B). Cyt treatment enhanced the levels of active caspase-3 as compared with those after no treatment, and PRL blocked the Cyt-induced increase of active caspase-3. The graph in Figure 1B shows quantification of active caspase-3 after normalization for the amount of total procaspase-3 on the blot. We also investigated the expression of proteins that regulate apoptosis. Upon treatment with Cyt, there was a 15-fold increase in the mRNA expression of proapoptotic *p53*, as determined by qRT-PCR, and this increase was significantly reduced by PRL (Figure 1C). Also, Western blot analysis showed that PRL prevented the increase in the levels of proapoptotic BAX induced by Cyt and increased the levels of antiapoptotic BCL-2, resulting in a significant reduction in the BAX/BCL-2 ratio (Figure 1D).

Because NO produced by iNOS is a main factor mediating the effect of TNF-α, IL-1β, and IFN-γ on chondrocyte apoptosis (3, 4, 18), we tested whether the inhibition of Cyt-induced iNOS protein expression/NO production mediates the survival effect of PRL. Similar to PRL, addition of the NOS inhibitor N^{ω}-nitro-L-arginine methyl ester (L-NAME) (19) prevented Cyt-induced chondrocyte apoptosis (Figure 2A). However, PRL had no apparent effect on Cyt-induced upregulation of iNOS protein measured by Western blot (Figure 2B) or of the NO metabolites, nitrite (NO_2^-) and nitrate (NO_3^-), evaluated by the Griess reaction (Figure 2C) in chondrocyte lysates or conditioned media, respectively. This indicates that inhibition of Cyt-induced apoptosis by PRL occurs through a NO-independent pathway. We next examined activation of JAK2/STAT3, a known PRL signaling pathway (20) that is implicated in chondrocyte survival (21). In the absence and presence of Cyt, addition of PRL to cultured chondrocytes stimulated the phosphorylation/activation of JAK2, as indicated by Western blotting (Figure 2D), and the activation of STAT3, as measured by its nuclear translocation (Figure 2E). STAT3 immunoreactivity was predominantly distributed throughout the cytoplasm, and treatment with PRL increased the localization of STAT3 immunostaining in the cell nucleus, indicative of STAT3 activation. Because incubation of chondrocytes with the STAT3 inhibitor S31-201 (22) resulted in chondrocyte apoptosis (Figure 2F), it is possible that activation of the JAK2/STAT3 pathway by PRL mediates its inhibitory effect on Cyt-induced chondrocyte apoptosis.

PRL inhibits the apoptosis of chondrocytes induced by the intra-articular injection of Cyt. To assess the survival action of PRL in vivo, Cyt with or without PRL were injected into the intra-articular space of knee joints of normoprolactinemic rats. Also, Cyt were injected in rats rendered hyperprolactinemic by placing 2 anterior pituitary glands (APs) under a kidney capsule for 15 days (23). After 48 hours, Cyt-injected knees showed a positive TUNEL signal on the outer border of the articular cartilage, visualized as a continuous fluorescent line, which was absent in the vehicle-injected controls (Figure 3A). The TUNEL-positive signal was located in chondrocytes (Figure 3A, inset), in which apoptosis was confirmed by active caspase-3 immunostaining and DAPI-DNA labeling (Figure 3B). There was no positive TUNEL reaction in the articular cartilage of knees coinjected with Cyt and PRL (Figure 3C) or in AP-grafted rats injected with Cyt (Figure 3E). Inhibition of the Cyt effect by PRL and AP grafts was statistically significant after quantifying

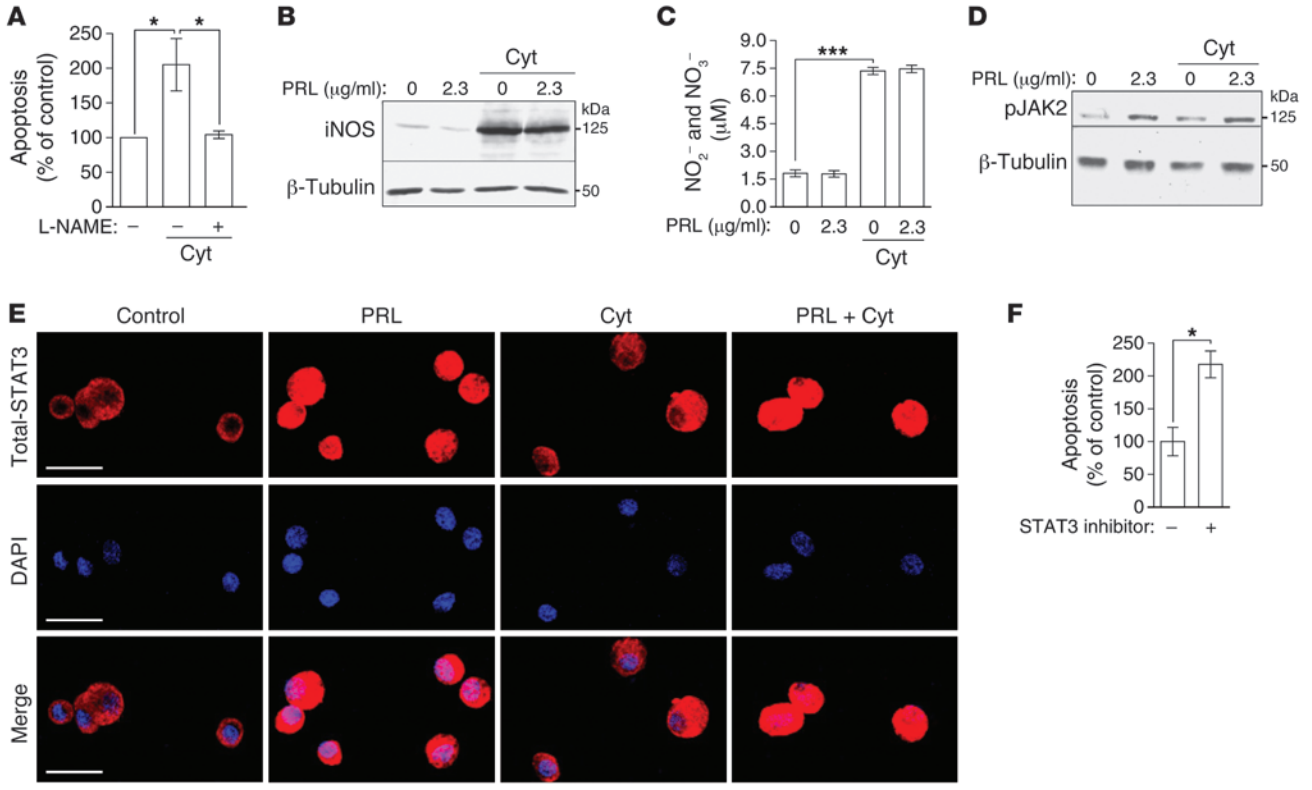

Figure 2

PRL inhibits Cyt-induced chondrocyte apoptosis by a NO-independent, JAK2/STAT3–dependent pathway. (**A**) Apoptosis evaluated by ELISA in chondrocytes incubated with Cyt in the presence or absence of the NO inhibitor L-NAME for 24 hours (n = 3–6). (**B**) Western blot analysis of iNOS (n = 3) and (**C**) NO_2^- and NO_3^- concentrations (n = 7) after incubating or not incubating chondrocytes with Cyt in the absence or presence of PRL for 6 and 24 hours, respectively. (**D**) Representative Western blot of phosphorylated JAK2 (pJAK2) in chondrocytes incubated with the various treatments for 30 minutes (n = 3). (**E**) Representative immunostaining for total STAT3 and DAPI in cultured chondrocytes treated with or without (control) PRL (2.3 μg/ml), Cyt, or PRL and Cyt (PRL + Cyt) for 1 hour (n = 3). Scale bar: 25 μm. (**F**) Apoptosis evaluated by ELISA in chondrocytes incubated in the absence or presence of 100 nM STAT3 inhibitor S31-201 for 24 hours (n = 3–4). Bars represent mean ± SEM. $^*P < 0.05$, $^{***}P < 0.001$.

the TUNEL signal (Figure 3, D and F). AP transplants resulted in a significant increase in circulating PRL levels (Figure 3G). These higher PRL levels were responsible for the reduction of Cyt-induced chondrocyte apoptosis, because this reduction was abrogated (Figure 3, E and F) by lowering circulating PRL with CB154 (Figure 3G), a dopamine D2 receptor agonist that inhibits AP PRL release (24). Therefore, intra-articular treatment with PRL or induction of high prolactinemia inhibits Cyt-induced chondrocyte apoptosis.

Cyt-induced chondrocyte apoptosis is enhanced in PRL receptor–null mice. In order to explore whether endogenous PRL helps maintain chondrocyte survival under inflammatory conditions, mice null for the PRL receptor ($Prlr^{-/-}$) were injected or not with Cyt in one knee and, after 48 hours, both the injected and noninjected knees were evaluated by TUNEL. In the absence of Cyt, there was no apparent histological alteration (data not shown) or positive TUNEL signal in the articular cartilage of $Prlr^{-/-}$ mice (Figure 4, A and B), indicating that PRL is not required for the survival of articular chondrocytes under normal conditions. After Cyt treatment, $Prlr^{-/-}$ mice showed TUNEL staining in the articular cartilage similar to that in wild-type counterparts (Figure 4, A and B). However, in $Prlr^{-/-}$ mice, but not in $Prlr^{+/+}$ mice, the noninjected knee, i.e., contralateral to the knee injected with Cyt, also showed a positive TUNEL reaction (Figure 4, C and D). These findings suggest that normal levels of PRL inhibit the proapoptotic effect of Cyt but that this action is only detected in response to lower levels of Cyt, such as those reaching a knee after contralateral intra-articular injection.

PRL prevents and reduces chondrocyte apoptosis in the adjuvant-induced model of inflammatory arthritis. Since PRL protects against Cyt-induced chondrocyte apoptosis, and Cyt can cause apoptosis-mediated cartilage loss in RA (1, 2, 6–9), we investigated whether PRL reduces chondrocyte apoptosis in the adjuvant-induced model of inflammatory arthritis in rats. Osmotic minipumps delivering PRL or subcutaneous tablets releasing haloperidol (Hal), a dopamine D2 receptor antagonist leading to hyperprolactinemia (25), were implanted 3 days before the injection of CFA (Figure 5A). On the day of CFA injection (day 0), infusion of PRL or Hal treatment elevated circulating PRL levels by 7 fold or 8 fold, respectively (Figure 5B). The hyperprolactinemic effect of PRL infusion was maintained and that of Hal decreased with time and resulted, at the end of the experiment (day 21 after CFA) (Figure 5B), in a 6-fold and 2-fold increase in serum PRL, respectively.

Consistent with cartilage destruction being a feature of adjuvant-induced arthritis (26), CFA treatment resulted in chondrocyte apoptosis, as revealed by TUNEL- and active caspase-3–

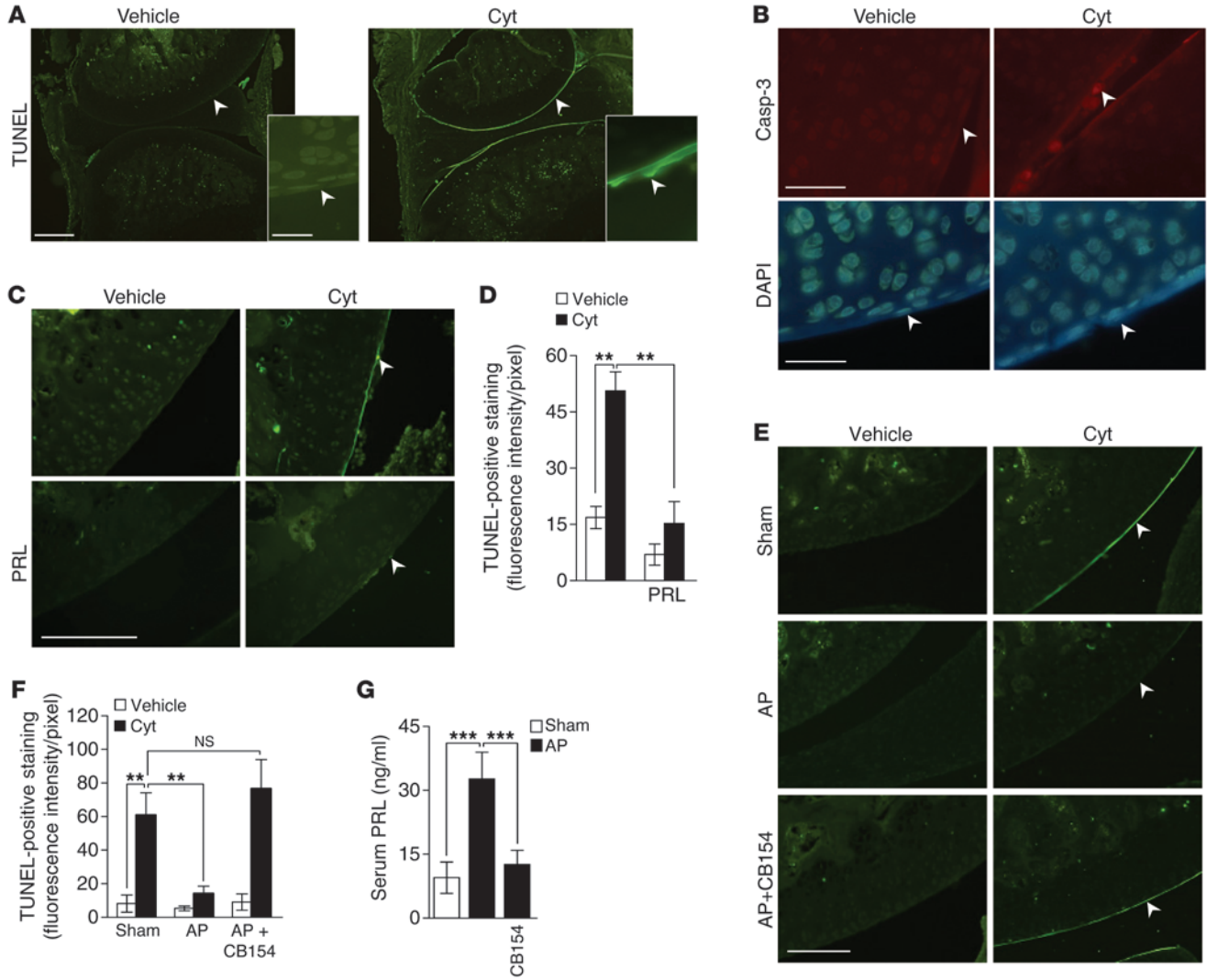

Figure 3

PRL inhibits the apoptosis of chondrocytes induced by the intra-articular injection of Cyt. (**A** and **B**) Apoptosis was assessed in rat knees injected with vehicle or Cyt by TUNEL and active caspase-3 staining. The bottom right images in **A** show enlarged views of knee cartilage. Scale bar: 500 μm (top); 25 μm (bottom). (**B**) Nucleic acids in chondrocytes were stained by DAPI. Scale bar: 50 μm. (**C** and **D**) TUNEL-positive staining and quantification in outer border cartilage of rat knees coinjected with Cyt and PRL (n = 4). Scale bar: 100 μm. (**E** and **F**) TUNEL-positive staining and quantification in outer border cartilages of rat knees from nontransplanted (sham) and AP-transplanted rats exposed to vehicle or Cyt, in the presence or absence of dopamine D2 receptor antagonist, CB154 (n = 4–6). (**A**–**C** and **E**) White arrowheads indicate cartilage outer border. Scale bar: 250 μm. (**G**) Serum PRL levels in sham or AP-transplanted rats treated or not with CB154 (n = 5–10). Bars represent mean ± SEM. $^{**}P < 0.01$, $^{***}P < 0.001$.

positive cells in the cartilage of knee joints on day 21 after CFA (Figure 5C), i.e., when joint swelling is at its peak, as seen below. At this time, CFA also produced a significant increase in the mRNA expression of *Casp3*, *Bax*, and *p53* in ankle joints (Figure 5D). Treatment with PRL or Hal lowered CFA-TUNEL and active caspase-3 staining and expression of proapoptotic mediators, indicating that this hormone prevents chondrocyte apoptosis in arthritic joints. We then investigated curative properties of PRL by placing osmotic minipumps delivering PRL 15 days after the injection of CFA (Figure 6A), i.e., when joint swelling is evident, as seen below. On day 21, PRL infusion had elevated serum PRL by 5 fold and 2 fold in control and CFA-treated animals, respectively (Figure 6B). Higher PRL levels correlated with reduced chondrocyte apoptosis (Figure 6C) and lower expression of proapoptotic mediators (Figure 6D) in the CFA-injected rats. These findings suggest that high prolactinemia prevents and reduces chondrocyte apoptosis in inflammatory arthritis.

PRL prevents and reduces adjuvant-induced arthritis. Because PRL has immunoregulatory properties (17), it may also promote cartilage survival in RA by attenuating joint inflammation. Early studies reported that AP-induced hyperprolactinemia reduces CFA-induced arthritis (27) and that Hal chronically suppresses inflammation in patients with RA (28, 29). Here, we show that PRL infusion, initiated 3 days before CFA injection (Figure 7A), delayed the onset and ameliorated the severity of joint inflammation, as indicated by a reduction in hind paw swelling (ankle circumference)

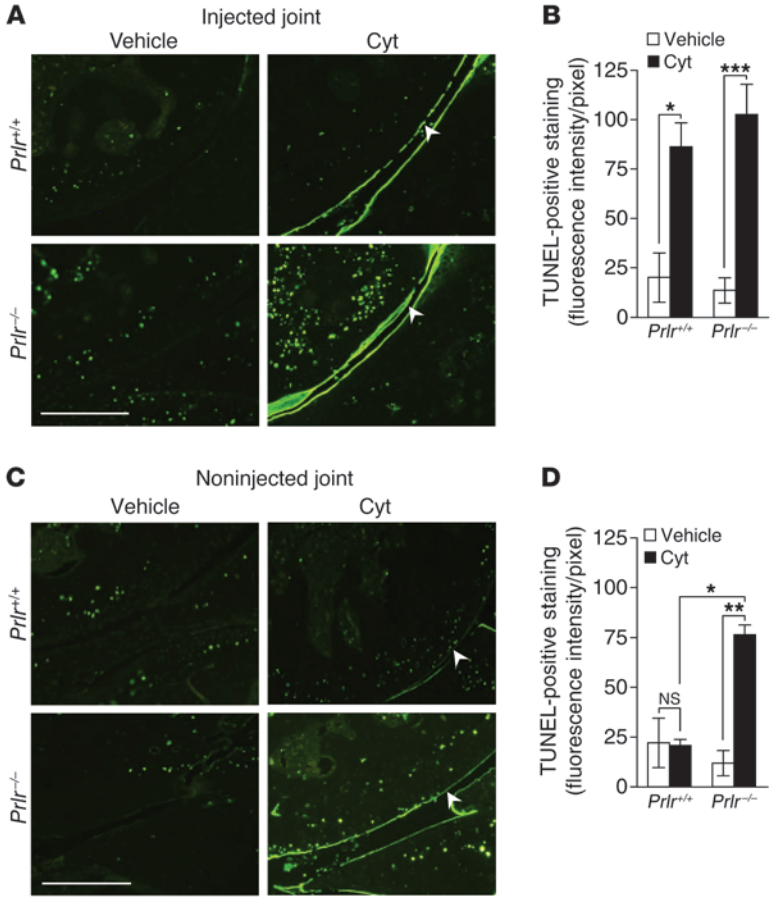

Figure 4
Cyt-induced chondrocyte apoptosis is enhanced in *Prlr*$^{-/-}$ mice. Apoptosis was assessed by TUNEL staining in knees of *Prlr*$^{-/-}$ and *Prlr*$^{+/+}$ mice intra-articularly injected or not with Cyt. (**A** and **B**) Both injected and (**C** and **D**) noninjected knee joints, i.e., ipsilateral and contralateral to the injection site, respectively, were analyzed. White arrowheads indicate cartilage outer border. Scale bar: 250 μm. Bars represent mean ± SEM. (n = 3–5). $^{*}P < 0.05$, $^{**}P < 0.01$, $^{***}P < 0.001$.

(Figure 7, B and C) and the lower mRNA expression of proinflammatory mediators (*Ifng*, *Il6*, *iNos*, *Il1b*, and *Tnfa*) in the ankle joint at day 21 after CFA (Figure 7E). Also, Hal treatment 3 days before CFA (Figure 7A) counteracted inflammation even more effectively than PRL infusion. Hal suppressed ankle swelling (Figure 7F) and reduced ankle pain (Figure 7G) and proinflammatory mediator expression (Figure 7H). Consistent with these findings, the histopathological examination of knee sections stained by hematoxylin and eosin showed that PRL infusion, and to a lesser extent Hal treatment, reduced the progression of inflammatory arthritis, as revealed by the absence of pannus formation, and the thinning and destruction of bone trabeculae that occur in normoprolactinemic, adjuvant-injected rats (Figure 8).

Notably, even when started after inflammatory onset (day 15 after CFA) (Figure 9A), PRL treatment mitigated ankle swelling, pain, and expression of proinflammatory mediators (Figure 9, B–D). These findings support the antiinflammatory action of PRL and its therapeutic value for the prevention and reduction of joint destruction in inflammatory arthritis.

Discussion

Chondrocytes are responsible for the production and maintenance of the articular cartilage extracellular matrix, which largely determines the biomechanical properties of joints (30). Adult articular cartilage is postmitotic and cannot compensate for loss of chondrocytes occurring in aging (31) and in arthropathies such as osteoarthritis (3) and RA (7). In these diseases, abnormal exposure to cytokines produced by resident cells and infiltrating inflammatory cells leads to chondrocyte apoptosis and matrix degradation (1, 2, 6–9). Natural chondrocyte survival factors have the potential to be developed for therapeutic application. This study demonstrates for the first time that PRL inhibits cytokine- and arthritis-driven chondrocyte apoptosis. This effect involves the reduced expression of proinflammatory cytokines in joint tissue and the blockage of their proapoptotic effect at the chondrocyte level. Moreover, raising circulating PRL levels reduces joint swelling, pain, pannus formation, and bone erosion in the arthritic joint.

Consistent with previous studies (2, 32, 33), here we show that a combination of TNF-α, IL-1β, and IFN-γ stimulated the in vitro apoptosis of chondrocytes, as evaluated by enhanced mRNA expression of *p53*, increased BAX/BCL-2 ratio, activated caspase-3, and increased DNA fragmentation. Cyt concentrations were similar to those (1–10 ng/ml) found in synovial fluid of patients with RA with severe disease activity (34, 35) or produced by activated chondrocytes (36). PRL opposed the Cyt proapoptotic effect in a dose-dependent manner at concentrations (0.2–2.3 μg/ml) higher than those reported in RA synovial fluid (0.007–0.02 μg/ml) (14, 15) but similar to those (0.2–0.3 μg/ml) circulating in pregnancy and lactation (37). Also, PRL may be higher in cartilage than in synovial fluid due to its local synthesis in chondrocytes (12). Previous findings showed that PRL attenuates the stimulatory effect of Cyt on the expression of iNOS and the production of NO in cultured fibroblasts (38) and NO is a major mediator of Cyt-induced chondrocyte apoptosis (ref. 3 and present data). In chondrocytes, however, PRL did not inhibit Cyt-induced iNOS protein expression/NO production, indicating that its survival effect is independent of NO. On the other hand, PRL activated JAK2 and STAT3, which signal to inhibit chondrocyte apoptosis. STAT3 activation promotes the survival of growth plate chondrocytes by inducing the transcription of BCL-2 (21), and we found that the pharmacological inhibition of STAT3 leads to the apoptosis of articular chondrocytes. It is possible that STAT3-independent, JAK2-dependent mechanisms also contribute to the antiapoptotic effect of PRL. Activation of JAK2 by PRL stimulates PI3K/Akt to promote the survival of various cells (39–42), and activation of Akt inhibits the apoptosis of chondrocytes induced by endoplasmic reticulum stress or the osteoarthritic condition (43, 44).

The fact that PRL activates molecular mechanisms in chondrocytes to counteract the proapoptotic effect of Cyt argues in favor of its prosurvival effect on cartilage under inflammatory

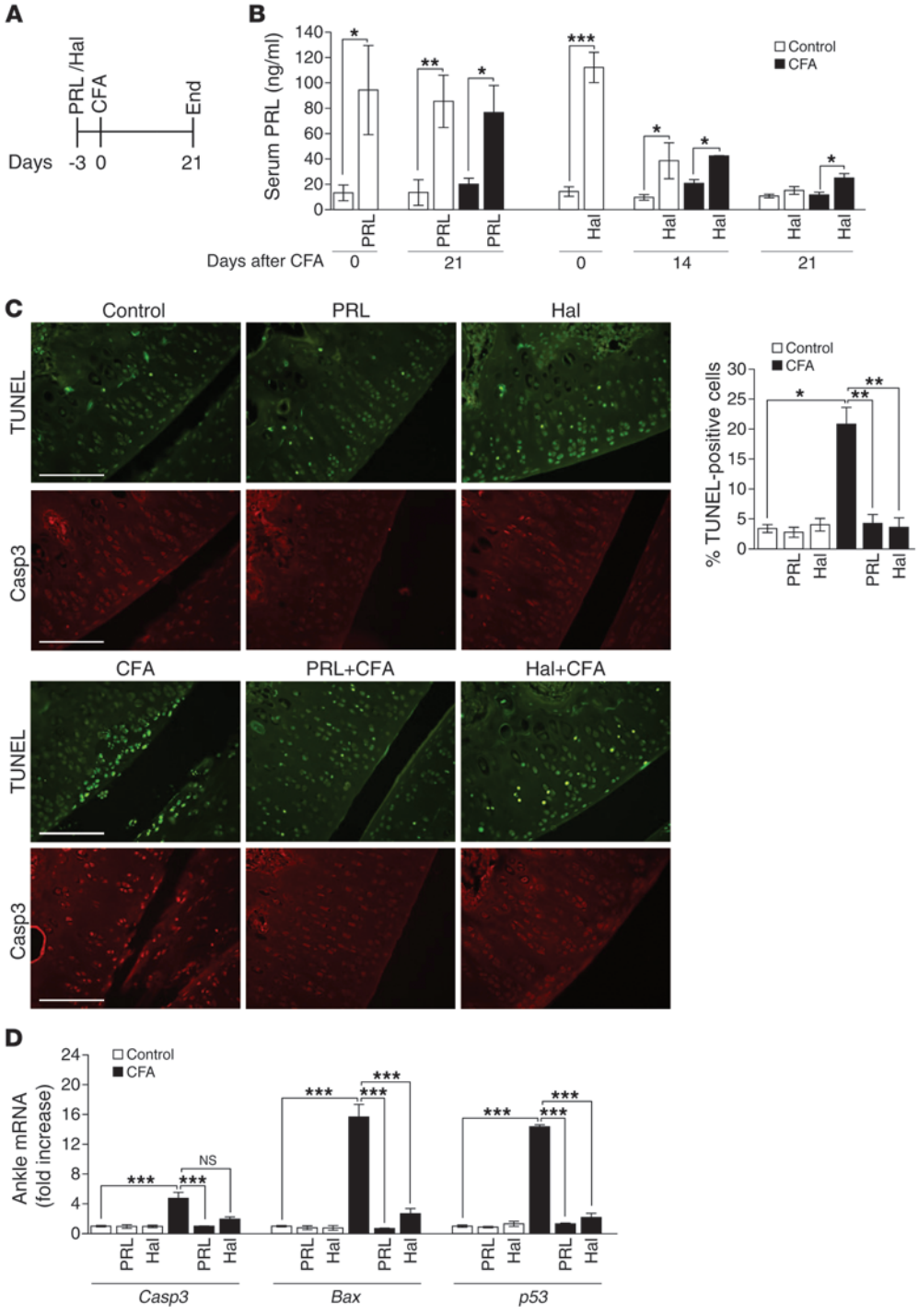

Figure 5

PRL and Hal prevent chondrocyte apoptosis in adjuvant-induced arthritis. (**A**) Experimental design diagram: osmotic minipumps delivering PRL or subcutaneous tablets releasing Hal were placed 3 days before injecting the rats with CFA, and the experiment ended on day 21 after CFA. (**B**) Serum PRL levels on days 0 and 21 after CFA in PRL-treated rats (n = 3–8) and on days 0, 14, and 21 after CFA in Hal-treated rats (n = 4–8). (**C**) TUNEL and active caspase-3 staining of articular cartilage of knees from rats treated or not with PRL or Hal under control and CFA-injected conditions on day 21 after CFA. Scale bar: 100 μm. The graph shows the quantification of TUNEL-positive cells in articular cartilage (n = 4–8). (**D**) qRT-PCR–based quantification of *Casp3*, *Bax*, and *p53* mRNA levels in ankle joints from PRL- and Hal-treated rats on day 21 after CFA (n = 5–14). Bars represent mean ± SEM. $^{*}P < 0.05$, $^{**}P < 0.01$, $^{***}P < 0.001$.

conditions. To investigate this concept, we extended the in vitro observations to the articular cartilage in situ. To our knowledge, this is the first report showing that the intra-articular delivery of Cyt induces the apoptosis of chondrocytes. Cyt were used at pharmacological concentrations, since, in contrast to cell-culture conditions, their intra-articular delivery results in a much shorter contact with chondrocytes (45). Apoptosis occurred at the outer surface of articular cartilage, which is the most exposed and susceptible area of the tissue. Superficial articular chondrocytes display higher numbers of IL-1 binding sites than cells in deep cartilage (46), and enhanced iNOS expression (47) and large numbers of apoptotic chondrocytes have been reported in the superficial and middle zones of osteoarthritic (48) and RA (8) cartilage. Cotreatment with a pharmacological concentration of PRL (60 μg/ml) or increasing serum PRL to levels similar to those (0.03 μg/ml) found in the circulation of patients with RA (49) blunted Cyt-induced chondrocyte apoptosis. These findings demonstrate the survival effect of PRL on articular cartilage in vivo and suggest that systemic PRL can enter the joint to protect against chondrocyte apoptosis in RA.

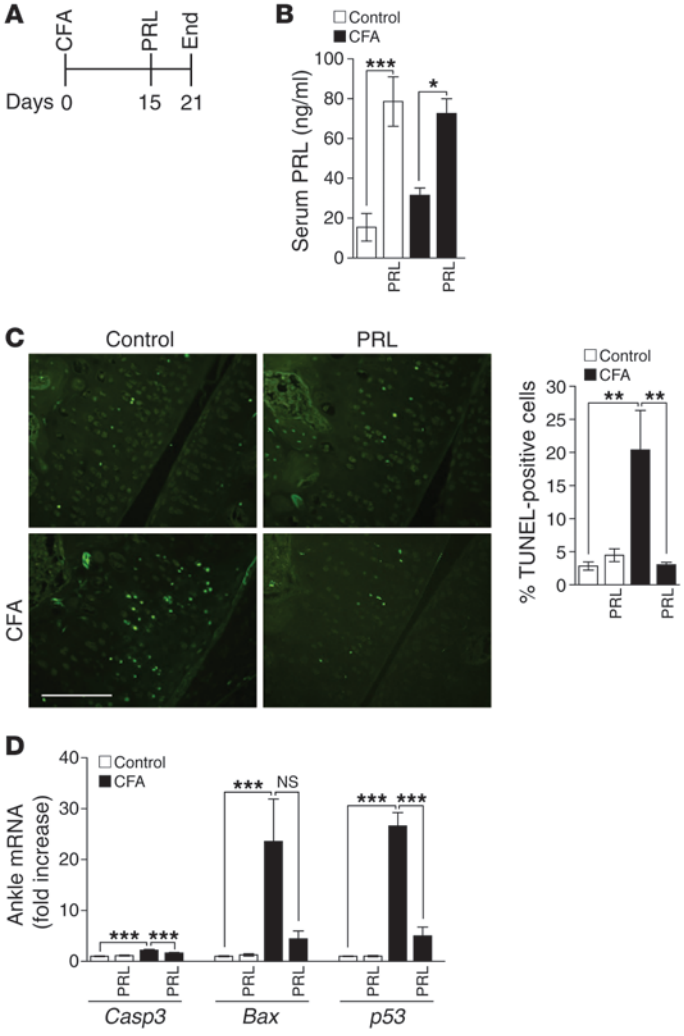

Figure 6

PRL reduces chondrocyte apoptosis in already arthritic rats. (**A**) Experimental design diagram: osmotic minipumps delivering PRL were placed 15 days after the injection of CFA in rats, and the experiment ended on day 21 after CFA. (**B**) Serum PRL levels on day 21 after CFA in PRL-treated and nontreated rats (n = 4–8). (**C**) TUNEL and active caspase-3 staining of articular cartilage of knees from rats treated or not with PRL under control and CFA-injected conditions on day 21 after CFA. Scale bar: 100 μm. The graph shows the quantification of TUNEL-positive cells in articular cartilage (n = 5–8). (**D**) qRT-PCR–based quantification of *Casp3*, *Bax*, and *p53* mRNA levels in ankle joints from PRL-treated and nontreated rats on day 21 after CFA (n = 3–8). Bars represent mean ± SEM. $^*P < 0.05$, $^{**}P < 0.01$, $^{***}P < 0.001$.

PRL is not essential for cartilage survival under normal conditions. Targeted disruption of the PRL receptor gene has no phenotype in endochondral bone formation (50), a process involving the apoptosis of growth plate chondrocytes, and it causes no apparent alteration indicative of a defect in articular cartilage survival (present study). However, Cyt-induced chondrocyte apoptosis was enhanced in the absence of the PRL receptor, indicating that the survival effect of PRL becomes apparent in the context of inflammation. The fact that in *Prlr*$^{-/-}$ mice enhanced apoptosis was also seen in the knee contralateral to the one injected with the Cyt, suggests that the antiapoptotic effect of PRL depends on Cyt levels and thus, that higher values of PRL are needed to promote cartilage survival under highly inflammatory conditions.

Here, we show that increasing systemic PRL levels prevents and reduces chondrocyte apoptosis in CFA-induced arthritis. This model is well documented for the induction of inflammation within joint tissues and for having cartilage and bone destruction similar to that in RA (26, 51). Consistent with a previous study (52), we found that CFA-induced arthritis enhances the expression of apoptotic mediators in joints and showed for the first time that apoptosis occurs in large numbers of articular chondrocytes. Thus, in CFA-induced arthritis as in other models of inflammatory arthritis (53) and in RA (8), chondrocyte apoptosis is associated with joint destruction. Increasing prolactinemia, either by PRL infusion or Hal treatment, before or after inducing arthritis, reduced chondrocyte apoptosis and Cyt expression in joints. Also, PRL and Hal ameliorated the severity of arthritis, as evaluated by joint swelling, pain, pannus formation, and bone erosion. The effect of Hal on joint swelling and pain was stronger than that of PRL but weaker on pannus formation and bone erosion. These differences may reflect the fact that, in addition to blocking D2 receptors on the AP, which causes the release of PRL, Hal also blocks dopamine D2 receptors on immune cells, thereby modifying both cytokine release and action (29, 54). Indeed, Cyt are key mediators of CFA-induced arthritis. Their concentration and expression are significantly elevated in serum (26) and joint tissues (present results) of CFA-injected rats, respectively, and IL-1 antagonists and TNF-α–neutralizing antibodies reduce disease severity in these animals (51, 52). We propose that PRL protects against CFA-induced inflammatory arthritis by reducing Cyt levels and counteracting their proapoptotic and proinflammatory actions on synovial cells, cartilage, and bone. However, contrary to these findings, PRL enhances proliferation of cultured RA synovial cells and their release of proinflammatory cytokines and MMP (16). While the in vitro condition may contribute to this discrepancy, in vivo evidence supporting our proposal shows that AP-induced hyperprolactinemia ameliorates CFA-induced inflammation by increasing the circulating levels of corticosterone (23, 27). Because glucocorticoids and inhibitors of TNF-α and IL-1β are current treatments for RA (55), sustained PRL administration offers promise for mitigating susceptibility to the onset or flare-up of RA and disease severity, and current medications known to increase prolactinemia constitute therapeutic options in RA, as indicated by clinical studies using Hal (28, 29).

The idea of inducing high prolactinemia to help control the progression of joint damage in RA is novel and unexpected. A large body of literature has focused on PRL having a pathogenic role in RA and also in other autoimmune diseases, like SLE, Sjögren's syndrome, Hashimoto's thyroiditis, celiac disease, MS, etc. Its pathogenic role is largely based on the preponderance of autoimmune diseases in women (56) and on PRL being a sex-linked hormone, on the higher levels of circulating PRL detected in some patients (6%–45%, depending on the disease and specific study), on the therapeutic effects of the dopamine agonist bromocriptine, and on the immunoenhancing properties of PRL (57–61). However, in RA, as in the other autoimmune diseases, treatment with bromocriptine is not always effective and the association between PRL levels

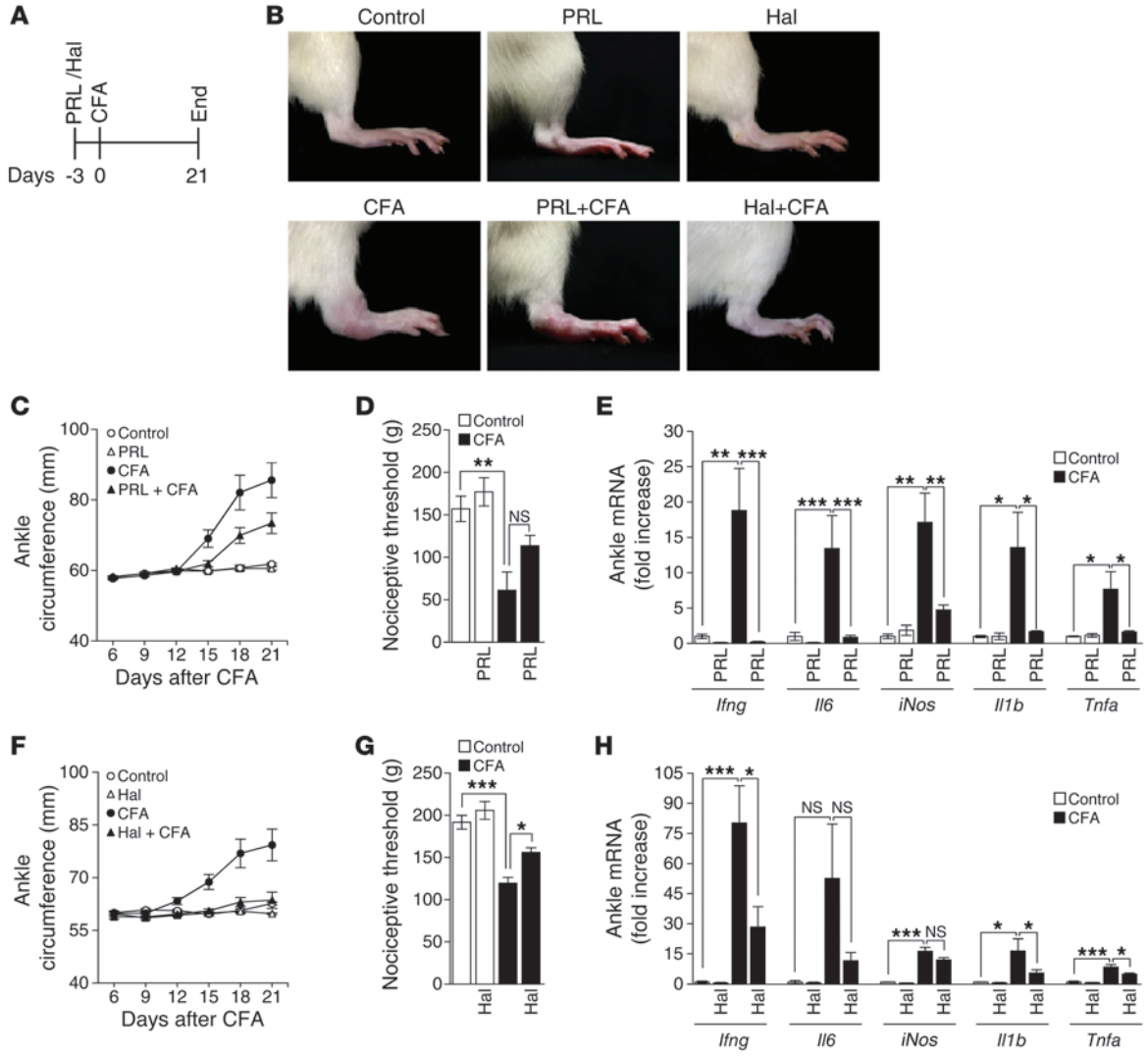

Figure 7

PRL and Hal prevent joint inflammation in adjuvant-induced arthritis. (**A**) Experimental design diagram: osmotic minipumps delivering PRL or subcutaneous tablets releasing Hal were implanted 3 days before the injection of CFA in rats. (**B**) Representative photographs of hind paws from groups injected or not with CFA. (**C** and **F**) Time course of ankle circumference in groups infused with PRL (n = 10) or treated with Hal (n = 16) under control and CFA-injected conditions. (**C**) Days 15, 18, and 21, $P < 0.001$, CFA vs. control. Days 18 and 21, $P < 0.001$, PRL vs. PRL plus CFA. (**F**) Days 15 and 18, $P < 0.001$, CFA vs. control. Days 12, 15, 18, and 21, $P < 0.001$, CFA vs. Hal plus CFA. (**D** and **G**) Nociceptive threshold in groups infused with PRL (n = 5–9) or treated with Hal (n = 5–9). (**E** and **H**) qRT-PCR–based quantification of *Infg*, *Il6*, *iNos*, *Il1b*, and *Tnfa* mRNA levels in ankle joints from rats treated with PRL (n = 3–10) or with Hal (n = 3–10) under control and CFA-injected conditions on day 21 after CFA. Bars are mean ± SEM. *$P < 0.05$, **$P < 0.01$, ***$P < 0.001$.

and disease activity has been inconsistent (58–62). Generalizations are confounded by the contribution of PRL synthesized locally by cells like chondrocytes (12), synoviocytes and immune cells (16), and endothelial cells (63), which can potentiate the action of systemic PRL. Moreover, PRL has the ability to exert immunostimulatory or immunosuppressive effects, depending on its level and the pathophysiological conditions (17). For example, physiological concentrations of PRL (<0.02 μg/ml) are more effective than high PRL levels (0.1 μg/ml) in stimulating antibody production by SLE lymphocytes (64), low PRL levels stimulate and high levels inhibit NK cell proliferation (65), and hyperprolactinemic patients (mean serum PRL of 0.98 μg/ml or 0.20 μg/ml) show reduced NK cell numbers (66) and function (67). Also, hyperprolactinemia protects against inflammatory arthritis in rats (present study), and treatment with a high, but not a low, dose of PRL exacerbates experimental MS (61). In the latter, however, the low dose of PRL is beneficial when combined with IFN-β, and *Prlr*$^{-/-}$ mice display a significantly worse outcome than wild-type mice (61). The variability of the relationship between PRL and autoimmune diseases is further highlighted under physiological hyperprolactinemia. During pregnancy, when PRL levels are high, SLE flare-ups occur, but RA and MS go into remission (59, 68). Breastfeeding, a stimulus elevating circulating PRL, exacerbates SLE in humans (69), but it is protective in the B/W mouse model of SLE (70). Breastfeeding also

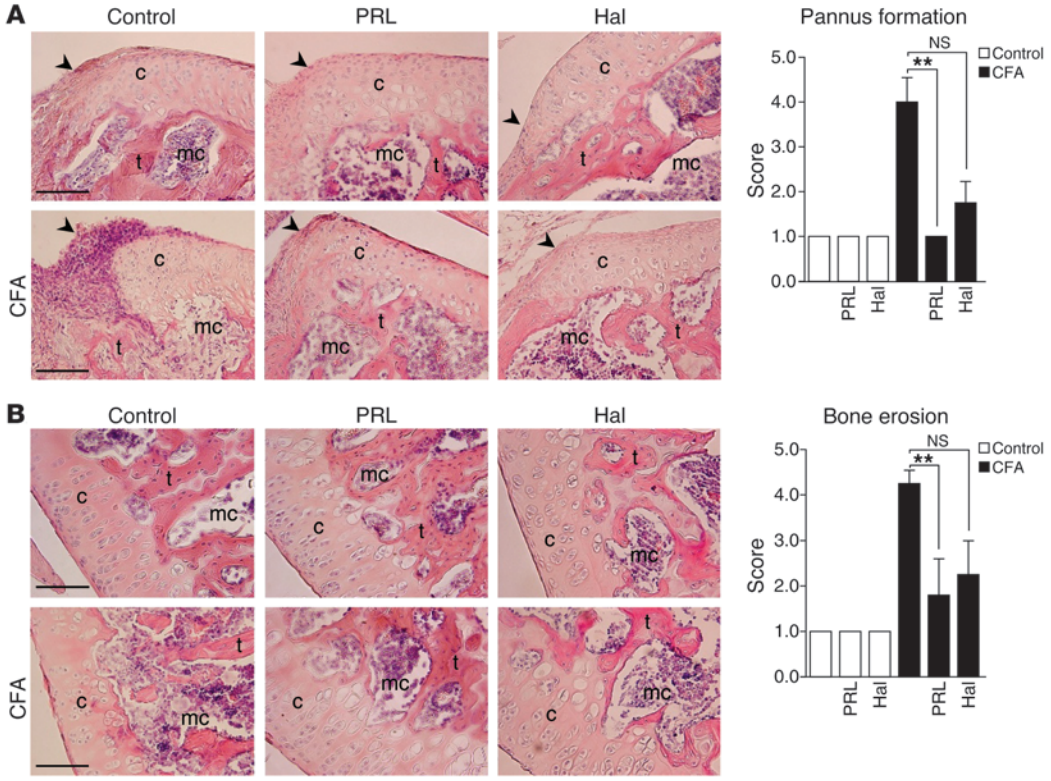

Figure 8

PRL reduces pannus formation and bone erosion in adjuvant-induced arthritis. Histological evaluation of (**A**) pannus formation and (**B**) bone erosion in sections of knee joints stained by hematoxylin and eosin from nonimplanted rats (control) or rats implanted with osmotic minipumps delivering PRL or with subcutaneous tablets releasing Hal 3 days before injecting or not injecting CFA; the histological evaluation was carried out on day 21 after CFA (n = 3–8). Pannus-associated regions in each group are indicated (arrows). c, cartilage; t, bone trabeculae; mc, bone marrow cavity. Scale bar: 100 μm. Graphs show histological scores for (**A**) pannus formation (synovial membrane hyperplasia and infiltration of leukocytes) and (**B**) bone erosion (thinning and destruction of bone trabeculae). Values are mean ± SEM. $^{**}P < 0.01$.

worsens RA (71) but protects against postpartum MS relapse (72). These contrasting observations indicate that PRL exerts opposing influences on immune function that depend on complex immune and hormonal interactions.

Although the role of endogenous PRL in autoimmune diseases has generated controversies (57–62, 73), our study reveals that elevating serum PRL levels significantly attenuates cartilage death and joint inflammation in inflammatory arthritis. This strategy may be comparable to the well-established use of glucocorticoids in patients with RA, in which levels of the endogenous hormones appear insufficient to control the disease (74). While PRL is not essential for normal immune system development and function (75, 76), it is a major stress-related hormone (77), balancing immune system homeostasis in the context of stress, trauma, and inflammation (17, 78). Studies clarifying how circulating and local PRL levels are being regulated in the proinflammatory milieu of pathological situations will help establish appropriate PRL levels for controlling ongoing inflammation and the better use of PRL for therapeutic purposes in RA and other inflammatory-related disorders.

Methods

Reagents. Recombinant human TNF-α, IL-1β, and IFN-γ were purchased from R&D Systems. Rat PRL and rat PRL radioimmunoassay reagents were obtained from A.F. Parlow (National Hormone and Pituitary Program, Los Angeles, California, USA). Ovine PRL and L-NAME were purchased from Sigma-Aldrich, and the STAT-3 inhibitor S31-201 and anti-BAX (Sc-493) and anti–BCL-2 (Sc-492) antibodies from Santa Cruz Biotechnology Inc. Antibodies anti–caspase-3 (9662) and anti-pJAK2 (Tyr1007/1008, 3771) were from Cell Signaling Technology Inc., anti-iNOS (06-573) was from Upstate, and CFA was from Difco.

Animals. Male Lewis and Sprague-Dawley rats (200–250 g), Wistar rats (130–150 g), and *Prlr*$^{-/-}$ mice (6–8 months, 129Sv/J background) were housed under standard laboratory conditions (22°C; 12-hour/12-hour light/dark cycle, free access to food and water). Animals were anesthetized with 70% ketamine and 30% xylazine (1 μl/g body weight, i.p.) for surgeries and intra-articular injections, and all procedures were performed between 9:00 and 12:00 AM. To avoid stress-induced alterations, animals were handled daily for 7 days before euthanization by carbon dioxide inhalation and decapitation.

Chondrocyte culture. Articular chondrocytes were isolated from femoral epiphyseal cartilage of male Wistar rats as described previously (12). Cells were seeded at 2 × 10^5 cells per cm^2 and incubated in DMEM containing 10% FBS and 1% penicillin/streptomycin at 37°C for 24 hours. Nonadherent cells were removed, and adherent cells were incubated for 24 hours in either fresh medium or medium containing Cyt (25 ng/ml TNF-α, 10 ng/ml IL-1β, and 10 ng/ml IFN-γ) combined or not with different concentrations of rat PRL or the NOS inhibitor L-NAME (1 mM). Other cell cultures were incubated with 100 nM of the STAT3 inhibitor, S31-201. All

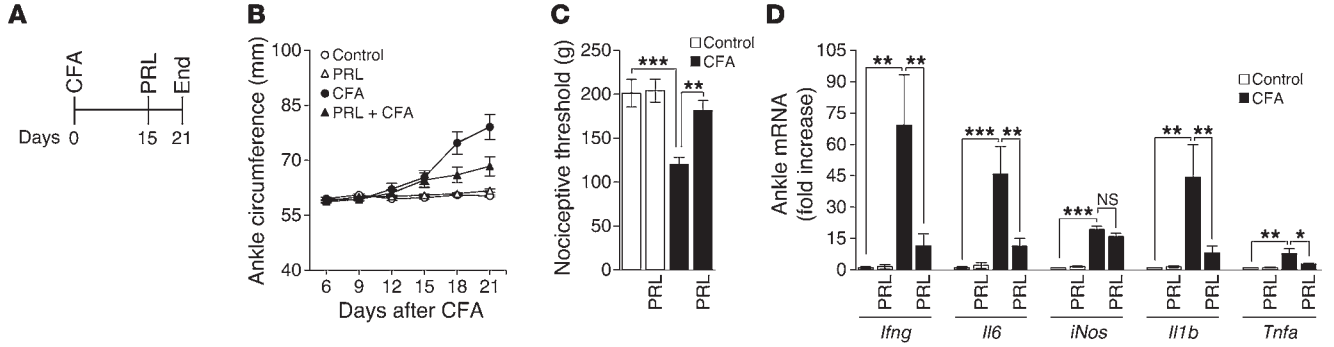

Figure 9

PRL reduces joint inflammation in already arthritic rats. (**A**) Experimental design diagram: osmotic minipumps delivering PRL were placed 15 days after the injection of CFA in rats, and the experiment ended on day 21 after CFA. (**B**) Time course of ankle circumference (n = 10–15) (days 18 and 21, $P < 0.001$, CFA vs. control), (**C**) evaluation of ankle joint nociceptive threshold (n = 5–8), and (**D**) qRT-PCR–based quantification of *Ifng*, *Il6*, *iNos*, *Il1b*, and *Tnfa* mRNA levels (n = 5–8) in ankle joints under control and CFA-injected conditions on day 21 after CFA. Bars are mean ± SEM. *$P < 0.05$, **$P < 0.01$, ***$P < 0.001$.

experiments were performed in the first passage of culture. Both detached and adherent chondrocytes were assayed for apoptosis by measuring fragmented nucleosomal DNA using the Cell Death Detection ELISA Kit (Roche Diagnostics). To investigate PRL-induced nuclear translocation of STAT3, chondrocytes were seeded on glass coverslips and treated with or without Cyt in the presence or absence of PRL for 1 hour. Cells were then fixed in 4% PFA at room temperature (RT) for 1 hour, washed, incubated 1 hour at RT with 5% normal goat serum in 0.05% Triton-PBS, and then incubated overnight at 4°C with a 1:100 dilution of anti-total STAT3. Cells were then washed and incubated at RT with the second antibody, Alexa Fluor 546 (1:500; Invitrogen), for 2 hours, and their nuclei were counterstained with DAPI (1 μg/ml; Sigma-Aldrich).

Western blot. Chondrocytes incubated with or without Cyt in the absence or presence of PRL were analyzed for JAK2 phosphorylation after 30 minutes, for BAX and BCL-2 after 4 hours, and for total caspase-3 (procaspase-3 and active caspase-3) and iNOS after 6 hours of treatment. Cells were resuspended in lysis buffer (0.5% Igepal, 0.1% SDS, 50 mM Tris, 150 mM NaCl, 1 μg/ml aprotinin, and 100 μg/ml PMSF, pH 7.0) and subjected to SDS/PAGE, and total protein (40 μg) was blotted and probed overnight with a 1:1,000 dilution of anti–caspase-3, anti-iNOS, or anti-pJAK2; a 1:300 dilution of anti-BAX; or a 1:200 dilution of anti–BCL-2. Secondary antibodies conjugated to alkaline phosphatase (Jackson ImmunoResearch Laboratories Inc.) were used. Densitometric analysis was performed using the Quantity One 1-D image analysis software (Bio-Rad Laboratories Inc.).

The Griess colorimetric assay was used to measure the NO_2^- and NO_3^- concentrations in conditioned media of chondrocytes treated or not with Cyt with or without PRL for 24 hours.

Intra-articular injection of Cyt. Lewis rats and *Prlr*$^{-/-}$ mice were injected in the articular space of right knee joints with Cyt in a final volume of 60 μl (375 ng TNF-α, 150 ng IL-1β, and 150 ng IFN-γ) and 10 μl (62.5 ng TNF-α, 25 ng IL-1β, and 25 ng IFN-γ), respectively. A group of rats was coinjected with the Cyt and 8 μg rat PRL. As the estimated volume of rat synovial fluid is 130 μl, the intra-articular concentration of PRL was 60 μg/ml. Thirteen days before Cyt injection, other groups of rats were implanted with 2 AP grafts under the kidney capsule in order to induce hyperprolactinemia (23), and half of them were injected i.p. with 1.25 mg/d of CB154 (Parlodel, Novartis), starting 5 days before Cyt injection. Endotoxin-free water (60 μl and 10 μl for rats and mice, respectively) was used as a control vehicle. Forty-eight hours after vehicle or Cyt injection, animals were euthanized to evaluate apoptosis in knee cartilage and assess serum PRL levels by radioimmunoassay.

Adjuvant-induced arthritis. Sprague-Dawley rats were immunized intradermally at the base of the tail with 0.2 ml CFA (10 mg heat-killed *Mycobacterium tuberculosis* H37Ra per 1 ml of Freund's adjuvant). Three days before CFA injection, some rats were rendered hyperprolactinemic by the subcutaneous implantation of a 28-day Alzet osmotic minipump (Alza) containing 1.6 mg ovine PRL or a tablet releasing 35 mg Hal over the 60 days of treatment (Innovative Research of America). Other rats were implanted 15 days after CFA injection with 14-day Alzet osmotic minipumps containing 0.8 mg ovine PRL. Arthritis development was evaluated every 3 days by the hind ankle circumference determined by measuring 2 perpendicular diameters, the laterolateral diameter (a) and the anteroposterior diameter (b), with a digital caliper and using the following formula: circumference = $2\pi(\sqrt{(a^2+b^2)}/2)$. On day 21 after CFA, hind paw pain was assessed using an Analgesy-Meter (Ugo Basile S.R.L.), and knee joints and hind paws were dissected to evaluate in situ apoptosis and expression of proapoptotic and proinflammatory markers, respectively. In addition, adjuvant-induced arthritis was evaluated histologically. Knee joints were fixed, decalcified, and dehydrated for paraffin embedding. Knee sections (7 μm) stained by hematoxylin and eosin were scored as reported previously (79), with the following modifications: 1 (no detectable change), 2 (slight change), 3 (moderate change), 4 (remarkable change), and 5 (severe change) for pannus formation (synovial membrane hyperplasia and infiltration of leukocytes) and bone erosion (thinning and destruction of bone trabeculae). Histological parameters were scored by 4 single-blind, independent observers (N. Adán, M.G. Ledesma-Colunga, S. Thebault, and C. Clapp).

In situ apoptosis. Seven-μm knee sections were deparaffinized, rehydrated, and permeabilized with 0.1% Triton X-100 and 0.1% sodium citrate for 7 minutes followed by incubation in sodium citrate buffer (10 mM sodium citrate, 0.5% Tween 20, pH 6.0) for 1 minute at 86°C. Apoptosis was detected by the TUNEL method using the In Situ Cell Death Detection Kit (Roche Diagnostics) and by immunohistochemistry using a polyclonal antibody against active caspase-3 (1:25; Millipore) and Alexa Fluor 546 secondary antibody (1:500) as well as by staining the condensed/fragmented DNA with DAPI (1 μg/ml, Sigma-Aldrich). Apoptotic signals were visualized under fluorescence microscopy (Microscope BX60F5, Olympus Optical Co. LTD) and quantified by the image analysis system software Pro-Plus (Media Cybernetics Inc.).

qRT-PCR. Frozen whole ankle joints were pulverized in liquid nitrogen using a mortar and pestle. Total RNA was isolated using TRIzol reagent (Invitrogen) and reverse transcribed using the High-Capacity cDNA Reverse

Transcription Kit (Applied Biosystems). PCR products were detected and quantified with Maxima SYBR Green qPCR Master Mix (Thermo Scientific) in a 10 μl final reaction volume containing template and 0.5 μM of each of the primer pairs for *Casp3*, forward 5′-GAAAGCCGAAACTCTTCATCA-3′, reverse 5′-ATAGTAACCGGGTGCGGTAT-3′; *Bax*, forward 5′-ACTGGACAACAACATGGTGC-3′, reverse 5′-ATCAGCTCGGGCACTTTAGT-3′; *p53*, forward 5′-AGAGACCCAGCAACTACCAACA-3′, reverse 5′-CTCAGACTGACAGCCTCTGCAT-3′; *Ifng*, forward 5′-AGCACAAAGCTGTCAATGAA-3′, reverse 5′-TTCTTCTTATTGGGCACACTC-3′; *Il6*, forward 5′-TCCAACTCATCTTGAAAGCA-3′, reverse 5′-TTCATATTGCCAGTTCTTCG-3′; *Tnfa*, forward 5′-GGGCTTGTCACTCGAGTTTT-3′, reverse 5′-TGCCTCAGCCTCTTCTCATT-3′; *iNos*, forward 5′-TTTTAGAGACGCTTCTGAGG-3′, reverse 5′-GTCCTTTTCCTCTTTCAGGT-3′; *Il1b*, forward 5′-AAAAGCGGTTTGTCTTCAAC-3′, reverse 5′-GGAATAGTGCAGCCATCTTT-3′; and *Ubc*, forward 5′-CTGACAGGGTGCGGCCATCTT-3′, reverse 5′-ACTGCAGCCAACACCGCTGAC-3′. Amplification performed in the CFX96 real-time PCR detection system (Bio-Rad) included a denaturation step of 10 minutes at 95°C, followed by 40 cycles of amplification (10 seconds at 95°C, 30 seconds at the primer pair–specific annealing temperature, and 30 seconds at 72°C). The PCR data were analyzed by the $2^{-\Delta\Delta CT}$ method, and cycle thresholds normalized to the housekeeping gene *Ubc* were used to calculate the mRNA levels of interest.

Serum PRL. Rat PRL was measured in serum by conventional radioimmunoassay, and infused ovine PRL was measured by the Nb2 cell bioassay, a standard procedure based on the proliferative response of the Nb2 lymphoma cells to PRL, carried out as described previously (80).

Statistics. All data were replicated in 3 or more independent experiments. The statistical analyses were performed using the Sigma Stat 7.0 (Sigma Stat 7.0, Systat Software Inc.) and the GraphPad Prism (GraphPad Software Inc.) software. Data distribution and equality of variances were determined by D'Agostino-Pearson omnibus and Levene's tests. In case of data with normal distribution and/or equal variances, statistical differences between 2 and more than 3 groups were determined by 2-tailed Student's *t* test and 1-way ANOVA followed by Bonferroni's post-hoc comparison test, respectively. In case of data with nonparametric distribution, statistical differences between 2 and more than 3 groups were determined by Mann Whitney's and Kruskal-Wallis followed by Dunn's post-hoc comparison tests, respectively. The threshold for significance was set at $P < 0.05$.

Study approval. All experiments were approved by the Bioethics Committee of the Institute of Neurobiology of the National University of Mexico and comply with the US National Research Council's Guide for the Care and Use of Laboratory Animals (Eighth Edition, National Academy Press, Washington, DC, USA).

Acknowledgments

The authors thank Gabriel Nava, Martín García, Daniel Mondragón, and Antonio Prado for excellent technical assistance as well as Dorothy D. Pless for critically editing the manuscript. N. Adán, J. Guzmán-Morales, S.I. Perales-Canales, and M.G. Ledesma-Colunga were supported by fellowships from the Council of Science and Technology of Mexico and the PhD Program in Biomedical Sciences of the National University of Mexico (UNAM). The study was supported by UNAM grants IN200509 and IN200312 to C. Clapp.

Received for publication February 21, 2013, and accepted in revised form June 6, 2013.

Address correspondence to: Carmen Clapp, Instituto de Neurobiología, Universidad Nacional Autónoma de México (UNAM), Campus UNAM-Juriquilla, 76230 Querétaro, Querétaro, México. Phone: 52.442.238.1028; Fax: 52.442.238.1005; E-mail: clapp@unam.mx.

1. McInnes IB, Schett G. Cytokines in the pathogenesis of rheumatoid arthritis. *Nat Rev Immunol*. 2007; 7(6):429–442.
2. Schuerwegh AJ, et al. Influence of pro-inflammatory (IL-1 alpha, IL-6, TNF-alpha, IFN-gamma) and anti-inflammatory (IL-4) cytokines on chondrocyte function. *Osteoarthritis Cartilage*. 2003;11(9):681–687.
3. Goggs R, et al. Apoptosis and the loss of chondrocyte survival signals contribute to articular cartilage degradation in osteoarthritis. *Vet J*. 2003; 166(2):140–158.
4. Christodoulou C, Choy EH. Joint inflammation and cytokine inhibition in rheumatoid arthritis. *Clin Exp Med*. 2006;6(1):13–19.
5. Keffer J, et al. Transgenic mice expressing human tumour necrosis factor: a predictive genetic model of arthritis. *EMBO J*. 1991;10(13):4025–4031.
6. Polzer K, Schett G, Zwerina J. The lonely death: chondrocyte apoptosis in TNF-induced arthritis. *Autoimmunity*. 2007;40(4):333–336.
7. Kim HA, Song YW. Apoptotic chondrocyte death in rheumatoid arthritis. *Arthritis Rheum*. 1999; 42(7):1528–1537.
8. Yatsugi N, et al. Apoptosis of articular chondrocytes in rheumatoid arthritis and osteoarthritis: correlation of apoptosis with degree of cartilage destruction and expression of apoptosis-related proteins of p53 and c-myc. *J Orthop Sci*. 2000;5(2):150–156.
9. Lotz M. Cytokines in cartilage injury and repair. *Clin Orthop Relat Res*. 2001;(391 suppl):S108–S115.
10. Lo MY, Kim HT. Chondrocyte apoptosis induced by collagen degradation: inhibition by caspase inhibitors and IGF-1. *J Orthop Res*. 2004;22(1):140–144.
11. Andreas K, et al. Key regulatory molecules of cartilage destruction in rheumatoid arthritis: an in vitro study. *Arthritis Res Ther*. 2008;10(1):R9.
12. Macotela Y, et al. Matrix metalloproteases from chondrocytes generate an antiangiogenic 16 kDa prolactin. *J Cell Sci*. 2006;119(pt 9):1790–1800.
13. Zermeno C, et al. Prolactin inhibits the apoptosis of chondrocytes induced by serum starvation. *J Endocrinol*. 2006;189(2):R1–R8.
14. Ogueta S, et al. Prolactin is a component of the human synovial liquid and modulates the growth and chondrogenic differentiation of bone marrow-derived mesenchymal stem cells. *Mol Cell Endocrinol*. 2002;190(1–2):51–63.
15. Rovensky J, et al. Hormone concentrations in synovial fluid of patients with rheumatoid arthritis. *Clin Exp Rheumatol*. 2005;23(3):292–296.
16. Nagafuchi H, et al. Prolactin locally produced by synovium infiltrating T lymphocytes induces excessive synovial cell functions in patients with rheumatoid arthritis. *J Rheumatol*. 1999;26(9):1890–1900.
17. Yu-Lee LY. Prolactin modulation of immune and inflammatory responses. *Recent Prog Horm Res*. 2002; 57:435–455.
18. Wu GJ, et al. Nitric oxide from both exogenous and endogenous sources activates mitochondria-dependent events and induces insults to human chondrocytes. *J Cell Biochem*. 2007;101(6):1520–1531.
19. Teixeira CC, et al. Phosphate-induced chondrocyte apoptosis is linked to nitric oxide generation. *Am J Physiol Cell Physiol*. 2001;281(3):C833–C839.
20. DaSilva L, et al. Prolactin recruits STAT1, STAT3 and STAT5 independent of conserved receptor tyrosines TYR402, TYR479, TYR515 and TYR580. *Mol Cell Endocrinol*. 1996;117(2):131–140.
21. Suemoto H, et al. Trps1 regulates proliferation and apoptosis of chondrocytes through Stat3 signaling. *Dev Biol*. 2007;312(2):572–581.
22. Siddiquee K, et al. Selective chemical probe inhibitor of Stat3, identified through structure-based virtual screening, induces antitumor activity. *Proc Natl Acad Sci U S A*. 2007;104(18):7391–7396.
23. Adler RA. The anterior pituitary-grafted rat: a valid model of chronic hyperprolactinemia. *Endocr Rev*. 1986;7(3):302–313.
24. Schuff KG, et al. Lack of prolactin receptor signaling in mice results in lactotroph proliferation and prolactinomas by dopamine-dependent and -independent mechanisms. *J Clin Invest*. 2002; 110(7):973–981.
25. Kapur S, et al. Relationship between dopamine D(2) occupancy, clinical response, and side effects: a double-blind PET study of first-episode schizophrenia. *Am J Psychiatry*. 2000;157(4):514–520.
26. Cai X, et al. The comparative study of Sprague-Dawley and Lewis rats in adjuvant-induced arthritis. *Naunyn Schmiedebergs Arch Pharmacol*. 2006; 373(2):140–147.
27. Neidhart M, Fluckiger EW. Hyperprolactinaemia in hypophysectomized or intact male rats and the development of adjuvant arthritis. *Immunology*. 1992;77(3):449–455.
28. Grimaldi MG. Long-term low dose haloperidol treatment in rheumatoid patients: effects on serum sulphydryl levels, technetium index, ESR, and clinical response. *Br J Clin Pharmacol*. 1981;12(4):579–581.
29. Moots RJ, et al. Old drug, new tricks: haloperidol inhibits secretion of proinflammatory cytokines. *Ann Rheum Dis*. 1999;58(9):585–587.
30. Aigner T, et al. Osteoarthritis: pathobiology-targets and ways for therapeutic intervention. *Adv Drug Deliv Rev*. 2006;58(2):128–149.
31. Adams CS, Horton WE Jr. Chondrocyte apoptosis increases with age in the articular cartilage of adult animals. *Anat Rec*. 1998;250(4):418–425.
32. Heraud F, Heraud A, Harmand MF. Apoptosis in normal and osteoarthritic human articular cartilage. *Ann Rheum Dis*. 2000;59(12):959–965.

33. Cho TJ, et al. Tumor necrosis factor alpha activation of the apoptotic cascade in murine articular chondrocytes is associated with the induction of metalloproteinases and specific pro-resorptive factors. *Arthritis Rheum*. 2003;48(10):2845–2854.
34. Westacott CI, et al. Synovial fluid concentration of five different cytokines in rheumatic diseases. *Ann Rheum Dis*. 1990;49(9):676–681.
35. Schlaak JF, et al. Different cytokine profiles in the synovial fluid of patients with osteoarthritis, rheumatoid arthritis and seronegative spondylarthropathies. *Clin Exp Rheumatol*. 1996;14(2):155–162.
36. Rohner E, et al. Inflammatory synovial fluid microenvironment drives primary human chondrocytes to actively take part in inflammatory joint diseases. *Immunol Res*. 2012;52(3):169–175.
37. Ben-Jonathan N, LaPensee CR, LaPensee EW. What can we learn from rodents about prolactin in humans? *Endocr Rev*. 2008;29(1):1–41.
38. Corbacho AM, et al. Cytokine induction of prolactin receptors mediates prolactin inhibition of nitric oxide synthesis in pulmonary fibroblasts. *FEBS Lett*. 2003;544(1–3):171–175.
39. Hunter S, Koch BL, Anderson SM. Phosphorylation of cbl after stimulation of Nb2 cells with prolactin and its association with phosphatidylinositol 3-kinase. *Mol Endocrinol*. 1997;11(9):1213–1222.
40. al-Sakkaf KA, Dobson PR, Brown BL. Prolactin induced tyrosine phosphorylation of p59fyn may mediate phosphatidylinositol 3-kinase activation in Nb2 cells. *J Mol Endocrinol*. 1997;19(3):347–350.
41. Bailey JP, et al. Prolactin and transforming growth factor-beta signaling exert opposing effects on mammary gland morphogenesis, involution, and the Akt-forkhead pathway. *Mol Endocrinol*. 2004; 18(5):1171–1184.
42. Tessier C, et al. PRL antiapoptotic effect in the rat decidua involves the PI3K/protein kinase B-mediated inhibition of caspase-3 activity. *Endocrinology*. 2001;142(9):4086–4094.
43. Price J, et al. Akt-1 mediates survival of chondrocytes from endoplasmic reticulum-induced stress. *J Cell Physiol*. 2010;222(3):502–508.
44. Chen Q, et al. Increased apoptosis in human knee osteoarthritis cartilage related to the expression of protein kinase B and protein kinase Cα in chondrocytes. *Folia Histochem Cytobiol*. 2012;50(1):137–143.
45. van Beuningen HM, Arntz OJ, van den Berg WB. In vivo effects of interleukin-1 on articular cartilage. Prolongation of proteoglycan metabolic disturbances in old mice. *Arthritis Rheum*. 1991;34(5):606–615.
46. Hauselmann HJ, et al. The superficial layer of human articular cartilage is more susceptible to interleukin-1-induced damage than the deeper layers. *Arthritis Rheum*. 1996;39(3):478–488.
47. Amin AR, Abramson SB. The role of nitric oxide in articular cartilage breakdown in osteoarthritis. *Curr Opin Rheumatol*. 1998;10(3):263–268.
48. Hashimoto S, et al. Linkage of chondrocyte apoptosis and cartilage degradation in human osteoarthritis. *Arthritis Rheum*. 1998;41(9):1632–1638.
49. Leiderman S, et al. Prolactin and IgG-prolactin complex levels in patients with rheumatic arthritis. *Ann N Y Acad Sci*. 2002;966:252–257.
50. Clement-Lacroix P, et al. Osteoblasts are a new target for prolactin: analysis of bone formation in prolactin receptor knockout mice. *Endocrinology*. 1999; 140(1):96–105.
51. Bendele A. Animal models of rheumatoid arthritis. *J Musculoskelet Neuronal Interact*. 2001;1(4):377–385.
52. Spears R, et al. Tumour necrosis factor-alpha and apoptosis in the rat temporomandibular joint. *Arch Oral Biol*. 2003;48(12):825–834.
53. Gonzalez C, et al. Inflammation, synovial angiogenesis and chondroid apoptosis in the evolution of type II collagen-induced arthritis. *Eur Cytokine Netw*. 2007;18(3):127–135.
54. Song C, et al. Immunosuppressive effects of clozapine and haloperidol: enhanced production of the interleukin-1 receptor antagonist. *Schizophr Res*. 2000; 42(2):157–164.
55. Resman-Targoff BH, Cicero MP. Aggressive treatment of early rheumatoid arthritis: recognizing the window of opportunity and treating to target goals. *Am J Manag Care*. 2010;16(9 suppl):S249–S258.
56. Whitacre CC, Reingold SC, O'Looney PA. A gender gap in autoimmunity. *Science*. 1999; 283(5406):1277–1278.
57. Neidhart M, Gay RE, Gay S. Prolactin and prolactin-like polypeptides in rheumatoid arthritis. *Biomed Pharmacother*. 1999;53(5–6):218–222.
58. Orbach H, Shoenfeld Y. Hyperprolactinemia and autoimmune diseases. *Autoimmun Rev*. 2007; 6(8):537–542.
59. Jara LJ, et al. Prolactin and autoimmunity. *Clin Rev Allergy Immunol*. 2011;40(1):50–59.
60. Shelly S, Boaz M, Orbach H. Prolactin and autoimmunity. *Autoimmun Rev*. 2012;11(6–7):A465–A470.
61. Zhornitsky S, et al. Prolactin in multiple sclerosis. *Mult Scler*. 2013;19(1):15–23.
62. Chuang E, Molitch ME. Prolactin and autoimmune diseases in humans. *Acta Biomed*. 2007; 78(suppl 1):255–261.
63. Corbacho AM, et al. Human umbilical vein endothelial cells express multiple prolactin isoforms. *J Endocrinol*. 2000;166(1):53–62.
64. Jacobi AM, et al. Prolactin enhances the in vitro production of IgG in peripheral blood mononuclear cells from patients with systemic lupus erythematosus but not from healthy controls. *Ann Rheum Dis*. 2001;60(3):242–247.
65. Matera L, et al. Modulatory effect of prolactin on the resting and mitogen-induced activity of T, B, and NK lymphocytes. *Brain Behav Immun*. 1992; 6(4):409–417.
66. Gerli R, et al. Reduced number of natural killer cells in patients with pathological hyperprolactinemia. *Clin Exp Immunol*. 1986;64(2):399–406.
67. Vidaller A, et al. Hyperprolactinemia inhibits natural killer (NK) cell function in vivo and its bromocriptine treatment not only corrects it but makes it more efficient. *J Clin Immunol*. 1992;12(3):210–215.
68. Vukusic S, et al. Pregnancy and multiple sclerosis (the PRIMS study): clinical predictors of postpartum relapse. *Brain*. 2004;127(pt 6):1353–1360.
69. Mok CC, Wong RW, Lau CS. Exacerbation of systemic lupus erythematosus by breast feeding. *Lupus*. 1998;7(8):569–570.
70. McMurray RW, et al. Effects of parturition, suckling and pseudopregnancy on variables of disease activity in the B/W mouse model of systemic lupus erythematosus. *J Rheumatol*. 1993;20(7):1143–1151.
71. Barrett JH, et al. Breast-feeding and postpartum relapse in women with rheumatoid and inflammatory arthritis. *Arthritis Rheum*. 2000;43(5):1010–1015.
72. Langer-Gould A, et al. Exclusive breastfeeding and the risk of postpartum relapses in women with multiple sclerosis. *Arch Neurol*. 2009;66(8):958–963.
73. McMurray RW. Bromocriptine in rheumatic and autoimmune diseases. *Semin Arthritis Rheum*. 2001; 31(1):21–32.
74. Hardy RS, Raza K, Cooper MS. Endogenous glucocorticoids in inflammation: contributions of systemic and local responses. *Swiss Med Wkly*. 2012; 142:w13650.
75. Horseman ND, et al. Defective mammopoiesis, but normal hematopoiesis, in mice with a targeted disruption of the prolactin gene. *EMBO J*. 1997; 16(23):6926–6935.
76. Bouchard B, et al. Immune system development and function in prolactin receptor-deficient mice. *J Immunol*. 1999;163(2):576–582.
77. Gala RR. The physiology and mechanisms of the stress-induced changes in prolactin secretion in the rat. *Life Sci*. 1990;46(20):1407–1420.
78. Dorshkind K, Horseman ND. The roles of prolactin, growth hormone, insulin-like growth factor-I, and thyroid hormones in lymphocyte development and function: insights from genetic models of hormone and hormone receptor deficiency. *Endocr Rev*. 2000;21(3):292–312.
79. Hamada T, et al. Suppression of adjuvant arthritis of rats by a novel matrix metalloproteinase-inhibitor. *Br J Pharmacol*. 2000;131(8):1513–1520.
80. Tanaka T, et al. A new sensitive and specific bioassay for lactogenic hormones: measurement of prolactin and growth hormone in human serum. *J Clin Endocrinol Metab*. 1980;51(5):1058–1063.

Prolactin promotes normal liver growth, survival, and regeneration in rodents: effects on hepatic IL-6, suppressor of cytokine signaling-3, and angiogenesis

Bibiana Moreno-Carranza, Maite Goya-Arce, Claudia Vega, Norma Adán, Jakob Triebel, Fernando López-Barrera, Andrés Quintanar-Stéphano, Nadine Binart, Gonzalo Martínez de la Escalera and Carmen Clapp

Am J Physiol Regul Integr Comp Physiol 305:R720-R726, 2013. First published 15 August 2013; doi:10.1152/ajpregu.00282.2013

American Journal of Physiology - Regulatory, Integrative and Comparative Physiology publishes original investigations that illuminate normal or abnormal regulation and integration of physiological mechanisms at all levels of biological organization, ranging from molecules to humans, including clinical investigations. It is published 12 times a year (monthly) by the American Physiological Society, 9650 Rockville Pike, Bethesda MD 20814-3991. ISSN: 0363-6119, ESSN: 1522-1490. Visit our website at http://www.the-aps.org/.

Am J Physiol Regul Integr Comp Physiol 305: R720–R726, 2013.
First published August 15, 2013; doi:10.1152/ajpregu.00282.2013.

Prolactin promotes normal liver growth, survival, and regeneration in rodents: effects on hepatic IL-6, suppressor of cytokine signaling-3, and angiogenesis

Bibiana Moreno-Carranza,[1] Maite Goya-Arce,[1] Claudia Vega,[1] Norma Adán,[1] Jakob Triebel,[1] Fernando López-Barrera,[1] Andrés Quintanar-Stéphano,[2] Nadine Binart,[3] Gonzalo Martínez de la Escalera,[1] and Carmen Clapp[1]

[1]*Instituto de Neurobiología, Universidad Nacional Autónoma de México, Querétaro, México;* [2]*Departamento de Fisiología y Farmacología, Centro de Ciencias Básicas, Universidad Autónoma de Aguascalientes, Aguascalientes, México; and* [3]*Institut National de la Santé et de la Recherche Médicale, U693, Université Paris-Sud, Le Kremlin-Bicêtre, France*

Submitted 7 June 2013; accepted in final form 12 August 2013

Moreno-Carranza B, Goya-Arce M, Vega C, Adán N, Triebel J, López-Barrera F, Quintanar-Stéphano A, Binart N, Martínez de la Escalera G, Clapp C. Prolactin promotes normal liver growth, survival, and regeneration in rodents: effects on hepatic IL-6, suppressor of cytokine signaling-3, and angiogenesis. *Am J Physiol Regul Integr Comp Physiol* 305: R720–R726, 2013. First published August 15, 2013; doi:10.1152/ajpregu.00282.2013.—Prolactin (PRL) is a potent liver mitogen and proangiogenic hormone. Here, we used hyperprolactinemic rats and PRL receptor-null mice ($PRLR^{-/-}$) to study the effect of PRL on liver growth and angiogenesis before and after partial hepatectomy (PH). Liver-to-body weight ratio (LBW), hepatocyte and sinusoidal endothelial cell (SEC) proliferation, and hepatic expression of VEGF were measured before and after PH in hyperprolactinemic rats, generated by placing two anterior pituitary glands (AP) under the kidney capsule. Also, LBW and hepatic expression of IL-6, as well as suppressor of cytokine signaling-3 (SOCS-3), were evaluated in wild-type and $PRLR^{-/-}$ mice before and after PH. Hyperprolactinemia increased the LBW, the proliferation of hepatocytes and SECs, and VEGF hepatic expression. Also, liver regeneration was increased in AP-grafted rats and was accompanied by elevated hepatocyte and SEC proliferation, and VEGF expression compared with nongrafted controls. Lowering circulating PRL levels with CB-154, an inhibitor of AP PRL secretion, prevented AP-induced stimulation of liver growth. Relative to wild-type animals, $PRLR^{-/-}$ mice had smaller livers, and soon after PH, they displayed an approximately twofold increased mortality and elevated and reduced hepatic IL-6 and SOCS-3 expression, respectively. However, liver regeneration was improved in surviving $PRLR^{-/-}$ mice. PRL stimulates normal liver growth, promotes survival, and regulates liver regeneration by mechanisms that may include hepatic downregulation of IL-6 and upregulation of SOCS-3, increased hepatocyte proliferation, and angiogenesis. PRL contributes to physiological liver growth and has potential clinical utility for ensuring survival and regulating liver mass in diseases, injuries, or surgery of the liver.

liver growth and regeneration; prolactin; vascular endothelial growth factor; interleukin-6; suppressor of cytokine signaling-3; liver angiogenesis

HEPATOCYTES ARE LONG-LIVED and rarely divide under normal conditions except soon after birth and in association with female reproductive events. In rodents, hepatocyte replication peaks during the first 2 wk of age (18), doubles during pregnancy (15), and continues to increase throughout lactation (27). Pathological conditions such as toxic injury and infection trigger hepatocyte proliferation to replace damaged tissue (17). Numerous growth factors and cytokines stimulate liver growth, and cross-circulation experiments (32) and liver tissue transplants into extrahepatic sites (25) indicate that triggering agents are present in the circulation. Prolactin (PRL), the hormone fundamental for lactation, may contribute to these triggering mechanisms.

PRL increases in the circulation under conditions of physiological and pathological liver growth. Its levels are high in neonates (21), in pregnant and lactating females (3), in patients with liver cirrhosis (33), and in rodents after partial hepatectomy (PH) (9). Liver is the organ that expresses the highest levels of PRL receptors (34), and injection of PRL increases hepatic DNA synthesis, the liver-to-body weight ratio (LBW) (10), and activity of transcription factors involved in hepatic cell proliferation [activator protein-1 (AP-1), Jun, STAT-3] (36). PRL triggers mitogenic signaling pathways in isolated hepatocytes (4) and may also promote liver growth by inducing angiogenesis. PRL stimulates endothelial cell proliferation in various organs through direct stimulation of endothelial cells (13) but also indirectly by inducing the synthesis of VEGF and fibroblast growth factor-2 in nonendothelial cells (13), and it promotes VEGF expression in regenerating livers (36).

Here, we tested the hypothesis that PRL contributes to physiological liver growth and regeneration using hyperprolactinemic rats and PRL receptor-null ($PRLR^{-/-}$) mice that were either intact or subjected to PH. The results support our hypothesis and identify regulation of IL-6, suppressor of cytokine signaling-3 (SOCS-3), sinusoidal endothelial cell (SEC) proliferation, and VEGF expression as mechanisms mediating the actions of PRL.

MATERIALS AND METHODS

Animal experimentation. Male Wistar rats (200–250 g) and $PRLR^{-/-}$ and wild-type ($PRLR^{+/+}$) mice (16-wk-old males and females of *129SvJ* background) were maintained and treated according to local institutional guidelines and in compliance with the *Guide for the Care and Use of Laboratory Animals* published by the U.S. National Institutes of Health. The Bioethics Committee of the Institute of Neurobiology of the National University of Mexico approved all animal experiments. All surgical procedures were performed between 8:00 AM and 12:00 PM. To avoid stress-induced PRL release, animals were handled daily for 7 days before death. Seventy or 60% PH was carried out in rats and mice, respectively, according to the method of Higgins and Anderson (22). Animals were weighed before PH and at the time of death when resected liver and regenerating liver remnants were weighed, formalin-fixed, or frozen; blood was then collected for subsequent analysis. Fifteen days before PH, hyperprolactinemia was induced in rats by implanting two anterior pituitary

Address for reprint requests and other correspondence: C. Clapp, Instituto de Neurobiología, Universidad Nacional Autónoma de México (UNAM), Campus UNAM-Juriquilla, 76230 Querétaro, México (e-mail: clapp@unam.mx).

glands (AP) under the kidney capsule, as previously described (2). Control rats were subjected to similar surgery without implantation. Groups of AP-implanted and control rats received a daily, intraperitoneal injection of saline or CB-154 (5 mg/kg body wt) 4 or 7 days before death.

Liver-to-body weight ratio. Liver growth was assessed by the liver-to-body weight ratio (LBW), calculated as 100 times the weight of the organ divided by the body weight of the animal at death. The rate of recovery of liver mass after PH was evaluated by comparing the LBW of the remnant liver immediately after (*day 0*) and at *days 2*, *4*, and *6* after surgery.

Hepatocyte and SEC proliferation. Liver samples were fixed in 10% formalin, dehydrated in a graded alcohol series, and embedded in paraffin. Eight-micrometer paraffin sections were incubated with a 1:500 dilution of anti-PCNA antibody (clone PC10; DakoCytomation, Freiberg, Germany) overnight at 4°C. Immunoreactive cells were detected using the avidin-biotin-peroxidase kit (Vectastain ABC kit; Vector Laboratories, Burlingame, CA). The slides were cover-slipped with Permount, scanned, and analyzed using the ScanScope Digital Scanner (Aperio Technologies, Vista, CA) and Pro-Plus software (Media Cybernetics, Silver Spring, MD). Cell proliferation was evaluated by quantifying the number of PCNA-positive nuclei in hepatocytes or SEC per square millimeter The spindle-shaped sinusoid-lining cells in the open sinusoids were considered to be SEC. Three areas per section and three different sections were evaluated per rat.

Serum PRL. Serum PRL was measured in rats by RIA using standard procedures and reagents provided by the National Hormone and Pituitary Program and by Dr. A. F. Parlow (Harbor-University of California, Los Angeles Medical Center, Los Angeles, CA).

Real-time quantitative RT-PCR. Total RNA was extracted from liver tissue using TRIzol reagent (Invitrogen, Carlsbad, CA), cDNA was synthesized using the high-capacity cDNA reverse transcription kit (Applied Biosystems, Foster City, CA), and real-time quantitative reverse-transcriptase PCR was performed using the Maxima SYBR Green/ROX qPCR Master Mix (Fermentas, Hanover, MD) with a Bio-Rad CFX96 PCR detection system (Bio-Rad Laboratories, Hercules, CA). The sequences of primers used were as follows: *VEGF*: 5′-TGCCAAGTGGTCCCAG-3′ (forward) and 5′-GTGAGGTTTGATCCGC-3′ (reverse); *IL-6*: 5′-GAGGATACCACTCCCAACAGACC-3′ (forward) and 5′-AAGTGCATCATCGTTGTTCATACA-3′ (reverse); *SOCS-3*: 5′-CCCGCGGGCACCTTTCTTAT-3′ (forward) and 5′-CACTGGATGCGTAGGTTCTTGGTC-3′ (reverse); and *ppia* 5′-GGCGGCAGGTCCATCTACG-3′ (forward) and 5′-CTTGCCATCCAGCCATTCAGTC-3′ (reverse). All primers distinguished between genomic and cDNA amplification. Results are expressed as fold induction compared with baseline after normalization to *ppia*.

Serum IL-6. IL-6 serum levels were determined using the BD OptEIA Mouse IL-6 ELISA Set (BD Biosciences Pharmigen, San Diego, CA) following the instructions of the manufacturer.

Statistics. Results are expressed as means ± SE. Differences between two groups at a single time point (Figs. 1 and 2) were evaluated by unpaired Student's *t*-test, whereas comparisons between two and more than two groups at various time points were examined by two-way ANOVA followed by Tukey's post hoc test (Figs. 3 and 4). SigmaStat 7.0 software (Systat Software, San Jose, CA) was used. Survival of $PRLR^{+/+}$ vs. $PRLR^{-/-}$ was analyzed by Cox's *F* test using Statistica software (StatSoft, Tulsa, OK). Differences in means with $P < 0.05$ were considered statistically significant.

RESULTS

PRL promotes growth, hepatocyte and SEC proliferation, and VEGF expression in intact livers. To determine the effect of PRL on normal liver growth, we evaluated the LBW in rats rendered hyperprolactinemic by placing two AP under the kidney capsule for 15 days and in $PRLR^{-/-}$ mice. LBW was elevated in AP-grafted rats, confirmed to be hyperprolactinemic ($P = 0.006$, Fig. 1*A*). Hyperprolactinemia was responsible for the increase in LBW, because the effect was abrogated by lowering PRL levels with CB-154, a dopamine D_2 receptor agonist that inhibits AP PRL release (38) (Fig. 1*A*). Liver growth was then assessed by the immunohistochemical evaluation of PCNA, a marker of cell proliferation (7). PCNA-positive hepatocytes were detectable in the nongrafted rats, and their number was significantly elevated in the AP-implanted animals ($P = 0.01$, Fig. 2, *A* and *B*). PCNA-positive SEC were identified by the immunoreactivity to PCNA located in elongated nuclei of spindle-shaped sinusoid-lining cells, and their number was found to be significantly higher in the AP-grafted animals ($P = 0.04$, Fig. 2, *A* and *C*). Hyperprolactinemia-induced liver angiogenesis was further suggested by the increased hepatic expression of VEGF in AP-implanted vs. nonimplanted rats ($P < 0.01$, Fig. 2*D*). Consistent with the findings, LBW was reduced in $PRLR^{-/-}$ mice relative to wild-type mice ($P < 0.001$, Fig. 1*B*).

Effect of hyperprolactinemia on liver growth and angiogenesis after PH. Liver regeneration over time was then evaluated in hyperprolactinemic rats subjected to PH 15 days after AP implantation. Circulating PRL levels increase during the first 15 min after PH and return to control values thereafter (9). Consistent with this report, no differences in PRL serum concentrations were found in the nongrafted controls at 2, 4, and 6 days after PH (Fig. 3*A*). AP-grafted rats showed a 7- to 12-fold increase in serum PRL levels over nongrafted controls throughout the 6-day period following PH ($P \leq 0.01$, Fig. 3*A*). LBW was higher at *day 0* and continued to be elevated at *days 2*, *4*, and *6* post-PH ($P \leq 0.01$ - 0.04 vs. control, nongrafted rats, Fig. 3*B*). Because hyperprolactinemic rats start out with a higher LBW value prior to PH, recovery of liver mass was evaluated by plotting LBW levels after PH relative to estimated whole LBW values immediately after surgery (*day 0*) (Fig. 3*C*). Two days after PH, hyperprolactinemic animals showed a significantly higher recovery of liver mass that leveled out thereafter, indicating a faster recovery of liver mass in hyperprolactinemic compared with normoprolactinemic rats. To assess the causal relationship with hyperprolactinemia, AP-im-

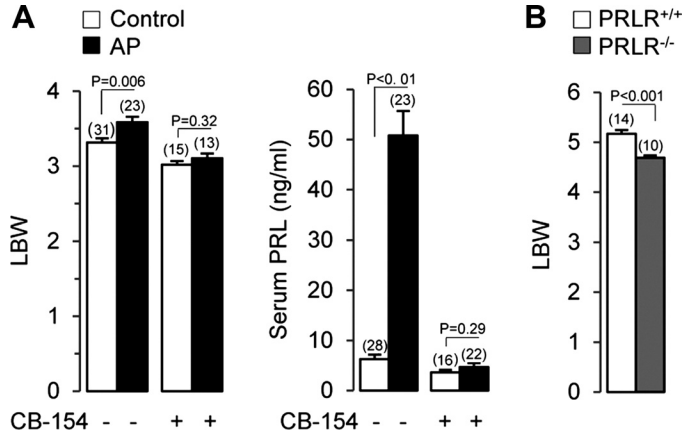

Fig. 1. Prolactin (PRL) promotes growth in intact livers. (*A*) Liver-to-body weight ratio (LBW) and serum PRL levels in rats nontransplanted (control) or transplanted with two anterior pituitary glands under the kidney capsule (AP) and injected or not with the dopamine D_2 receptor antagonist, CB-154. *B*: LBW in wild-type ($PRLR^{+/+}$) and PRL receptor-deficient ($PRLR^{-/-}$) mice. Bars represent means ± SE. Numbers inside parentheses indicate *n* values.

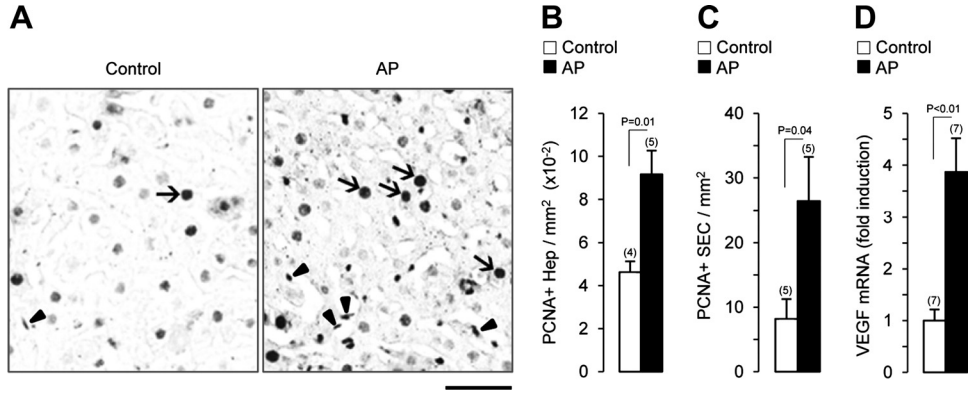

Fig. 2. PRL stimulates the proliferation of hepatocytes (Hep) and sinusoidal endothelial cells (SEC) and the expression of VEGF in intact livers. *A*: representative photographs of hepatocytes and SEC immunostained for PCNA in liver sections from rats nontransplanted (control) or transplanted with two anterior pituitary glands under the kidney capsule (AP). Arrows and arrowheads indicate some PCNA-positive Hep and SEC, respectively. Scale bar = 100 μm. Quantification of hepatocytes (*B*) and SEC (*C*) positive for PCNA/mm^2 of liver tissue in Control and AP rats. *D*: quantitative RT-PCR-based evaluation of VEGF mRNA levels in livers from control and AP-implanted rats. Bars represent means ± SE. Numbers inside parentheses indicate n values.

planted and nonimplanted rats were injected with CB-154 before and after being subjected to PH and killed 2 days after surgery. Treatment with CB-154 reduced circulating PRL to basal levels and blunted the increase in LBW in AP-implanted rats (Fig. 3, *A* and *B*), indicating that hyperprolactinemia is responsible for this increase. Liver growth and angiogenesis were then evaluated in hyperprolactinemic rats by measuring the proliferation of hepatocytes and SEC after PH. Immunohistochemical analysis of PCNA staining in regenerating livers of control rats showed higher numbers of proliferating hepatocytes and SEC that peaked at 2 and 4 days after surgery (Fig. 3, *D–F*). Hepatocyte proliferation was significantly increased on postoperative *days 0*, *2*, and *4* in hyperprolactinemic vs. control rats ($P \leq 0.01–0.04$, Fig. 3*E*). Also, hyperprolactinemic animals showed elevated SEC proliferation on *days 0* and *4* post-PH ($P \leq 0.01$, Fig. 3*F*) and enhanced *VEGF* mRNA levels on *days 0* and *2* after surgery ($P \leq 0.01–0.05$, Fig. 3*G*). These results confirm the mitogenic effect of PRL on hepatocytes and suggest that enhanced angiogenesis contributes to its stimulatory effect on liver regeneration.

PRLR$^{-/-}$ mice show increased mortality, elevated hepatic expression, and serum levels of IL-6, reduced hepatic SOCS-3 expression, and reduced liver growth after PH. Mortality after PH was higher [Cox's *F* test: $F(22,42) = 1.87$, $P = 0.038$] in PRLR$^{-/-}$ mice (21 of 53, 40%) compared with wild-type animals (11 of 47, 23%). PRLR-null mice died between 1 and 2 days post-PH, suggesting that mortality was not related to the surgical procedure. IL-6 is a key cytokine produced and released into the circulation mainly by Kupffer cells during the first hours of liver regeneration that promotes hepatoprotection and mitogenesis (43). However, overproduction of IL-6 can also inhibit hepatocyte growth and cause liver injury (47) and mortality (28). Because PRL reduces LPS-induced IL-6 synthesis in Kupffer cells (49), we tested whether PH-induced production of IL-6 is altered in PRLR$^{-/-}$ mice and may, thus, contribute to enhanced mortality. As expected (44), expression and circulating levels of IL-6 were elevated at 3 and 6 h after PH in wild-type mice ($P < 0.01–0.001$; Fig. 4, *A* and *B*). In PRLR$^{-/-}$ mice, hepatic *IL-6* mRNA levels were 3- to 15-fold higher throughout the first 24 h after PH ($P < 0.01–0.001$, Fig. 4*A*) and were associated with significantly higher levels of IL-6 in the circulation at 3 and 6 h post-PH ($P = 0.02–0.047$, Fig. 4*B*). Because SOCS-3 is a negative regulator of IL-6 synthesis and signaling that is transiently expressed during liver regeneration (11) and is upregulated by PRL in the liver (37), we examined whether deficiency of PRLR affected hepatic SOCS-3 expression in the early phases of PH. PRLR-null mice showed significantly lower levels of *SOCS-3* mRNA at 3 and 6 h after PH compared with wild-type mice ($P < 0.001–0.006$, Fig. 4*C*).

To further evaluate the involvement of PRL in the control of liver regeneration, we compared the LBW values after PH between control and PRLR$^{-/-}$ mice (Fig. 4*D*). Consistent with the reduced LBW found in intact PRLR$^{-/-}$ mice (Fig. 1*B*), LBW was significantly lower immediately after PH (*day 0*) ($P = 0.029$ PRLR$^{+/+}$ vs. PRLR$^{-/-}$, Fig. 4*D*). The LBW continued to be reduced in PRLR$^{-/-}$ mice 2 days after PH ($P = 0.043$ PRLR$^{+/+}$ vs. PRLR$^{-/-}$) but was similar to the LBW of control mice at *days 4* and *6* after PH (Fig. 4*D*). Because PRLR$^{-/-}$ mice start out with a lower LBW prior to PH, recovery of liver mass was evaluated by plotting LBW levels after PH relative to estimated whole LBW values immediately after surgery (*day 0*) (Fig. 4*E*). A similar recovery of liver mass was found between PRLR$^{-/-}$ and PRLR$^{+/+}$ mice 2 days after PH ($P = 0.47$ PRLR$^{+/+}$ vs. PRLR$^{-/-}$, Fig. 4*E*), indicating that the reduction in LBW found in PRLR$^{-/-}$ mice at this time (Fig. 4*D*) is due not to decreased liver regeneration but to the fact that these mice have lower LBW values prior to PH. Moreover, PRLR$^{-/-}$ mice showed a higher liver mass recovery 4 and 6 days after PH ($P < 0.02–0.03$, Fig. 4*E*), indicating that the absence of PRL signaling enhances the final phases of liver regeneration.

DISCUSSION

The central role of endocrine factors in physiological liver growth and hepatic regeneration has been known for decades (6, 25, 27, 32), but the contribution of specific hormones is still unclear. The present study demonstrates that PRL can act both on the normal and regenerating liver to stimulate their growth and angiogenesis. Moreover, we show that PRL promotes animal survival after PH by mechanisms that may involve the

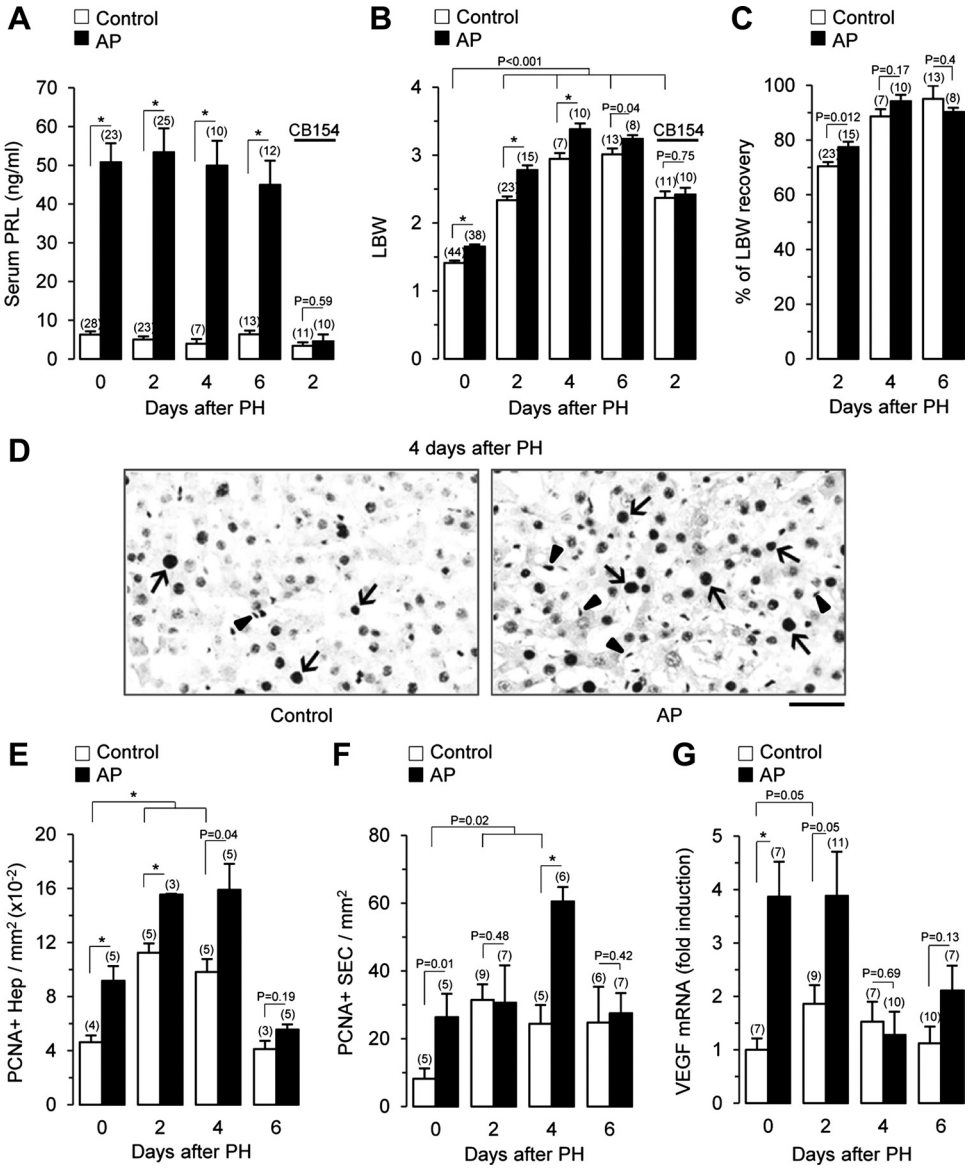

Fig. 3. PRL stimulates liver growth, hepatocyte (Hep), and SEC proliferation, and expression of VEGF after PH. Serum PRL levels (*A*) and LBW (*B*) in rats nontransplanted (control) or transplanted with two anterior pituitary glands under the kidney capsule (AP) immediately (*day 0*), and 2, 4, and 6 days after partial hepatectomy (PH). Some control and AP-transplanted animals were injected with CB-154 and evaluated 2 days after PH. *C*: percentage of recovery of LBW in control and AP rats 2, 4, and 6 days after PH. *D*: representative photographs of Hep and SEC immunostained for PCNA in liver sections from rats nontransplanted (control) or transplanted with two anterior pituitary glands under the kidney capsule (AP) and evaluated 4 days after PH. Arrows and arrowheads indicate some PCNA-positive Hep and SEC, respectively. Scale bar = 100 μm. Quantification of hepatocytes (*E*) and SEC (*F*) positive for PCNA/mm^2 of liver tissue in control and AP rats immediately (*day 0*), and 2, 4, and 6 days after PH. *G*: qRT-PCR-based evaluation of VEGF mRNA levels in livers from control and AP rats on *days 0*, *2*, *4*, and *6* after PH. Bars represent means ± SE. Numbers inside parentheses indicate *n* values. *$P \leq 0.01$.

downregulation and upregulation of hepatic IL-6 and SOCS-3, respectively.

PRL is a versatile hormone that acts on a wide variety of target tissues to regulate reproduction, osmoregulation, energy metabolism, brain function, immune response, growth, and angiogenesis (3, 6, 13). The liver is the organ with the largest number of PRL receptors (34), and PRL regulates liver function and growth, yet these actions are poorly understood. PRL acts on fetal liver to promote the differentiation of red blood progenitor cells (40) and stimulate lipid metabolism (30). It induces adult liver to produce Hageman factor (20) and may contribute to bile secretion by promoting the proliferation of cholangiocytes under normal and diseased conditions (41). PRL was reported to be a mitogen for normal liver nearly 30 years ago, when repeated injections of pharmacological doses of the hormone stimulated hepatic DNA synthesis and the mitotic index, caused hepatomegaly, and promoted the expression of preneoplastic lesions when given after a hepatocarcinogen (10).

Here, we have used mice carrying a homozygous deletion of the *PRLR* gene to investigate the role of PRL in normal liver growth. We found that absence of the PRLR confers reduced liver mass. It is possible that nonspecific effects of PRL during development contribute to this phenotype. Placental lactogens and pituitary PRL lead to metabolic adaptations in the mother, such as increased food intake, β-cell expansion, and insulin

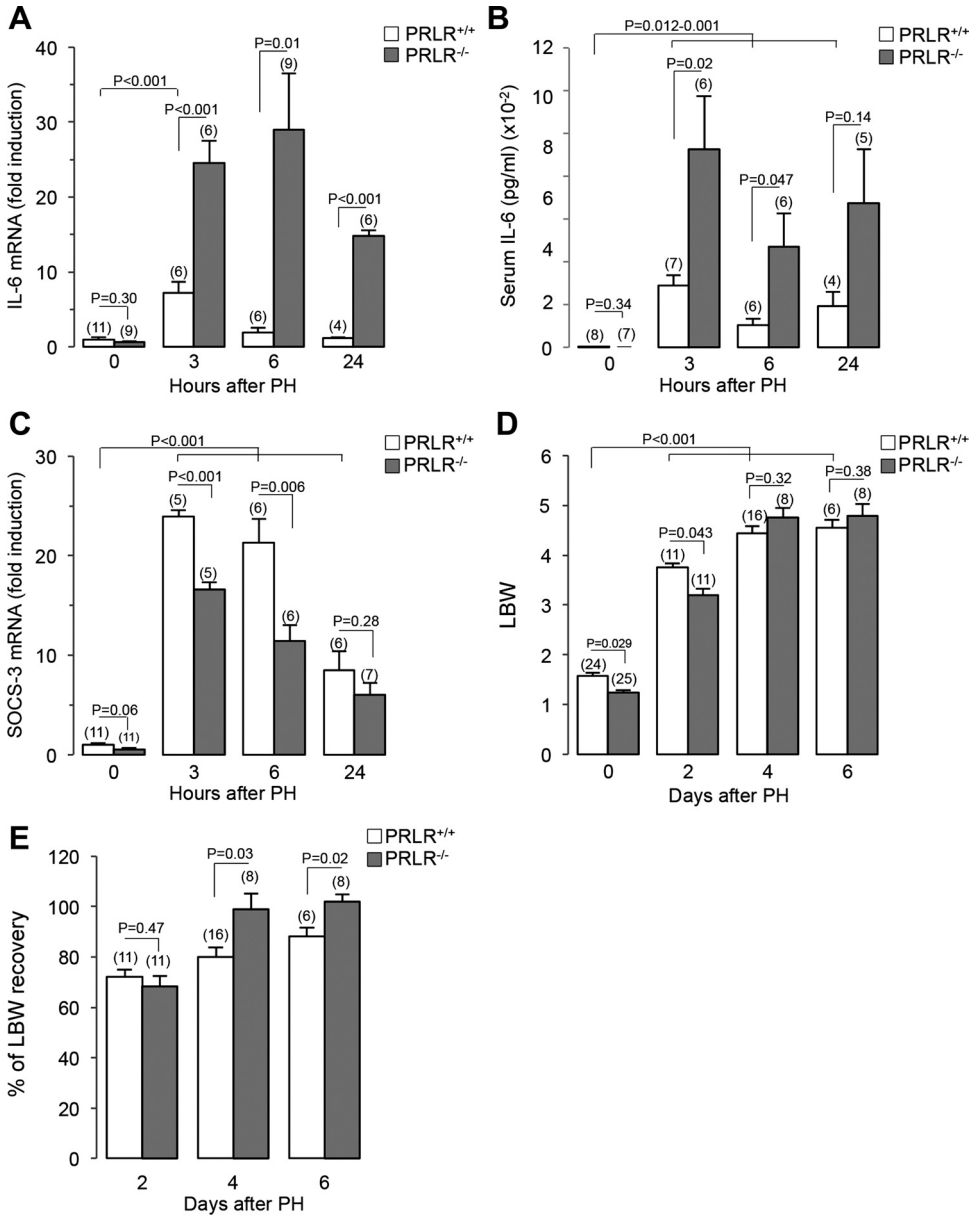

Fig. 4. PRL receptor-deficient ($PRLR^{-/-}$) mice show increased hepatic expression and circulating levels of IL-6, lower hepatic expression of SOCS-3, and reduced liver growth. $PRLR^{-/-}$ and wild-type ($PRLR^{+/+}$) mice were evaluated at 0, 3, 6, and 24 h post-PH for the hepatic expression of IL-6 mRNA (*A*), circulating IL-6 (*B*), hepatic SOCS-3 mRNA (*C*), and LBW (*D*). mRNA was quantified by quantitative RT-PCR. *E*: percentage of recovery of LBW in $PRLR^{+/+}$ and $PRLR^{-/-}$ mice 2, 4, and 6 days after PH. Bars represent means ± SE. Numbers inside parentheses indicate *n* values.

production (35), which may promote fetal and neonatal liver development. However, the facts that fetal liver expresses the PRLR (19) and that PRL stimulates the proliferation of cultured hepatocytes isolated from 20-day-old rats (45) suggest that PRL can signal directly to stimulate liver growth during development and that this action is required to achieve normal liver size. Consistent with this finding, we also showed that inducing persistent hyperprolactinemia, to levels similar to those (50–250 ng/ml) circulating in pregnancy and lactation (3), stimulates liver mass, and that this effect disappears when PRL levels are lowered to basal with CB-154.

Hyperprolactinemia-induced liver growth entailed the enhanced proliferation of hepatocytes. Adult hepatocytes express the PRLR (39), and PRL acts on cultured hepatocytes to stimulate expression of the growth-related genes *Fos, Jun,* and *Src* (4) and to promote proliferation (45). In addition, hyperprolactinemia stimulated SEC proliferation and hepatic VEGF expression, indicating that PRL promotes angiogenesis in intact livers. Because liver growth requires angiogenesis (5, 42) and SEC proliferation strongly depends on VEGF (48), angiogenesis may be an important component of the PRL effect on liver growth. While PRL may be acting through VEGF to stimulate SEC proliferation, a direct effect of PRL on SEC is suggested by the detection of the PRLR on hepatic sinusoidal membranes (39), and by the mitogenic action of PRL on cultured endothelial cells (12).

The facts that deletion of the PRL receptor reduces liver mass and that hyperprolactinemia makes normally quiescent hepatocytes and SEC become proliferating cells, suggest that PRL has an effect on physiological liver growth. Indeed, studies in rats show that LBW is high in nursing pups during lactation (18) when they are being exposed to high levels of PRL in milk (46). Moreover, the PRLR is upregulated in the pregnant liver (23), and hyperprolactinemia associates with liver enlargement during pregnancy and lactation (3, 15, 27).

PRL also influences early events of liver regeneration leading to animal survival and hepatic growth. Circulating PRL levels increase shortly after PH (9), and PRL administration stimulates the binding activity of AP-1, JUN, and STAT-3 within the first 5 to 12 h following PH (36). Activation of these transcriptional factors is part of the signaling cascade elicited by important cytokines, including IL-6, to promote hepatoprotection and mitogenesis (14, 43). Here, we found that the elimination of PRL signaling in $PRLR^{-/-}$ mice results in increased mortality, indicating that PRL stimulates the adaptive response to PH required for animal survival.

IL-6 is a key cytokine mediating homeostatic adaptations involved in animal survival and liver growth after resection. IL-6 deficiency increases mortality and reduces hepatocyte proliferation after PH (14, 43). However, the levels of IL-6 must be carefully adjusted since exposure to higher levels of IL-6 causes liver failure, increased mortality, and reduced regenerative capacity (24, 28, 47). Because, the hepatic expression and serum levels of IL-6 are elevated in $PRLR^{-/-}$ mice throughout the first 24 h of liver regeneration, PRL may signal to adjust IL-6 levels after PH. Although a nonhepatic source of serum IL-6 in $PRLR^{-/-}$ mice cannot be excluded, hepatic Kupffer cells are the primary source of serum IL-6 after liver resection (1), and PRL may, thus, reduce IL-6 levels by upregulating the production of SOCS-3 in the remnant liver. SOCS-3 is an important negative regulator of IL-6 production and signaling, and it acts by preventing the activity of NF-κB (8) and the tyrosine phosphorylation/activation of STAT-3 (11). PRL induces SOCS-3 expression in liver (37), and, thus, deletion of the PRLR reduces mRNA levels of *SOCS-3* during the first 24 h after PH (present study).

Consistent with PRL playing a role in liver regeneration, LBW after PH was increased in hyperprolactinemic rats. These findings agree with previous reports showing that the injection of PRL before PH stimulates the early proliferation of hepatocytes and the activity of factors promoting growth, differentiation, and energy metabolism in the liver (36). Contrary to our observations, an earlier study failed to show enhanced LBW in hyperprolactinemic, AP-grafted rats 2 days after PH (26). The reason for this discrepancy is unclear, but the lack of a significant difference may relate to a small number of animals.

The stimulatory effect of hyperprolactinemia on liver regeneration correlates with enhanced hepatocyte proliferation and angiogenesis. As expected from the proliferation dynamics of hepatic cells following PH (43), the mitogenic effect of PRL occurred earlier in hepatocytes than in SEC, and this effect could be functionally linked to VEGF. VEGF stimulates the proliferation of hepatocytes and SEC during regeneration (5, 29, 42), PRL treatment induces the early expression of VEGF in regenerating livers (36), and VEGF expression is elevated in hyperprolactinemic animals 2 days after PH (present study). However, in contrast to the stimulatory effects of hyperprolactinemia, deletion of the PRLR did not modify liver regeneration 2 days after PH but enhanced it thereafter. The reason for this discrepancy is unclear, but it is possible that compensatory mechanisms able to subserve the stimulatory role of PRL are activated in $PRLR^{-/-}$ mice and result not only in no reduction, but in enhancement of liver regeneration. Because this enhancement occurred late in the regeneration process, it may involve the overactivation of compensatory mechanisms promoting angiogenesis, which would warrant further investigation. Thus, in spite of $PRLR^{-/-}$ mice having a nearly twofold higher mortality after PH relative to wild-type mice, the surviving animals display an improved liver regeneration. Recovery after higher (4-fold) mortality occurs in surviving $IL\text{-}6^{-/-}$ mice (14), illustrating the functional redundancy of the liver regeneration process.

Perspectives and Significance

The present study shows that PRL is required for normal liver growth and that it regulates animal survival and liver regeneration after resection. It provides insights into the action of this hormone during early events leading to body homeostasis, hepatocyte proliferation, and liver angiogenesis. However, further investigation is needed to help establish causative links between these events and hormone action and to evaluate the cellular and molecular mechanisms activated by PRL that result in hepatoprotection, liver growth, function, and regeneration both in the absence and presence of the PRLR. Interestingly, hyperprolactinemia accompanies liver growth under normal and pathological conditions. Liver cirrhosis is commonly associated with elevated levels of PRL and with gynecomastia (16, 33). Because, hyperprolactinemia may help preserve hepatic cell function and growth in the advanced disease, efforts to correct PRL levels may be disadvantageous. Moreover, the use of current medications known to increase prolactinemia (31) constitutes potential therapeutic options in liver diseases, liver injuries, or after liver surgery and warrants further investigation.

ACKNOWLEDGMENTS

The authors thank Gabriel Nava, Martin Garcia, Daniel Mondragon, and Antonio Prado for excellent technical assistance as well as Dorothy D. Pless for critically editing the manuscript.

GRANTS

The present work was supported by the National Council of Science and Technology of Mexico Grant 127496 to C. Clapp.

DISCLOSURES

No conflicts of interest, financial or otherwise, are declared by the authors.

AUTHOR CONTRIBUTIONS

Author contributions: B.M.-C., M.G.-A., C.V., and C.C. conception and design of research; B.M.-C., M.G.-A., C.V., N.A., F.L.-B., and A.Q.-S. performed experiments; B.M.-C., M.G.-A., C.V., N.A., and C.C. analyzed data; B.M.-C., M.G.-A., C.V., J.T., G.M.d.l.E., and C.C. interpreted results of experiments; B.M.-C. and M.G.-A. prepared figures; B.M.-C. and C.C. drafted manuscript; B.M.-C., M.G.-A., J.T., N.B., G.M.d.l.E., and C.C. edited and revised manuscript; B.M.-C., M.G.-A., C.V., N.A., J.T., F.L.-B., A.Q.-S., N.B., G.M.d.l.E., and C.C. approved final version of manuscript.

REFERENCES

1. **Abshagen K, Eipel C, Kalff JC, Menger MD, Vollmar B.** Loss of NF-κB activation in Kupffer cell-depleted mice impairs liver regeneration after partial hepatectomy. *Am J Physiol Gastrointest Liver Physiol* 292: G1570–G1577, 2007.
2. **Adler RA.** The anterior pituitary-grafted rat: a valid model of chronic hyperprolactinemia. *Endocr Rev* 7: 302–313, 1986.
3. **Ben-Jonathan N, LaPensee CR, LaPensee EW.** What can we learn from rodents about prolactin in humans? *Endocr Rev* 29: 1–41, 2008.
4. **Berlanga JJ, Fresno Vara JA, Martin-Perez J, Garcia-Ruiz JP.** Prolactin receptor is associated with c-src kinase in rat liver. *Mol Endocrinol* 9: 1461–1467, 1995.

5. **Bockhorn M, Goralski M, Prokofiev D, Dammann P, Grunewald P, Trippler M, Biglarnia A, Kamler M, Niehues EM, Frilling A, Broelsch CE, Schlaak JF.** VEGF is important for early liver regeneration after partial hepatectomy. *J Surg Res* 138: 291–299, 2007.
6. **Bole-Feysot C, Goffin V, Edery M, Binart N, Kelly PA.** Prolactin (PRL) and its receptor: actions, signal transduction pathways and phenotypes observed in PRL receptor knockout mice. *Endocr Rev* 19: 225–268, 1998.
7. **Bravo R, Frank R, Blundell PA, Macdonald-Bravo H.** Cyclin/PCNA is the auxiliary protein of DNA polymerase-delta. *Nature* 326: 515–517, 1987.
8. **Bruun C, Heding PE, Ronn SG, Frobose H, Rhodes CJ, Mandrup-Poulsen T, Billestrup N.** Suppressor of cytokine signalling-3 inhibits Tumor necrosis factor-α-induced apoptosis and signalling in beta cells. *Mol Cell Endocrinol* 311: 32–38, 2009.
9. **Buckley AR, Crowe PD, Bauman PA, Neumayer LA, Laird HE, 2nd, Russell DH, Putnam CW.** Prolactin-provoked alterations of cytosolic, membrane, and nuclear protein kinase C following partial hepatectomy. *Dig Dis Sci* 36: 1313–1319, 1991.
10. **Buckley AR, Putnam CW, Russell DH.** Prolactin is a tumor promoter in rat liver. *Life Sci* 37: 2569–2575, 1985.
11. **Campbell JS, Prichard L, Schaper F, Schmitz J, Stephenson-Famy A, Rosenfeld ME, Argast GM, Heinrich PC, Fausto N.** Expression of suppressors of cytokine signaling during liver regeneration. *J Clin Invest* 107: 1285–1292, 2001.
12. **Castilla A, Garcia C, Cruz-Soto M, Martinez de la Escalera G, Thebault S, Clapp C.** Prolactin in ovarian follicular fluid stimulates endothelial cell proliferation. *J Vasc Res* 47: 45–53, 2009.
13. **Clapp C, Thebault S, Jeziorski MC, Martinez de la Escalera G.** Peptide hormone regulation of angiogenesis. *Physiol Rev* 89: 1177–1215, 2009.
14. **Cressman DE, Greenbaum LE, DeAngelis RA, Ciliberto G, Furth EE, Poli V, Taub R.** Liver failure and defective hepatocyte regeneration in interleukin-6-deficient mice. *Science* 274: 1379–1383, 1996.
15. **Dai G, Bustamante JJ, Zou Y, Myronovych A, Bao Q, Kumar S, Soares MJ.** Maternal hepatic growth response to pregnancy in the mouse. *Exp Biol Med (Maywood)* 236: 1322–1332, 2011.
16. **Dickson G.** Gynecomastia. *Am Fam Physician* 85: 716–722, 2012.
17. **Fausto N.** Liver regeneration. *J Hepatol* 32: 19–31, 2000.
18. **Fausto N, Laird AD, Webber EM.** Liver regeneration. 2. Role of growth factors and cytokines in hepatic regeneration. *FASEB J* 9: 1527–1536, 1995.
19. **Freemark M, Driscoll P, Maaskant R, Petryk A, Kelly PA.** Ontogenesis of prolactin receptors in the human fetus in early gestation. Implications for tissue differentiation and development. *J Clin Invest* 99: 1107–1117, 1997.
20. **Gordon EM, Douglas JG, Ratnoff OD, Arafah BM.** The influence of estrogen and prolactin on Hageman factor (factor XII) titer in ovariectomized and hypophysectomized rats. *Blood* 66: 602–605, 1985.
21. **Guyda HJ, Friesen HG.** Serum prolactin levels in humans from birth to adult life. *Pediatr Res* 7: 534–540, 1973.
22. **Higgins GM, Anderson RM.** Experimental pathology of the liver. Restoration of the liver of the white rat following partial surgical removal. *Arch Pathol* 12: 186–202, 1931.
23. **Jahn GA, Edery M, Belair L, Kelly PA, Djiane J.** Prolactin receptor gene expression in rat mammary gland and liver during pregnancy and lactation. *Endocrinology* 128: 2976–2984, 1991.
24. **Jin X, Zimmers TA, Perez EA, Pierce RH, Zhang Z, Koniaris LG.** Paradoxical effects of short- and long-term interleukin-6 exposure on liver injury and repair. *Hepatology* 43: 474–484, 2006.
25. **Jirtle RL, Michalopoulos G.** Effects of partial hepatectomy on transplanted hepatocytes. *Cancer Res* 42: 3000–3004, 1982.
26. **Kahn D, Gavaler JS, Makowka L, Chapchap P, Mazzaferro V, Casavilla A, Smith MS, Eagon PK, Starzl TE, Van Thiel DH.** Does hyperprolactinemia affect hepatic regeneration independent of sex steroids? *J Lab Clin Med* 112: 644–651, 1988.
27. **Kennedy GC, Pearce WM, Parrott DM.** Liver growth in the lactating rat. *J Endocrinol* 17: 158–160, 1958.
28. **Kusashio K, Shimizu H, Kimura F, Yoshidome H, Ohtsuka M, Kato A, Yoshitomi H, Furukawa K, Fukada T, Miyazaki M.** Effect of excessive acute-phase response on liver regeneration after partial hepatectomy in rats. *Hepatogastroenterology* 56: 824–828, 2009.
29. **LeCouter J, Moritz DR, Li B, Phillips GL, Liang XH, Gerber HP, Hillan KJ, Ferrara N.** Angiogenesis-independent endothelial protection of liver: role of VEGFR-1. *Science* 299: 890–893, 2003.
30. **Machida T, Taga M, Minaguchi H.** Effect of prolactin (PRL) on lipoprotein lipase (LPL) activity in the rat fetal liver. *Asia Oceania J Obstet Gynaecol* 16: 261–265, 1990.
31. **Molitch ME.** Medication-induced hyperprolactinemia. *Mayo Clin Proc* 80: 1050–1057, 2005.
32. **Moolten FL, Bucher NL.** Regeneration of rat liver: transfer of humoral agent by cross circulation. *Science* 158: 272–274, 1967.
33. **Mukherjee S, Kar M, Dutta S.** Observation on serum prolactin in hepatic cirrhosis. *J Indian Med Assoc* 89: 307–308, 1991.
34. **Nagano M, Kelly PA.** Tissue distribution and regulation of rat prolactin receptor gene expression. Quantitative analysis by polymerase chain reaction. *J Biol Chem* 269: 13337–13345, 1994.
35. **Newbern D, Freemark M.** Placental hormones and the control of maternal metabolism and fetal growth. *Curr Opin Endocrinol Diabetes Obes* 18: 409–416, 2011.
36. **Olazabal IM, Munoz JA, Rodriguez-Navas C, Alvarez L, Delgado-Baeza E, Garcia-Ruiz JP.** Prolactin's role in the early stages of liver regeneration in rats. *J Cell Physiol* 219: 626–633, 2009.
37. **Pezet A, Favre H, Kelly PA, Edery M.** Inhibition and restoration of prolactin signal transduction by suppressors of cytokine signaling. *J Biol Chem* 274: 24497–24502, 1999.
38. **Schuff KG, Hentges ST, Kelly MA, Binart N, Kelly PA, Iuvone PM, Asa SL, Low MJ.** Lack of prolactin receptor signaling in mice results in lactotroph proliferation and prolactinomas by dopamine-dependent and -independent mechanisms. *J Clin Invest* 110: 973–981, 2002.
39. **Smirnova OV, Petraschuk OM, Kelly PA.** Immunocytochemical localization of prolactin receptors in rat liver cells. I. Dependence on sex and sex steroids. *Mol Cell Endocrinol* 105: 77–81, 1994.
40. **Socolovsky M, Fallon AE, Lodish HF.** The prolactin receptor rescues EpoR−/− erythroid progenitors and replaces EpoR in a synergistic interaction with c-kit. *Blood* 92: 1491–1496, 1998.
41. **Taffetani S, Glaser S, Francis H, DeMorrow S, Ueno Y, Alvaro D, Marucci L, Marzioni M, Fava G, Venter J, Vaculin S, Vaculin B, Lam IP, Lee VH, Gaudio E, Carpino G, Benedetti A, Alpini G.** Prolactin stimulates the proliferation of normal female cholangiocytes by differential regulation of Ca^{2+}-dependent PKC isoforms. *BMC Physiol* 7: 6, 2007.
42. **Taniguchi E, Sakisaka S, Matsuo K, Tanikawa K, Sata M.** Expression and role of vascular endothelial growth factor in liver regeneration after partial hepatectomy in rats. *J Histochem Cytochem* 49: 121–130, 2001.
43. **Taub R.** Liver regeneration: from myth to mechanism. *Nat Rev Mol Cell Biol* 5: 836–847, 2004.
44. **Vaquero J, Campbell JS, Haque J, McMahan RS, Riehle KJ, Bauer RL, Fausto N.** Toll-like receptor 4 and myeloid differentiation factor 88 provide mechanistic insights into the cause and effects of interleukin-6 activation in mouse liver regeneration. *Hepatology* 54: 597–608, 2011.
45. **Vergani G, Mayerhofer A, Bartke A.** Acute effects of rat growth hormone (GH), human GH and prolactin on proliferating rat liver cells in vitro: a study of mitotic behaviour and ultrastructural alterations. *Tissue Cell* 26: 457–465, 1994.
46. **Whitworth NS, Grosvenor CE.** Transfer of milk prolactin to the plasma of neonatal rats by intestinal absorption. *J Endocrinol* 79: 191–199, 1978.
47. **Wustefeld T, Rakemann T, Kubicka S, Manns MP, Trautwein C.** Hyperstimulation with interleukin 6 inhibits cell cycle progression after hepatectomy in mice. *Hepatology* 32: 514–522, 2000.
48. **Yamane A, Seetharam L, Yamaguchi S, Gotoh N, Takahashi T, Neufeld G, Shibuya M.** A new communication system between hepatocytes and sinusoidal endothelial cells in liver through vascular endothelial growth factor and Flt tyrosine kinase receptor family (Flt-1 and KDR/Flk-1). *Oncogene* 9: 2683–2690, 1994.
49. **Zhu XH, Zellweger R, Ayala A, Chaudry IH.** Prolactin inhibits the increased cytokine gene expression in Kupffer cells following haemorrhage. *Cytokine* 8: 134–140, 1996.

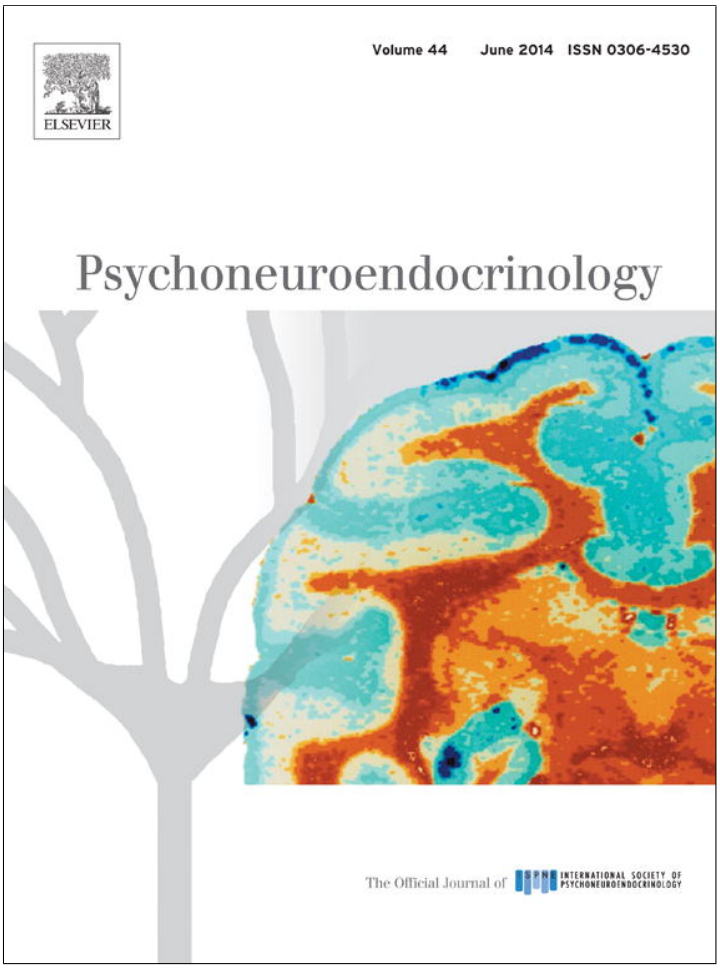

Psychoneuroendocrinology (2014) 44, 123—132

Available online at www.sciencedirect.com

ScienceDirect

journal homepage: www.elsevier.com/locate/psyneuen

Prolactin-derived vasoinhibins increase anxiety- and depression-related behaviors

Miriam Zamorano [a,1], Maria G. Ledesma-Colunga [a,1], Norma Adán [a], Camila Vera-Massieu [a], Maria Lemini [a], Isabel Méndez [a], Bibiana Moreno-Carranza [a], Inga D. Neumann [b], Stéphanie Thebault [a], Gonzalo Martínez de la Escalera [a], Luz Torner [c,2], Carmen Clapp [a,2,*]

[a] *Instituto de Neurobiología, Universidad Nacional Autónoma de México (UNAM), Campus UNAM-Juriquilla, Querétaro, Mexico*
[b] *Department of Behavioral and Molecular Neurobiology, University of Regensburg, Regensburg, Germany*
[c] *Centro de Investigación Biomédica de Michoacán, Instituto Mexicano del Seguro Social (IMSS), Morelia, Mexico*

Received 12 December 2013; received in revised form 12 March 2014; accepted 13 March 2014

KEYWORDS
Anxiety;
Depression;
Stress;
Prolactin;
Vasoinhibins;
16K prolactin;
Hypothalamus;
Proteolytic cleavage

Summary The hormone prolactin (PRL) regulates neuroendocrine and emotional stress responses. It is found in the hypothalamus, where the protein is partially cleaved to vasoinhibins, a family of N-terminal antiangiogenic PRL fragments ranging from 14 to 18 kDa molecular masses, with unknown effects on the stress response. Here, we show that the intracerebroventricular administration of a recombinant vasoinhibin, containing the first 123 amino acids of human PRL that correspond to a 14 kDa PRL, exerts anxiogenic and depressive-like effects detected in the elevated plus-maze, the open field, and the forced swimming tests. To investigate whether stressor exposure affects the generation of vasoinhibins in the hypothalamus, the concentrations of PRL mRNA, PRL, and vasoinhibins were evaluated in hypothalamic extracts of virgin female rats immobilized for 30 min at different time points after stress onset. The hypothalamic levels of PRL mRNA and protein were higher at 60 min but declined at 360 min to levels seen in non-stressed animals. The elevation of hypothalamic PRL did not correlate with the stress-induced increase in circulating PRL levels, nor was it modified by blocking adenohypophyseal PRL secretion with bromocriptine. A vasoinhibin having an electrophoretic migration rate corresponding to 17 kDa was detected in the hypothalamus. Despite the elevation in hypothalamic PRL, the levels of this hypothalamic vasoinhibin were similar in stressed and non-stressed rats. Stress reduced the rate

* Corresponding author at: Instituto de Neurobiología, Universidad Nacional Autónoma de México, Campus UNAM-Juriquilla, 76230 Querétaro, Mexico. Tel.: +52 442 238 1028; fax: +52 442 238 1005.
E-mail address: clapp@unam.mx (C. Clapp).
[1] These authors contributed equally to this work.
[2] Share senior authorship.

http://dx.doi.org/10.1016/j.psyneuen.2014.03.006
0306-4530/

of cleavage of PRL to this vasoinhibin as shown by the incubation of recombinant PRL with hypothalamic extracts from stressed rats. These results suggest that vasoinhibins are potent anxiogenic and depressive factors and that stress increases PRL levels in the hypothalamus partly by reducing its conversion to vasoinhibins. The reciprocal interplay between PRL and vasoinhibins may represent an effective mechanism to regulate anxiety and depression.

1. Introduction

Prolactin (PRL) regulates a wide range of biological effects in and beyond reproduction (Ben-Jonathan et al., 1996). Some of these effects occur in the brain, where PRL promotes maternal and feeding behaviors (Grattan and Kokay, 2008), suppresses fertility (Sonigo et al., 2012), stimulates neurogenesis and neuronal survival (Shingo et al., 2003), regulates neurotransmitter and neuropeptide release (Grattan and Kokay, 2008; Vega et al., 2010), and attenuates stress-induced neuroendocrine and anxiety responses (Torner et al., 2001; Torner and Neumann, 2002).

PRL is often referred to as ''stress hormone'' because a number of physical and emotional forms of stressors stimulate its secretion from the adenohypophysis into the circulation (Reichlin, 1988). The increase in circulating PRL is considered to be an adaptation to ensure competence of the immune system (Dorshkind and Horseman, 2000; Yu-Lee, 2002) and proper physiological and behavioral responses to stress (Torner et al., 2001; Torner and Neumann, 2002). The PRL receptor is expressed in several immune cells, in which this hormone regulates proliferation, survival, and the release of inflammatory mediators (Yu-Lee, 2002). PRL inhibits stress-induced production of immunosuppressive steroids (Cook, 1997) and the stress-induced increase of corticotropin secretion (Torner et al., 2001). Also, PRL reduces anxiety behavior, and blocking PRL receptors in the brain prevents both PRL inhibition of the hypothalamic—pituitary—adrenal (HPA) axis activation and its anxiolytic effect (Torner et al., 2001). These central actions may be mediated by circulating PRL accessing the brain after entering the cerebrospinal fluid via its receptors in the choroid plexus (Walsh et al., 1987; Mangurian et al., 1992). In addition, PRL mRNA is expressed in hypothalamic tissue (Clapp et al., 1994; Ben-Jonathan et al., 1996; Torner et al., 2004; Grattan and Kokay, 2008) and, although its neuronal localization has not been demonstrated, PRL may act as a neuropeptide to regulate stress-related responses.

Adding complexity to PRL actions is its structural polymorphism. In the hypothalamus, PRL is proteolytically cleaved to vasoinhibins (Clapp et al., 1994), a family of N-terminal PRL fragments with molecular masses ranging from 14 to 18 kDa that signal through receptors distinct from PRL receptors (Clapp and Weiner, 1992) to exert effects opposite to those of the full-length hormone on blood vessels. PRL stimulates blood vessel growth (angiogenesis), whereas vasoinhibins inhibit angiogenesis (Clapp et al., 2009). The structural diversity of vasoinhibins derives from the fact that different proteases generate the various fragments by cleaving near or within various sites of the large disulfide loop linking alpha helixes 3 and 4 of the PRL molecule (for reviews see Clapp et al., 2006, 2009). Vasoinhibins not only share blood vessel inhibitory properties but also non-vascular actions. 14 kDa Human and 16 kDa rat vasoinhibins act as proinflammatory cytokines upregulating inducible nitric oxide synthase (iNOS) in pulmonary fibroblasts (Corbacho et al., 2000), whereas PRL functions to attenuate proinflammatory cytokine-induced iNOS expression in these cells (Corbacho et al., 2003). On the other hand, both PRL and vasoinhibins stimulate the release of vasopressin by the hypothalamo-neurohypophyseal system (Mejia et al., 2003).

Since vasoinhibins are found in the hypothalamus and have actions that may or may not differ from those of PRL, here we investigated the hypothesis that vasoinhibins affect anxiety behavior and that their generation is modified under conditions of stress.

2. Methods

2.1. Reagents

A recombinant 14 kDa vasoinhibin containing the first 123 amino acids of the human PRL sequence and a tail of 7 histidines generated as described (Galfione et al., 2003) was used in behavioral tests. Recombinant rat PRL used in cleavage assays and as standard in Western blots was purchased from the National Hormone and Pituitary Program (NHPP) and Dr. A.F. Parlow (Harbor-University of California, Los Angeles Medical Center, Los Angeles, CA). PRL having a cleavage in the large disulfide loop and a 16 kDa vasoinhibin containing the first 145 amino acids of PRL were used as standards in Western blots and were generated by enzymatic proteolysis of rat PRL with a mammary gland extract enriched with cathepsin D, as reported (Clapp, 1987).

2.2. Animals

Virgin, female Wistar rats (230—250 g body weight) were maintained and treated according to local institutional guidelines and in compliance with the *Guide for the Care and Use of Laboratory Animals* published by the U.S. National Institutes of Health. The Bioethics Committee of the Institute of Neurobiology of the National University of Mexico (UNAM) approved all animal experiments. Rats were handled daily for five to seven days before the experiment. All experiments were performed between 0900 h and 1200 h. Behavioral tests were carried out on diestrous day. In non-behavioral studies,

the stage of estrous cycle was determined after completing the respective experiment. Because results of the latter studies showed no difference within the same experimental group, data were compiled and analyzed without regard to the estrous cycle. Rats were anesthetized in a CO_2-saturated chamber and euthanized by decapitation.

2.3. Acute intracerebroventricular administration

A guide cannula was stereotaxically cemented above the right lateral ventricle (Paxinos and Watson, 1986) under 70% ketamine and 30% xylazine anesthesia (1.0 μl/g body weight) injected intraperitoneally. Five days later, an infusion cannula was inserted into the guide cannula of conscious, freely moving rats. After 1 h, an injection delivered vasoinhibin (1.0 μg in 4 μl) or 4 μl of vehicle (25 mM HEPES, 0.01% Triton, 0.1% glycerol, pH 7.4) over a 2-min interval. The infusion system was left in place for two additional min and rats were then subjected to the elevated plus-maze, the open-field, or the forced swim tests.

2.4. Elevated plus-maze (EPM)

The EPM was performed during 5 min as described (Torner et al., 2001). A camera above the EPM apparatus connected to a computer set-up allowed assessment of behavior. An observer blind to the treatment determined the percentage of time spent on the open arms as an indicator of anxiety. The number of closed arm entries was used as an indicator of locomotor activity.

2.5. Open-field test (OF)

The OF was performed as described (Carola et al., 2002) using a square box (90 cm × 90 cm × 40 cm), with a 9-square grid floor (3 × 3 squares, 30 cm/side) and an overhead light illuminating the central square. The number of entries into the central and peripheral squares and the number of fecal boli laid during a 5-min test was assessed on-line via a video camera located above the box and scored by an observer blind to the treatment.

2.6. Forced swim test (FS)

The FS test was videotaped for 10 min to evaluate depressive behavior as reported and defined (Marti and Armario, 1993). An observer blind to treatment scored: (1) time spent struggling; (2) time spent swimming; (3) time spent floating; and (4) latency until first floating.

2.7. Physical restraint procedure

The animals were immobilized for 30 min by placing them into tapered plastic film tubes (DecapiCones, Braintree Scientific, Inc., Braintree, MA) with a front breathing hole. Some rats were euthanized immediately after termination of the stress exposure, and others were returned to their home cage to be killed 60 or 360 min after initiating stress. The control group was killed without prior stress exposure. Other rats were injected intraperitoneally with 5 mg/kg of bromocriptine (Parlodel, Novartis Pharmaceuticals Inc., Basel, Switzerland), the day before and 1 h prior to initiating or not stress. Blood was collected by decapitation and serum was kept at −70 °C until assayed. The hypothalamus was isolated by cutting rostral to the optic chiasm, lateral to either side of the median eminence, and caudal to the mammillary bodies, undercutting at a depth of 2 mm. Each hypothalamus was immediately placed on dry ice and stored at −70 °C for no more than two days, after which the frozen tissue was pulverized in liquid nitrogen and divided frozen into two aliquots, one for quantitative RT-PCR (qRT-PCR) and the other for Western blot analysis. qRT-PCR was carried out immediately, whereas the aliquot for Western blot analysis was kept at −70 °C until assayed.

2.8. Radioimmunoassay (RIA)

The RIA was carried out using standard procedures and reagents provided by the NHPP and Dr. A.F. Parlow, with rat PRL antigen (rPRL-I-6) and rat PRL reference (rPRL-RP-3) preparations.

2.9. Western blot

Pulverized frozen hypothalami were homogenized in lysis buffer (0.5% Igepal, 0.1% SDS, 50 mM Tris, 150 mM NaCl, 1 μg/ml aprotinin, and 100 μg/ml PMSF, pH 7.4) and analyzed for PRL by RIA and for PRL and vasoinhibins by Western blot. Sixty μg of protein was resolved by 15% SDS-PAGE, blotted, and probed overnight with C-1 anti-PRL antiserum (α-PRL; 1:250 dilution) or with monoclonal antibody INN-1 directed against the N-terminal end of PRL (N-Term; 1:100 dilution) as described (Duenas et al., 1999; Aranda et al., 2005). Secondary antibodies conjugated to alkaline phosphatase were used (Bio-Rad Laboratories, Hercules, CA) and optical density values determined using Quantity One, 1-D analysis software (Bio-Rad).

2.10. qRT-PCR

Total RNA was isolated from frozen, pulverized hypothalamic samples by placing them in TRIzol reagent (Invitrogen, Carlsbad, CA) followed by homogenization for 10 s. Reverse transcription was then performed using 1 μg total RNA and the High Capacity cDNA Reverse Transcription Kit (Applied Biosystems, Foster City, CA). PCR products were detected and quantified with Maxima SYBR Green qPCR Master Mix (Thermo Scientific, Waltham, MA) in a 10 μl final reaction volume containing template and 0.5 μM of each of the primer pairs for *Prl*: forward 5′-TTATTGCCAAGGCCATCAAT-3′, reverse 5′-TGAAACAGAGGGTCATTCCA-3′ and for *Gapdh*: forward 5′-GTCCACTGGCGTCTTCACCA-3′, reverse 5′-GTGGCAGTCATGGCATGGAC-3′. Amplification performed in the CFX96™ thermocycler (Bio-Rad) included a denaturation step of 10 min at 95 °C, followed by 35 cycles of amplification (10 s at 95 °C, 30 s at the primer pair-specific annealing temperature and 30 s at 72 °C). The PCR data were analyzed by the $2^{-\Delta\Delta CT}$ method, and cycle thresholds normalized to the housekeeping gene *Gapdh* allowed the mRNA levels of interest to be calculated. PRL transcripts were amplified at 24–28 cycles, and they displayed a single melting peak at 80.5 °C indicative of a single amplicon.

2.11. PRL cleavage analyses

The activity of PRL cleaving proteases was assessed by incubating 200 ng of recombinant PRL in 5 μl of incubation buffer (0.05 M Tris-HCl, 0.15 M NaCl, and 0.01 M $CaCl_2$, pH 7.0) with different amounts of hypothalamic lysate protein from stressed and non-stressed rats in a final volume of 20 μl for 24 h at 37 °C.

2.12. Statistical analysis

Statistics was performed using the Sigma Stat 7.0 (Systat Software Inc., San Jose, CA). Differences between two or more groups were evaluated by the two-tailed Student' *t*-test and one-way ANOVA followed by Tukey or the Holm—Sidak post hoc comparison test, respectively. Differences in means with $p < 0.05$ were considered statistically significant.

3. Results

3.1. Vasoinhibins stimulate anxiety and depressive-like behaviors

Compared to vehicle-treated controls, intracerebroventricular (icv) injection of a recombinant vasoinhibin containing the first 123 amino acids of human PRL increased anxiety-related behavior in the EPM (Fig. 1A), as indicated by a reduced percentage of time spent on the open arms ($p = 0.003$). This effect was not due to decreased locomotor activity, since the number of entries into closed arms was similar between vehicle- and vasoinhibin-treated rats ($p = 0.143$). Moreover, treatment with the vasoinhibin was also associated with increased anxiety behavior in the OF test reflected by a significant reduction in the number of entries into the central square ($p = 0.001$) and a significant increase in the number of fecal boli ($p < 0.001$) of the rats receiving the vasoinhibin compared with vehicle-treated rats (Fig. 1B). No differences were noted between the two groups in the number of entries into the peripheral squares (84 ± 5 vs. 89 ± 7, for vasoinhibin and vehicle, respectively; $p = 0.729$), further evidence that locomotor activity was not modified by icv administration of the vasoinhibin.

The recombinant vasoinhibin also increased depressive-related behavior in the FS test, where rats given the vasoinhibin displayed a shorter latency to floating ($p < 0.001$) and spent more time floating ($p = 0.001$) compared with control rats (Fig. 1C). The time spent struggling (107 ± 19 vs. 111 ± 9 s for the vasoinhibin and vehicle, respectively; $p = 0.836$) and swimming (477 ± 19 vs. 480 ± 10 s, for the vasoinhibin and vehicle, respectively; $p = 0.202$) was similar.

3.2. Physical restraint increases systemic PRL levels and hypothalamic levels of PRL mRNA and protein but not the levels of hypothalamic vasoinhibins

To investigate the stress-induced increase in hypothalamic levels of PRL and vasoinhibins, we exposed animals to 30 min of physical restraint and measured the circulating PRL levels (Fig. 2A). Consistent with previous reports (Moore et al., 1987; Reichlin, 1988), 30 min of physical restraint caused a transient, 6-fold increase in serum PRL levels ($p < 0.001$) that declined to control values by 60 min after the onset of stress. Treatment with the dopamine D2 receptor agonist bromocriptine, an inhibitor of PRL secretion by the adenohypophysis, prevented such increase and lowered the systemic levels of PRL throughout the experiment (Fig. 2A).

Because circulating PRL can enter the brain (Walsh et al., 1987), we analyzed by RIA whether the stress-induced increase in systemic PRL correlated with higher hypothalamic levels of PRL (Fig. 2B). In contrast to serum PRL, the levels of PRL in the hypothalamus were unchanged at the end of the 30-min immobilization period, but they were elevated at 60 min ($p < 0.001$) and 360 min ($p < 0.02$). This rise in hypothalamic PRL was not prevented by treatment with bromocriptine.

Consistent with a previous report (Torner et al., 2004), hypothalamic PRL mRNA was elevated 10-fold at 60 min post-stress ($p = 0.021$) and returned to the basal levels at 360 min (Fig. 2C).

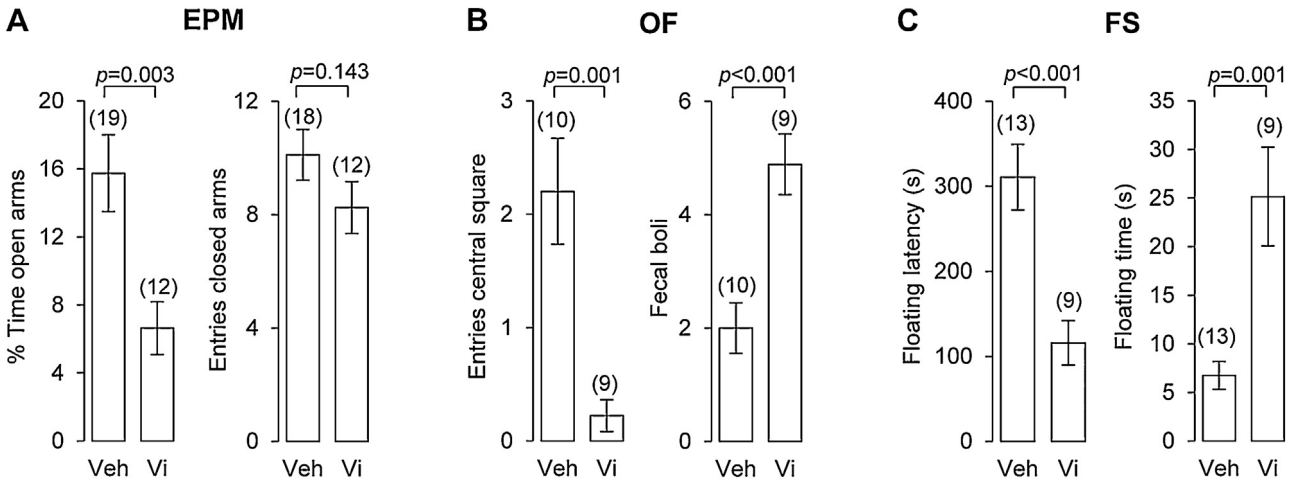

Figure 1 Vasoinhibins stimulate anxiety- and depressive-like behaviors. Intracerebroventricular administration of a vasoinhibin (Vi) or vehicle (Veh) 10 min before exposure to the elevated plus-maze (EPM) (A), open field (OF) (B), and forced swim (FS) tests (C). Bars are means ± SE. Numbers inside parentheses indicate *n* values.

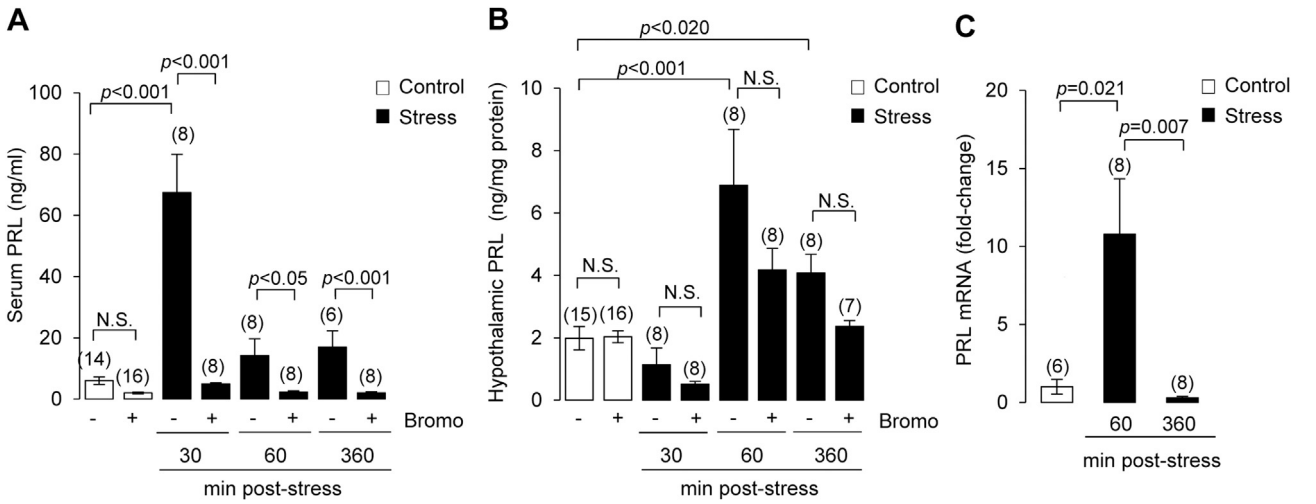

Figure 2 Stress increases hypothalamic PRL levels by stimulating local synthesis but not the uptake of systemic PRL. PRL levels, evaluated by RIA, in serum (A) or hypothalamic extracts (B) before (Control) or after (Stress) 30, 60, and 360 min after initiating a 30 min period of restraint stress in the absence (−) or presence (+) of bromocriptine (Bromo), an inhibitor of PRL secretion by the adenohypophysis. Quantitative RT-PCR-based evaluation of PRL mRNA in the hypothalamus of control and stressed rats (C). Bars are means ± SE. Numbers inside parentheses indicate *n* values. N.S., non-significant.

To discriminate between PRL and vasoinhibins, the hypothalamic levels of these proteins were evaluated by Western blot using polyclonal antibodies that target the entire PRL molecule (α-PRL) and the monoclonal INN-1 anti-PRL antibody that reacts with the N-terminal end of PRL (N-Term), which is the part of the PRL molecule present in vasoinhibins. The specificity of the N-Term antibody is illustrated by its reaction with rat PRL cleaved by cathepsin D in the large disulfide loop (cleaved PRL), which upon disulfide-bond reduction yields an N-terminal 16 kDa fragment (vasoinhibin) and a C-terminal 7 kDa fragment (Fig. 3A). Western blot analysis under reducing conditions of a combination of standards of rat PRL and of rat PRL cleaved by a mammary gland extract enriched with cathepsin D showed that α-PRL and N-Term antibodies react with PRL; however, while α-PRL reacts with both the 16 and the 7 kDa fragments of PRL, the N-Term antibody only reacted with the 16 kDa PRL fragment (Fig. 3B).

Hypothalamic lysates contained 23 kDa and 17 kDa PRL-like proteins that likely correspond to PRL and a vasoinhibin, respectively, as they are both detected by α-PRL antibodies (Fig. 3C) and the N-Term antibody (Fig. 3D). PRL and the vasoinhibin were quantified in blots probed with the α-PRL antibodies after normalization for the amount of β-tubulin (Fig. 3E). Consistent with the RIA data (Fig. 2A), Western blots showed that hypothalamic PRL was elevated at 60 min and declined thereafter (Fig. 3E). In contrast, levels of the vasoinhibin were similar in the hypothalamus of non-stressed and stressed animals (Fig. 3E).

3.3. Physical restraint downregulates the activity of PRL-cleaving enzymes in the hypothalamus

To understand why the stress-induced increase in hypothalamic PRL did not result in higher levels of the vasoinhibin, we investigated whether the activity of PRL cleaving enzymes is downregulated under stress. Recombinant PRL was incubated with three different protein concentrations of hypothalamic extracts harvested from either non-stressed or stressed rats at 60 and 360 min after stress onset (Fig. 4). Western blot revealed that incubation of PRL with hypothalamic extracts resulted in its partial conversion to a 17 kDa vasoinhibin in an extract-protein concentration-dependent manner. Incubation of PRL with hypothalamic extracts sampled from stressed rats at 60 min resulted in a significant reduction in vasoinhibin generation ($p = 0.025$), and this effect was reversed at 360 min (Fig. 4B).

4. Discussion

It is increasingly apparent that the PRL effects on blood vessels are influenced by its proteolytic cleavage to vasoinhibins, a family of peptides exerting effects opposite to those of PRL on blood vessels and inflammatory reactions (Clapp et al., 2009). Here, we extend these observations to PRL inhibition of stress-induced emotional responses. We show for the first time that the icv delivery of vasoinhibins increases anxiety- and depression-related behaviors, and that exposure to an acute stressor can downregulate the cleavage of PRL to vasoinhibins in the hypothalamus.

The acute icv infusion of a recombinant vasoinhibin increased stress-related behaviors on the EPM, the OF, and the FS tests, which are standard tests used to detect emotional responses to anxiogenic and depressive substances in rodents (Marti and Armario, 1993; Carola et al., 2002). As expected for an anxiogenic agent, the vasoinhibin reduced the time spent on the open arms of the EPM and the number of entries into the brightly lit central square of the OF, indicating enhanced aversion to unprotected elevated and open areas, respectively. These behavioral changes are not influenced by altered locomotion since parameters measuring locomotor activity (number of entries to closed arms and to peripheral squares) were not modified by the vasoinhibin.

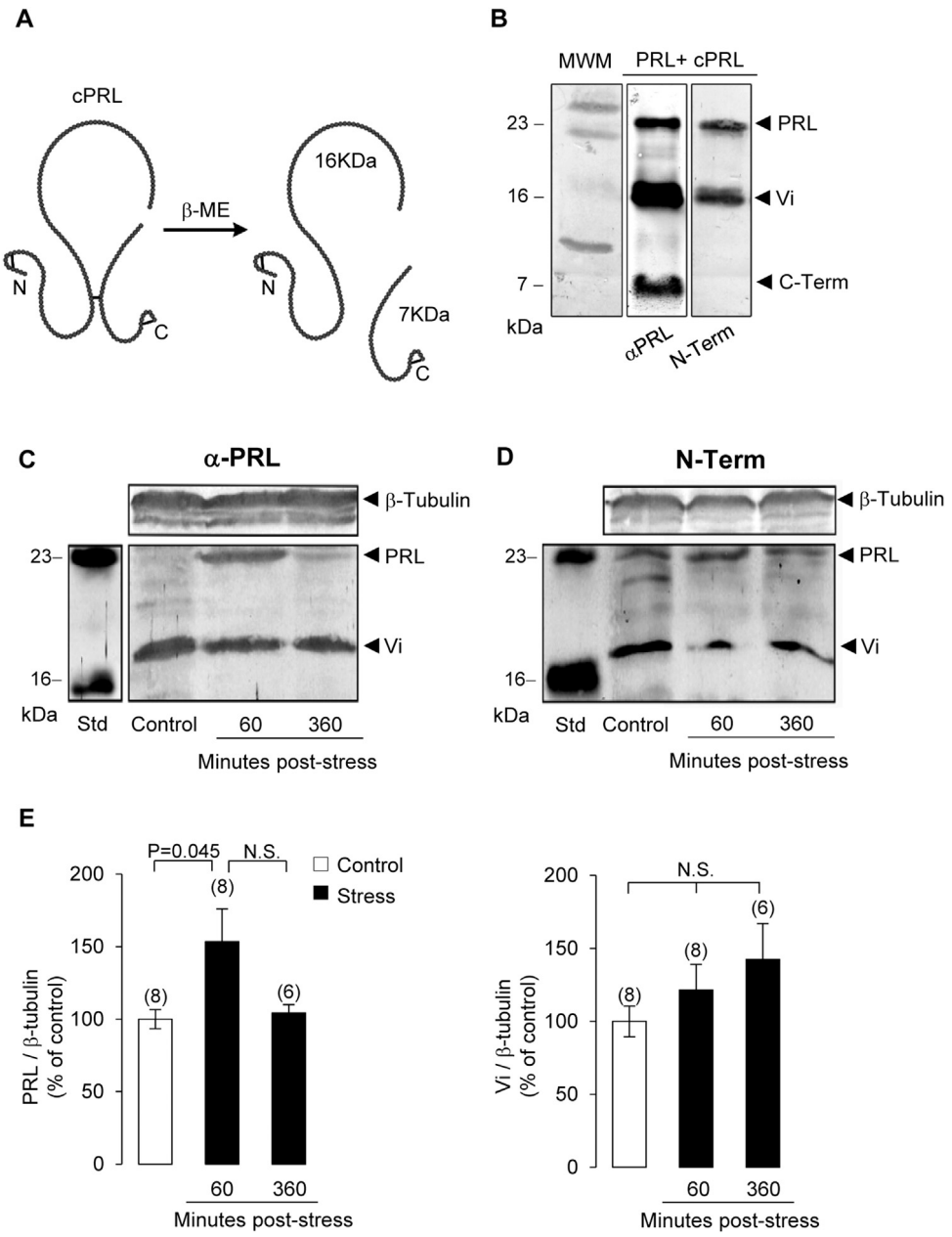

Figure 3 Stress increases hypothalamic levels of PRL but not of vasoinhibins. Rats were exposed (Stress) or not (Control) to a 30 min period of restrain stress and killed at 60 or 360 min after stress initiation. (A) Linear representation of rat PRL cleaved by cathepsin D in the large disulfide loop (cPRL), which upon β-mercaptoethanol (β-ME) reduction yields an N-terminal 16 kDa fragment (vasoinhibin) and a C-terminal 7 kDa fragment. (B) Reducing Western blot analysis of a combination of standards of rat PRL and of rat PRL cleaved by a mammary gland extract enriched with cathepsin D (cPRL) probed with anti-PRL antiserum (α-PRL) or with a monoclonal antibody directed against the N-terminal region of PRL (N-Term). MWM, molecular weight markers; Vi, vasoinhibin. Numbers on the left side show the molecular weights of PRL isoforms. Representative Western blot analysis of hypothalamic extracts as revealed by α-PRL (A) or N-Term (B) antibodies. Migration positions of PRL and Vi standards are indicated (Std), and numbers on the left side show their molecular weights. (C) Densitometric quantification of PRL and Vi in hypothalamic extracts as revealed by α-PRL antibodies and after normalization for β-tubulin used as loading control. Bars are means ± SE. Numbers inside parentheses indicate *n* values. N.S., non significant.

Moreover, vasoinhibin-treated rats displayed a shorter latency to floating and longer immobility in the FS, which is commonly linked to a depressive phenotype.

The dose of the vasoinhibin (1.0 μg) was similar to the one causing PRL anxiolytic effects (Torner et al., 2001) and was selected to compare relative potencies. However, this is likely a pharmacological dose, raising the possibility that vasoinhibins are acting as PRL antagonists. Vasoinhibins lack helix 4, which comprises several residues of the PRL binding site 1 required for the dimerization and activation of PRL receptors (Bole-Feysot et al., 1998). Moreover, there is evidence that vasoinhibins bind only weakly to PRL receptors

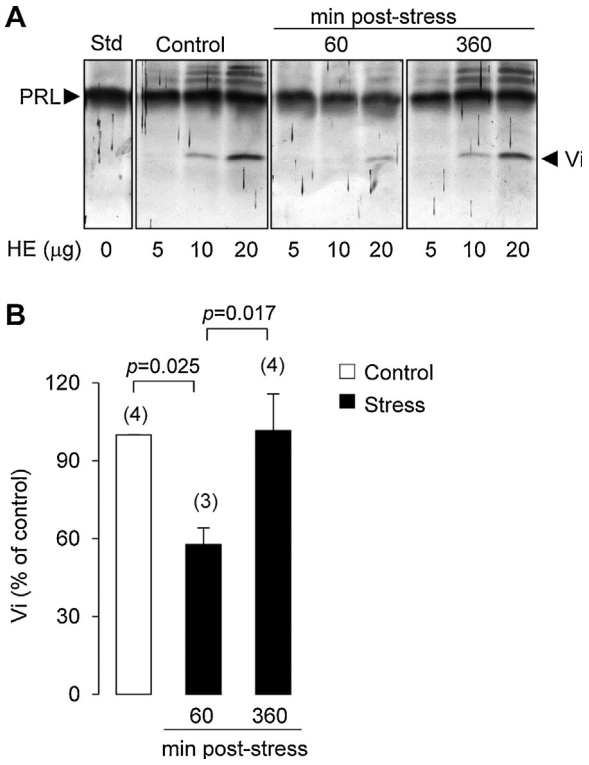

Figure 4 Stress downregulates the activity of PRL-cleaving enzymes in the hypothalamus. (A) Western blot analysis of the vasoinhibin generated when 200 ng of recombinant PRL was incubated at pH 7.0 with the indicated amounts of hypothalamic extract protein (HE) obtained from rats exposed or not (Control) to a 30 min period of restrain stress and killed 60 or 360 min after stress initiation. (B) The vasoinhibin (Vi) bands generated when 200 ng of recombinant PRL was incubated at pH 7.0 with 20 μg of HE protein from stressed rats were evaluated densitometrically and the results were expressed as a percentage of the Vi band evaluated after incubation with the same amount of HE protein from control rats. Bars are means ± SE. Numbers inside parentheses indicate *n* values.

(Clapp et al., 1989) and can act as partial agonists in PRL bioassays (Clapp et al., 1988). On the other hand, single, saturable, high-affinity (K_d of 1–10 nM) vasoinhibin binding sites that are distinct from the PRL receptor were reported in endothelial cell membranes (Clapp and Weiner, 1992), but these putative vasoinhibin receptors have not been identified. Specific vasoinhibin binding sites were also reported in brain membranes (Clapp et al., 1989). Whether these binding sites correspond to receptors mediating vasoinhibins' anxiogenic and depressive effects and are different from those in endothelial cells is unknown. It is possible that the central effects of vasoinhibins involve their vascular actions. Vasoinhibins act on endothelial cells to inhibit vasodilation (Gonzalez et al., 2004), and several studies have correlated anxiety and depression with an attenuated cerebral blood flow (Rauch et al., 2006; Giardino et al., 2007) that reflects endothelial cell dysfunction (Park and Pepine, 2010).

The fact that vasoinhibins can exert effects opposite to the anxiolytic and antidepressive effects of PRL (Torner et al., 2001) indicates that the PRL molecule contains the potential to both inhibit and stimulate stress-induced emotional responses and thus, that specific proteolytic cleavage can modify its action. Accordingly, conversion of PRL to vasoinhibins may provide an explanation for controversial findings associating elevated circulating PRL levels with high innate anxiety in rats (Torner and Neumann, 2002) or with increased anxiety in patients bearing prolactinomas (Reavley et al., 1997).

To establish a possible link between PRL cleavage and stress responses, we investigated whether immobilization stress regulates the hypothalamic levels of PRL and vasoinhibins. We found that physical restraint raises the levels of both systemic and hypothalamic PRL as measured by RIA, but with different temporal dynamics. The early and delayed elevation of systemic and hypothalamic PRL levels, respectively, may reflect the time required for the transport of PRL from blood. The dopamine antagonist, domperidone, induces an increase in circulating PRL that is followed 30–40 min later by a rise in the cerebrospinal fluid levels of the hormone (Felicio and Bridges, 1992). In addition, hypothalamic PRL may be partly independent of systemic PRL under conditions of stress. We found that blockage of the physical restraint-induced elevation of systemic PRL with bromocriptine failed to modify the hypothalamic levels of PRL. Also, it has been shown that ether stress, causing a pattern of PRL in blood similar to restraint stress (Reichlin, 1988), does not modify the levels of PRL in cerebrospinal fluid (Barbanel et al., 1986). Along this line, our findings confirmed a previous report (Torner et al., 2004) showing that physical restraint stimulates the expression of PRL mRNA in the hypothalamus, and suggest that local synthesis may contribute to the delayed elevation of hypothalamic PRL following stress.

However, it should be noted that the neuronal expression of PRL is under debate. There is no in situ hybridization study in rodents showing the expression of PRL mRNA in neurons or other brain cells. A report in adult and fetal sheep brain did visualize PRL mRNA by in situ hybridization in the hypothalamic paraventricular nucleus and other brain sites (Roselli et al., 2008), but provided no proof of neuronal identity. We do not know the nature of the cells expressing the PRL transcript in our study (neurons, glia, vascular endothelium, and/or circulating cells), nor can we eliminate the contribution of pituitary contaminants.

The RIA employed here essentially measures PRL and not vasoinhibins, as vasoinhibins have low RIA activity (2%) (Clapp et al., 1988). In the absence of a quantitative assay, the hypothalamic levels of vasoinhibins could only be determined semi-quantitatively by Western blotting combined with optical densitometry. This is a limitation of the study since small differences hypothalamic levels of vasoinhibins could have escaped detection. However, Western blot analysis confirmed the stress-induced increase in hypothalamic PRL measured by RIA, and support the use of this technique for studying stress-mediated changes of hypothalamic PRL isoforms.

In contrast to PRL, the hypothalamic levels of vasoinhibins appeared not to be modified by stress. Elevation of PRL levels leads to the accumulation of vasoinhibins in the retina (Arnold et al., 2010); however, the stress-induced increase in PRL levels was not followed by an elevation in hypothalamic vasoinhibins, which could imply that stress downregulates the activity of PRL-cleaving enzymes in the hypothalamus. Indeed, we found that the activity of

PRL-cleaving proteases is reduced at 60 min post-stress onset and recovers thereafter. The presence of acidic proteases able to cleave PRL to vasoinhibins has been previously reported in the hypothalamus (DeVito et al., 1992), but this is the first demonstration of hypothalamic PRL-cleaving activity at a neutral pH. The nature of these neutral proteases is unknown, but they may include matrix metalloproteases (MMP), as various MMP cleave PRL to vasoinhibins (Macotela et al., 2006), and restraint stress can downregulate MMP in the brain (Lee et al., 2009). In summary, we suggest that stress increases PRL levels in the hypothalamus both by stimulating PRL expression and by reducing its conversion to vasoinhibins.

The distribution of PRL and vasoinhibins in the hypothalamus includes the hypothalamo-neurohypophyseal system, the medial preoptic area, and the periventricular, and arcuate nuclei (Clapp et al., 1994; Ben-Jonathan et al., 1996; Grattan and Kokay, 2008). Subcellularly, PRL isoforms are localized in secretory granules within neuronal structures that might include dendrites, perikarya, or axon terminals, and a depolarizing stimulus (56 mM K^+) triggers their secretion by exocytosis (Torner et al., 1995, 2004; Mejia et al., 1997). Moreover, restraint stress elicits the release of PRL within both the paraventricular (PVN) and medial preoptic nuclei (Torner et al., 2004), which are important areas regulating the activation of the HPA axis, possibly via inhibition of corticotropin-releasing hormone secretion (Torner et al., 2001, 2002). However, to what extent PRL and vasoinhibins in the hypothalamus contribute to the regulation of stress-induced emotional responses remains unknown.

The central nucleus of the amygdala (CeA) plays a key role in generating anxiety, depression, and fear through its projections to the brain stem and hypothalamic structures (Debiec, 2005; Schulkin, 2006; Walker and Davis, 2008). Long-range axon collaterals originating from magnocellular PVN and supraoptic (SON) neurons release the neuropeptide oxytocin (OXT) in the CeA to suppress fear (Knobloch et al., 2012). It is possible that a similar hypothalamic connection leads to the release of PRL and vasoinhibins into the CeA. PRL and vasoinhibins are found in the magnocellular PVN and SON (Clapp et al., 1994); PRL-immunoreactive fibers have been reported in the CeA, and colchicine treatment indicates that some of these fibers originate in the hypothalamus (Siaud et al., 1989). Outside of the choroid plexus, however, most of the PRL receptors are located in the hypothalamus including the magnocellular neurons of the PVN and SON (Ben-Jonathan et al., 1996; Mejia et al., 2003; Grattan and Kokay, 2008). Therefore, it is also possible that PRL and vasoinhibins regulate anxiety by stimulating the magnocellular OXT and arginine vasopressin (AVP) system to release both peptides in the CeA, and also in the PVN, where they are known to regulate anxiety in an opposite manner (Debiec, 2005; Blume et al., 2008; Viviani and Stoop, 2008). Supporting this notion, PRL stimulates neuronal nitric oxide synthase activity in magnocellular PVN and SON neurons to release OXT and AVP (Vega et al., 2010), and vasoinhibins stimulate AVP release by hypothalamo-neurohypophyseal explants (Mejia et al., 2003).

The effects of the PRL-vasoinhibin system on stress responses may be particularly relevant during pregnancy and lactation, when there is an attenuation of physiological and behavioral stress responses (Torner and Neumann, 2002). The anti-stress effects of PRL, together with those of oxytocin (Neumann et al., 2000), have been viewed as an adaptation of the maternal brain to ensure maternal care under aversive situations (Torner and Neumann, 2002; Schulkin, 2006; Grattan and Kokay, 2008), albeit a reduced reaction to stress can be detrimental for parent survival. In this regard, the ability of PRL to both inhibit and stimulate anxiety and depression upon conversion to vasoinhibin represents an efficient mechanism for adjusting stress responses and maximizing reproduction and survival. However, PRL also counteracts stress responses in males (Torner et al., 2001), and the facts that our behavioral study was carried out on diestrous rats and that the stage of the estrous cycle showed no apparent correlation with stress-induced changes in hypothalamic PRL and vasoinhibins, imply that the PRL–vasoinhibin system regulates stress responses beyond female reproduction. Understanding the regulation of the protease(s) responsible for specific PRL cleavage under different physiological states and pathological conditions should help define the influence of PRL on stress-related responses.

Taken together, our findings demonstrate that PRL, an anxiolytic and anti-depressive hormone, acquires anxiogenic and depressive properties after undergoing proteolytic cleavage to vasoinhibins in the hypothalamus, and that such conversion can be downregulated by exposure to an acute stressor. This represents an efficient mechanism for the fine-tuning of stress-related emotional responses. Further research is needed to understand how PRL and vasoinhibin are mechanistically related and interact to affect specific behavioral and physiological components associated with stress.

Role of funding source

Ph.D. students from Programa de Doctorado en Ciencias Biomédicas, Universidad Nacional Autónoma de México (UNAM) were supported by fellowships from National Council of Science and Technology of Mexico (CONACYT): M. Zamorano (#181558), M.G. Ledesma-Colunga (#245828), N. Adán (#223363), and M. Lemini (#228328). The research was supported by CONACYT grants 127496 and 161594 to C. Clapp.

Conflict of interest

None declared.

Acknowledgments

We thank Fernando López-Barrera, Gabriel Nava, Daniel Mondragón, Antonio Prado, Martín García, Alejandra Castilla for their technical assistance and Dorothy D. Pless for critically editing the manuscript.

References

Aranda, J., Rivera, J.C., Jeziorski, M.C., Riesgo-Escovar, J., Nava, G., Lopez-Barrera, F., Quiroz-Mercado, H., Berger, P., Martinez de la Escalera, G., Clapp, C., 2005. Prolactins are natural inhibitors of angiogenesis in the retina. Invest. Ophthalmol. Vis. Sci. 46, 2947–2953.

Arnold, E., Rivera, J.C., Thebault, S., Moreno-Paramo, D., Quiroz-Mercado, H., Quintanar-Stephano, A., Binart, N., Martinez de la Escalera, G., Clapp, C., 2010. High levels of serum prolactin protect against diabetic retinopathy by increasing ocular vasoinhibins. Diabetes 59, 3192—3197.

Barbanel, G., Ixart, G., Arancibia, S., Assenmacher, I., 1986. Probable extrapituitary source of the immunoreactive prolactin measured in the cerebrospinal fluid of unanesthetized rats by push-pull cannulation of the 3rd ventricle. Neuroendocrinology 43, 476—482.

Ben-Jonathan, N., Mershon, J.L., Allen, D.L., Steinmetz, R.W., 1996. Extrapituitary prolactin: distribution, regulation, functions, and clinical aspects. Endocr. Rev. 17, 639—669.

Blume, A., Bosch, O.J., Miklos, S., Torner, L., Wales, L., Waldherr, M., Neumann, I.D., 2008. Oxytocin reduces anxiety via ERK1/2 activation: local effect within the rat hypothalamic paraventricular nucleus. Eur. J. Neurosci. 27, 1947—1956.

Bole-Feysot, C., Goffin, V., Edery, M., Binart, N., Kelly, P.A., 1998. Prolactin (PRL) and its receptor: actions, signal transduction pathways and phenotypes observed in PRL receptor knockout mice. Endocr. Rev. 19, 225—268.

Carola, V., D'Olimpio, F., Brunamonti, E., Mangia, F., Renzi, P., 2002. Evaluation of the elevated plus-maze and open-field tests for the assessment of anxiety-related behaviour in inbred mice. Behav. Brain Res. 134, 49—57.

Clapp, C., 1987. Analysis of the proteolytic cleavage of prolactin by the mammary gland and liver of the rat: characterization of the cleaved and 16K forms. Endocrinology 121, 2055—2064.

Clapp, C., Aranda, J., Gonzalez, C., Jeziorski, M.C., Martinez de la Escalera, G., 2006. Vasoinhibins: endogenous regulators of angiogenesis and vascular function. Trends Endocrinol. Metab. 17, 301—307.

Clapp, C., Sears, P.S., Nicoll, C.S., 1989. Binding studies with intact rat prolactin and a 16K fragment of the hormone. Endocrinology 125, 1054—1059.

Clapp, C., Sears, P.S., Russell, D.H., Richards, J., Levay-Young, B.K., Nicoll, C.S., 1988. Biological and immunological characterization of cleaved and 16K forms of rat prolactin. Endocrinology 122, 2892—2898.

Clapp, C., Thebault, S., Jeziorski, M.C., Martinez De La Escalera, G., 2009. Peptide hormone regulation of angiogenesis. Physiol. Rev. 89, 1177—1215.

Clapp, C., Torner, L., Gutierrez-Ospina, G., Alcantara, E., Lopez-Gomez, F.J., Nagano, M., Kelly, P.A., Mejia, S., Morales, M.A., Martinez de la Escalera, G., 1994. The prolactin gene is expressed in the hypothalamic-neurohypophyseal system and the protein is processed into a 14-kDa fragment with activity like 16-kDa prolactin. Proc. Natl. Acad. Sci. U. S. A. 91, 10384—10388.

Clapp, C., Weiner, R.I., 1992. A specific, high affinity, saturable binding site for the 16-kilodalton fragment of prolactin on capillary endothelial cells. Endocrinology 130, 1380—1386.

Cook, C.J., 1997. Oxytocin and prolactin suppress cortisol responses to acute stress in both lactating and non-lactating sheep. J. Dairy Res. 64, 327—339.

Corbacho, A.M., Macotela, Y., Nava, G., Eiserich, J.P., Cross, C.E., Martinez de la Escalera, G., Clapp, C., 2003. Cytokine induction of prolactin receptors mediates prolactin inhibition of nitric oxide synthesis in pulmonary fibroblasts. FEBS Lett. 544, 171—175.

Corbacho, A.M., Nava, G., Eiserich, J.P., Noris, G., Macotela, Y., Struman, I., Martinez De La Escalera, G., Freeman, B.A., Clapp, C., 2000. Proteolytic cleavage confers nitric oxide synthase inducing activity upon prolactin. J. Biol. Chem. 275, 13183—13186.

Debiec, J., 2005. Peptides of love and fear: vasopressin and oxytocin modulate the integration of information in the amygdala. Bioessays 27, 869—873.

DeVito, W.J., Avakian, C., Stone, S., 1992. Proteolytic modification of prolactin by the female rat brain. Neuroendocrinology 56, 597—603.

Dorshkind, K., Horseman, N.D., 2000. The roles of prolactin, growth hormone, insulin-like growth factor-I, and thyroid hormones in lymphocyte development and function: insights from genetic models of hormone and hormone receptor deficiency. Endocr. Rev. 21, 292—312.

Duenas, Z., Torner, L., Corbacho, A.M., Ochoa, A., Gutierrez-Ospina, G., Lopez-Barrera, F., Barrios, F.A., Berger, P., Martinez de la Escalera, G., Clapp, C., 1999. Inhibition of rat corneal angiogenesis by 16-kDa prolactin and by endogenous prolactin-like molecules. Invest. Ophthalmol. Vis. Sci. 40, 2498—2505.

Felicio, L.F., Bridges, R.S., 1992. Domperidone induces a probenecid-sensitive rise in immunoreactive prolactin in cerebroventricular perfusates in female rats. Brain Res. 573, 133—138.

Galfione, M., Luo, W., Kim, J., Hawke, D., Kobayashi, R., Clapp, C., Yu-Lee, L.Y., Lin, S.H., 2003. Expression and purification of the angiogenesis inhibitor 16-kDa prolactin fragment from insect cells. Protein Expr. Purif. 28, 252—258.

Giardino, N.D., Friedman, S.D., Dager, S.R., 2007. Anxiety, respiration, and cerebral blood flow: implications for functional brain imaging. Compr. Psychiatry 48, 103—112.

Gonzalez, C., Corbacho, A.M., Eiserich, J.P., Garcia, C., Lopez-Barrera, F., Morales-Tlalpan, V., Barajas-Espinosa, A., Diaz-Munoz, M., Rubio, R., Lin, S.H., Martinez de la Escalera, G., Clapp, C., 2004. 16K-prolactin inhibits activation of endothelial nitric oxide synthase, intracellular calcium mobilization, and endothelium-dependent vasorelaxation. Endocrinology 145, 5714—5722.

Grattan, D.R., Kokay, I.C., 2008. Prolactin: a pleiotropic neuroendocrine hormone. J. Neuroendocrinol. 20, 752—763.

Knobloch, H.S., Charlet, A., Hoffmann, L.C., Eliava, M., Khrulev, S., Cetin, A.H., Osten, P., Schwarz, M.K., Seeburg, P.H., Stoop, R., Grinevich, V., 2012. Evoked axonal oxytocin release in the central amygdala attenuates fear response. Neuron 73, 553—566.

Lee, K.W., Kim, J.B., Seo, J.S., Kim, T.K., Im, J.Y., Baek, I.S., Kim, K.S., Lee, J.K., Han, P.L., 2009. Behavioral stress accelerates plaque pathogenesis in the brain of Tg2576 mice via generation of metabolic oxidative stress. J. Neurochem. 108, 165—175.

Macotela, Y., Aguilar, M.B., Guzman-Morales, J., Rivera, J.C., Zermeno, C., Lopez-Barrera, F., Nava, G., Lavalle, C., Martinez de la Escalera, G., Clapp, C., 2006. Matrix metalloproteases from chondrocytes generate an antiangiogenic 16 kDa prolactin. J. Cell. Sci. 119, 1790—1800.

Mangurian, L.P., Walsh, R.J., Posner, B.I., 1992. Prolactin enhancement of its own uptake at the choroid plexus. Endocrinology 131, 698—702.

Marti, J., Armario, A., 1993. Effects of diazepam and desipramine in the forced swimming test: influence of previous experience with the situation. Eur. J. Pharmacol. 236, 295—299.

Mejia, S., Morales, M.A., Zetina, M.E., Martinez de la Escalera, G., Clapp, C., 1997. Immunoreactive prolactin forms colocalize with vasopressin in neurons of the hypothalamic paraventricular and supraoptic nuclei. Neuroendocrinology 66, 151—159.

Mejia, S., Torner, L.M., Jeziorski, M.C., Gonzalez, C., Morales, M.A., de la Escalera, G.M., Clapp, C., 2003. Prolactin and 16K prolactin stimulate release of vasopressin by a direct effect on hypothalamo-neurohypophyseal system. Endocrine 20, 155—162.

Moore, K.E., Demarest, K.T., Lookingland, K.J., 1987. Stress, prolactin and hypothalamic dopaminergic neurons. Neuropharmacology 26, 801—808.

Neumann, I.D., Torner, L., Wigger, A., 2000. Brain oxytocin: differential inhibition of neuroendocrine stress responses and anxiety-related behaviour in virgin, pregnant and lactating rats. Neuroscience 95, 567—575.

Park, K.E., Pepine, C.J., 2010. Pathophysiologic mechanisms linking impaired cardiovascular health and neurologic dysfunction: the year in review. Cleve. Clin. J. Med. 77 (Suppl. 3) S40L 45.

Paxinos, G., Watson, C., 1986. The Rat Brain in Stereotaxic Coordinates. American Press, San Diego.

Rauch, S.L., Shin, L.M., Phelps, E.A., 2006. Neurocircuitry models of posttraumatic stress disorder and extinction: human neuroimaging research — past, present, and future. Biol. Psychiatry 60, 376—382.

Reavley, A., Fisher, A.D., Owen, D., Creed, F.H., Davis, J.R., 1997. Psychological distress in patients with hyperprolactinaemia. Clin. Endocrinol. (Oxf.) 47, 343—348.

Reichlin, S., 1988. Prolactin and growth hormone secretion in stress. Adv. Exp. Med. Biol. 245, 353—376.

Roselli, C.E., Bocklandt, S., Stadelman, H.L., Wadsworth, T., Vilain, E., Stormshak, F., 2008. Prolactin expression in the sheep brain. Neuroendocrinology 87, 206—215.

Schulkin, J., 2006. Angst and the amygdala. Dialogues Clin. Neurosci. 8, 407—416.

Shingo, T., Gregg, C., Enwere, E., Fujikawa, H., Hassam, R., Geary, C., Cross, J.C., Weiss, S., 2003. Pregnancy-stimulated neurogenesis in the adult female forebrain mediated by prolactin. Science 299, 117—120.

Siaud, P., Manzoni, O., Balmefrezol, M., Barbanel, G., Assenmacher, I., Alonso, G., 1989. The organization of prolactin-like-immunoreactive neurons in the rat central nervous system. Light- and electron-microscopic immunocytochemical studies. Cell Tissue Res. 255, 107—115.

Sonigo, C., Bouilly, J., Carre, N., Tolle, V., Caraty, A., Tello, J., Simony-Conesa, F.J., Millar, R., Young, J., Binart, N., 2012. Hyperprolactinemia-induced ovarian acyclicity is reversed by kisspeptin administration. J. Clin. Invest. 122, 3791—3795.

Torner, L., Maloumby, R., Nava, G., Aranda, J., Clapp, C., Neumann, I.D., 2004. In vivo release and gene upregulation of brain prolactin in response to physiological stimuli. Eur. J. Neurosci. 19, 1601—1608.

Torner, L., Mejia, S., Lopez-Gomez, F.J., Quintanar, A., Martinez de la Escalera, G., Clapp, C., 1995. A 14-kilodalton prolactin-like fragment is secreted by the hypothalamo-neurohypophyseal system of the rat. Endocrinology 136, 5454—5460.

Torner, L., Neumann, I.D., 2002. The brain prolactin system: involvement in stress response adaptations in lactation. Stress 5, 249—257.

Torner, L., Toschi, N., Nava, G., Clapp, C., Neumann, I.D., 2002. Increased hypothalamic expression of prolactin in lactation: involvement in behavioural and neuroendocrine stress responses. Eur. J. Neurosci. 15, 1381—1389.

Torner, L., Toschi, N., Pohlinger, A., Landgraf, R., Neumann, I.D., 2001. Anxiolytic and anti-stress effects of brain prolactin: improved efficacy of antisense targeting of the prolactin receptor by molecular modeling. J. Neurosci. 21, 3207—3214.

Vega, C., Moreno-Carranza, B., Zamorano, M., Quintanar-Stephano, A., Mendez, I., Thebault, S., Martinez de la Escalera, G., Clapp, C., 2010. Prolactin promotes oxytocin and vasopressin release by activating neuronal nitric oxide synthase in the supraoptic and paraventricular nuclei. Am. J. Physiol. Regul. Integr. Comp. Physiol. 299, R1701—R1708.

Viviani, D., Stoop, R., 2008. Opposite effects of oxytocin and vasopressin on the emotional expression of the fear response. Prog. Brain Res. 170, 207—218.

Walker, D.L., Davis, M., 2008. Role of the extended amygdala in short-duration versus sustained fear: a tribute to Dr. Lennart Heimer. Brain Struct. Funct. 213, 29—42.

Walsh, R.J., Slaby, F.J., Posner, B.I., 1987. A receptor-mediated mechanism for the transport of prolactin from blood to cerebrospinal fluid. Endocrinology 120, 1846—1850.

Yu-Lee, L.Y., 2002. Prolactin modulation of immune and inflammatory responses. Recent Prog. Horm. Res. 57, 435—455.

General and Comparative Endocrinology 203 (2014) 132–136

Contents lists available at ScienceDirect

General and Comparative Endocrinology

journal homepage: www.elsevier.com/locate/ygcen

Review

Arthritis and prolactin: A phylogenetic viewpoint

Norma Adán [1], María G. Ledesma-Colunga [1], Ana L. Reyes-López, Gonzalo Martínez de la Escalera, Carmen Clapp *

Instituto de Neurobiología, Universidad Nacional Autónoma de México (UNAM), Campus UNAM-Juriquilla, 76230 Querétaro, Mexico

ARTICLE INFO

Article history:
Available online 4 February 2014

Keywords:
Inflammation
Stress
Reproduction
Spondyloarthritis
Osteoarthritis
Rheumatoid arthritis

ABSTRACT

Arthritic disorders are family of diseases that have existed since vertebrate life began. Their etiology is multifactorial with genetic, environmental, and gender factors driving chronic joint inflammation. Prolactin is a sexually dimorphic hormone in mammals that can act to both promote and ameliorate rheumatic diseases. It is found in all vertebrate groups where it exerts a wide diversity of actions. This review briefly addresses the presence and features of arthritic diseases in vertebrates, the effects of PRL on joint tissues and immune cells, and whether PRL actions could have contributed to the ubiquity of arthritis in nature. This comparative approach highlights the value of PRL as a biologically conserved factor influencing the development and progression of arthritis.

1. Introduction

The joint is made of cartilage, bone, tendon, and muscle and is essential for mechanical support and mobility. The articular joint functions to transmit force from one bone to another with the cartilage providing a resistant, elastic, and smooth surface distributing load while allowing movement. Joint inflammation (arthritis) causes pain, swelling, and dysfunction, and it is a major cause of impaired movement and disability. Attesting to the influence of the terrestrial environment, arthritis has never been reported in fish, but various forms of arthritis have been documented in contemporary amphibians, reptiles, birds, and mammals and in their ancestral past. Cases of arthritis have been identified in fossil records of Triassic dinosaurs (Cisneros et al., 2010), Pleistocene mammals (Rothschild et al., 2013, 2001b), and thousands of years ago in neolithic man (Rothschild et al., 1988), indicating that inflammatory arthropathies are ancient diseases. Because in humans the age of onset of many of the most common inflammatory arthritides is in the twenties (Braun and Sieper, 2007; Warrell et al., 2010), these diseases were likely to be experienced well before reproductive senescence, and natural selection should have had the opportunity to select against them. However, in spite of evolutionary pressures, inflammatory arthritides stand as prevalent disorders across taxa. A plausible explanation for this inconsistency proposes that the painful and limiting characteristics of arthritis represent a thrifty adaptation selected to compel organisms to slow down and refrain from physically demanding activities in order to minimize voluntary energy expenditure (Reser and Reser, 2010). Such a strategy would be particularly relevant for vertebrates experiencing adversity hardship such as the starving, the stressed, the pregnant or lactating, and the elderly. The close association between arthritis, stress, gender, and reproductive states (Golding et al., 2007; Huyser and Parker, 1998; van Vollenhoven, 2009; Warrell et al., 2010) points to a contribution of chemical mediators that are upregulated in these conditions. One such mediator is prolactin (PRL), a stress-related (Gala, 1990; Reichlin, 1988) and reproductive hormone that is essential for lactation in mammals and controls a wide variety of other actions (Ben-Jonathan et al., 2008; Bole-Feysot et al., 1998) including effects on joint tissues and immune cells. PRL regulates cartilage survival (Adan et al., 2013), bone development and growth (Clement-Lacroix et al., 1999), and the proliferation, apoptosis, and release of proinflammatory mediators by immune cells (Yu-Lee, 2002), and it can both promote and mitigate rheumatic diseases (Adan et al., 2013). In this review we briefly summarize known and speculative issues underlying the presence of arthritis in different vertebrate groups and discuss the possibility that PRL regulation of joint tissues and inflammation early in vertebrate phylogeny could have influenced arthritis development and progression.

2. Inflammatory arthritides: features and etiology

Inflammatory arthritides define a group of acute and chronic arthritic conditions that involve the articular joints, the spine, and

* Corresponding author. Fax: +52 442 238 1005.
E-mail address: clapp@unam.mx (C. Clapp).
[1] Contributed equally to this work.

http://dx.doi.org/10.1016/j.ygcen.2014.01.011
0016-6480/

other organ systems. In humans, they include rheumatoid arthritis, spondyloarthritis (comprising different diseases: ankylosing spondylitis, reactive arthritis, psoriatic arthritis, arthritis conditions associated with inflammatory bowel disease), septic arthritis, and gout. Osteoarthritis may also be included as it has an inflammatory component in its advanced stages (Berenbaum, 2013). The clinical features differ among these diseases and can include deforming and destructive monoarthritis or polyarthritis (symmetric or asymmetric), cartilage degradation, bone erosion or overgrowth, synovial hyperplasia, and various degrees of extra-articular manifestations (subcutaneous nodule formation, uveitis, skin rash, vasculitis, serositis, amyloidosis, fibrosing alveolitis), systemic features of inflammation (fatigue, anaemia, weight loss), and comorbidities (cardiovascular disease, infections, and B-cell lymphomas) (Dougados and Baeten, 2011; Scott et al., 2010; Warrell et al., 2010).

The etiology is known for gout (monosodium urate crystals inducing inflammation and joint destruction) and septic arthritis (infection of a joint by Gram-positive or negative pathogens, viruses, mycobacteria, and fungi), but it remains unclear for spondyloarthritis, rheumatoid arthritis, and osteoarthritis. The latter three are multifactorial, with genetic factors (such as mutations in human leukocyte antigens and type 2 procollagen genes), environmental conditions (infectious agents, diet, physical activity, trauma) and host aspects (body size, metabolism, age, gender, reproductive state) playing a role (Dougados and Baeten, 2011; Haseeb and Haqqi, 2013; Scott et al., 2010; Sharkey et al., 2007; Warrell et al., 2010). In spondyloarthritis and rheumatoid arthritis, a complex interaction among the various contributing factors and an unidentified trigger initiates a biological response that results in the recruitment of immune cells into the joints and other sites of disease. Autoimmunity and inflammatory reactions then lead to structural joint damage and failure. In osteoarthritis, increased catabolic reactions result in cartilage damage and loss, local production of proinflammatory cytokines, and reactive bone formation (Dougados and Baeten, 2011; Berenbaum, 2013).

3. Arthritis in vertebrates

Spondyloarthritis is the most common form of arthritis in vertebrates (Rothschild, 2010; Rothschild et al., 2001b). Cases have been reported in amphibians (toads) (Brown et al., 2007), reptiles (lizards and crocodilians) (Rothschild, 2010), non-passerine birds (Rothschild and Panza, 2005), and mammals (primates, cetaceans, rhinoceros, bears, canids, and felids) (Kolmstetter et al., 2000; Kompanje, 1999; Nunn et al., 2007; Rothschild, 2005, 2001a, b). Gout and osteoarthritis have also been reported in the various vertebrates, but are rare in the wild and increase under captivity (Degernes et al., 2011; Greer et al., 2003; Rothschild, 2003, 2010; Warrell et al., 2010; Wobeser and Runge, 1975). In contrast, rheumatoid arthritis is limited to humans (Firestein, 2009), where it was first identified 5000 years ago (Rothschild, 2001) and is reported to have originated from the parent disease spondyloarthritis (Klepinger, 1978).

Prolonged locomotion and larger body size have been proposed as causative links for arthritis in vertebrates (Brown et al., 2007; Nunn et al., 2007), and joint infections increase with body size. The association of spondyloarthritis with pathogens (Dougados and Baeten, 2011; Rothschild, 2005; Shilton et al., 2008) suggests that molecular mimicry shared between micro-organisms and self antigens could help trigger an autoimmune response in susceptible individuals (Dougados and Baeten, 2011; Nunn et al., 2007). Moreover, sustained locomotion, infection, and other life-threatening scenarios (trauma, prolonged starvation, etc.) create high levels of stress, an internal condition that can precede and modify arthritis progression, given the ability of stress hormones to dampen or enhance immune function (Martin, 2009; McCray and Agarwal, 2011).

Other host factors influencing arthritis are age and gender. Spondyloarthritis and rheumatoid arthritis have a young adult onset (Dougados and Baeten, 2011; Warrell et al., 2010), whereas the incidence of osteoarthritis and gout rise with age (Haseeb and Haqqi, 2013; Saag and Choi, 2006; Warrell et al., 2010). Spondyloarthritis has no apparent gender specificity in non-human vertebrates (Rothschild et al., 2001a), albeit ankylosing spondylitis occurs preferentially in men (Dougados and Baeten, 2011), and rheumatoid arthritis and osteoarthritis are more frequent in women (Haseeb and Haqqi, 2013; Scott et al., 2010; Warrell et al., 2010). Gender correlations point to the influence of reproductive hormones in human arthritis, a conclusion supported by the amelioration of rheumatoid arthritis and psoriatic arthritis during pregnancy (Da Silva and Spector, 1992; Ostensen, 1992), and the exacerbation of rheumatoid arthritis in lactation (Barrett et al., 2000) and at menopause (Kuiper et al., 2001). A similar influence of pregnancy and lactation has been reported in rodents with induced inflammatory arthritis (Ratkay et al., 2000; Waites and Whyte, 1987), but to our knowledge there is no information concerning the influence of these reproductive states on arthritis development in wild non-mammalian and mammalian species, respectively.

PRL is a sexually dimorphic hormone in mammals that could play a role in arthritis development. Its levels are higher in mammalian females than in males, and pregnancy and lactation are states of physiological hyperprolactinemia (Ben-Jonathan et al., 2008). A number of physical and emotional forms of stress stimulate the secretion of pituitary PRL into the circulation (Gala, 1990; Reichlin, 1988), which may be an adaptation to ensure competence of the immune system (Dorshkind and Horseman, 2001; Yu-Lee, 2002), and proper physiological and behavioral responses to stress (Torner et al., 2001). Importantly, PRL promotes the growth and survival of joint tissues and protects against joint damage and inflammation in inflammatory arthritis (Adan et al., 2013).

4. PRL and arthritis

The PRL receptor is expressed in murine and human joint tissues including cartilage chondrocytes (Zermeno et al., 2006), osteoblasts (Clement-Lacroix et al., 1999), synovial cells (Nagafuchi et al., 1999), and immune cells (Yu-Lee, 2002). The human synovial fluid contains PRL (Ogueta et al., 2002) that may derive from the circulation or may be produced locally, since synovial cells (Nagafuchi et al., 1999), chondrocytes (Zermeno et al., 2006), immune cells (Montgomery, 2001), and endothelial cells (Corbacho et al., 2000) express PRL. In growing rats, treatment with PRL increases bone formation (Krishnamra and Seemoung, 1996), which slows down during embryonic development in the absence of the PRL receptor (Clement-Lacroix et al., 1999). However, targeted disruption of the PRL receptor has no articular cartilage phenotype (Adan et al., 2013), unless animals are subjected to an inflammatory challenge. Proinflammatory cytokines (cyt), including tumor necrosis factor α, interleukin 1β, and interferon γ, are major inflammatory mediators that destroy articular cartilage by inducing chondrocyte apoptosis and releasing matrix-degrading proteases (McInnes and Schett, 2007). Stimulation of chondrocyte apoptosis following the intraarticular injection of cyt is enhanced in PRL receptor null mice and reduced after inducing hyperprolactinemia in rats (Adan et al., 2013). Also, treatment with PRL inhibits the cyt-induced apoptosis of cultured chondrocytes by preventing the induction of p53 and decreasing the BAX/BCL-2 ratio through a NO-independent, JAK2/STAT3-dependent pathway (Adan et al.,

2013). Finally, eliciting hyperprolactinemia in the rat adjuvant model of inflammatory arthritis reduces chondrocyte apoptosis, proinflammatory cytokine expression, pannus formation, bone erosion, joint swelling, and pain (Adan et al., 2013). Therefore, high levels of circulating PRL protect against permanent joint damage and inflammation in experimental arthritis.

Nevertheless, the above findings are in contrast with clinical studies showing that PRL may exacerbate rheumatoid arthritis and other autoimmune diseases (systemic lupus erythematosus, Sjögren's syndrome, Hashimoto's thyroiditis, celiac disease, multiple sclerosis) (Chuang and Molitch, 2007; Jara et al., 2011; Orbach and Shoenfeld, 2007; Shelly et al., 2012). Evidence for this pathogenic action is largely circumstantial: the preponderance of these diseases in women, the higher levels of circulating PRL found in some patients, the therapeutic value of blocking PRL release with dopamine agonists, and the immunoenhancing properties of PRL (Chuang and Molitch, 2007; Jara et al., 2011; Orbach and Shoenfeld, 2007; Shelly et al., 2012). However, treatment with a dopamine agonist is not always effective, and the association between PRL levels and disease activity is inconsistent (Chuang and Molitch, 2007; Jara et al., 2011; Orbach and Shoenfeld, 2007; Shelly et al., 2012). Conclusions are confounded by locally produced PRL able to potentiate the actions of the systemic hormone, and by the ability of PRL to both stimulate or inhibit the immune system, depending on its level and the pathophysiological condition. Under stress conditions, higher levels of circulating PRL can be anti-inflammatory (Dugan et al., 2002; Oberbeck et al., 2003; Vidaller et al., 1992), whereas lower PRL levels, such as those in the non-stressed animal, are pro-inflammatory (Jacobi et al., 2001; Matera et al., 1992). When combined with interferon β, a low dose of PRL reduces inflammation in experimental multiple sclerosis and PRL receptor null mice display a significantly worse outcome than wild type mice (Zhornitsky et al., 2013). During pregnancy, when PRL levels are high, rheumatoid arthritis and multiple sclerosis go into remission (Langer-Gould and Beaber, 2013; Ostensen and Villiger, 2007) but systemic lupus erythematosus flares up (Jara et al., 2011). Also, breastfeeding, a stimulus that elevates circulating levels of PRL, exacerbates rheumatoid arthritis and systemic lupus erythematosus (Barrett et al., 2000; Mok et al., 1998), but reduces the risk of rheumatoid arthritis (Karlson et al., 2004) and protects against multiple sclerosis relapse (Langer-Gould et al., 2009). These observations indicate the ability of PRL to influence immune system homeostasis in the context of stress, inflammation, and reproduction, and support the possibility that PRL affects the development and progression of arthritis and other rheumatic diseases in mammals (Fig. 1).

5. Does PRL influence arthritis prevalence in non-mammalian vertebrates?

PRL is a multifunctional hormone with an ancient past. It is found in invertebrates (Hull et al., 1998; Quintanar et al., 2007) and thought to have evolved 400–800 million years ago to regulate water and electrolyte balance, growth and development, reproduction, endocrinology and metabolism, brain and behavior, the immune system, and angiogenesis in the various vertebrate groups (Bole-Feysot et al., 1998; Clapp et al., 2012). PRL gene sequences have been identified in all bony fish and tetrapods analyzed, they exhibit significant divergence, and their evolution may be branched into two lineages, the tetrapod lineage and the teleost lineage (Forsyth and Wallis, 2002; Huang et al., 2009). Recently, a new PRL-like gene was found in cartilaginous fish and in almost all the non-mammalian vertebrate classes but not in mammals (Huang et al., 2009). The protein encoded by this novel gene is homologous to PRL and can transactivate the PRL receptor (Huang et al., 2009).

While it is clear that PRL could play a role in regulating arthritis development in mammals, studies are incomplete or non-existent in non-mammalian species. There is evidence for the presence of PRL receptors in bone, muscle, and immune cells in fish (Manzon, 2002; Whittington and Wilson, 2013) and birds (Bu et al., 2013; Zhou et al., 1996), but no studies have addressed the presence of PRL receptor in other joint tissues of these vertebrates or in the joint tissues and immune cells of amphibians and reptiles. Notably, an energy-demanding condition that may have influenced the prevalence of arthritis in nature is that of providing nutrients to the young, the best-known effect of PRL. PRL promotes milk production in mammals, but also in fish and birds. It stimulates the surface of the skin of parent fish to produce a mucous ("discus milk") that is used to feed the developing young (Whittington

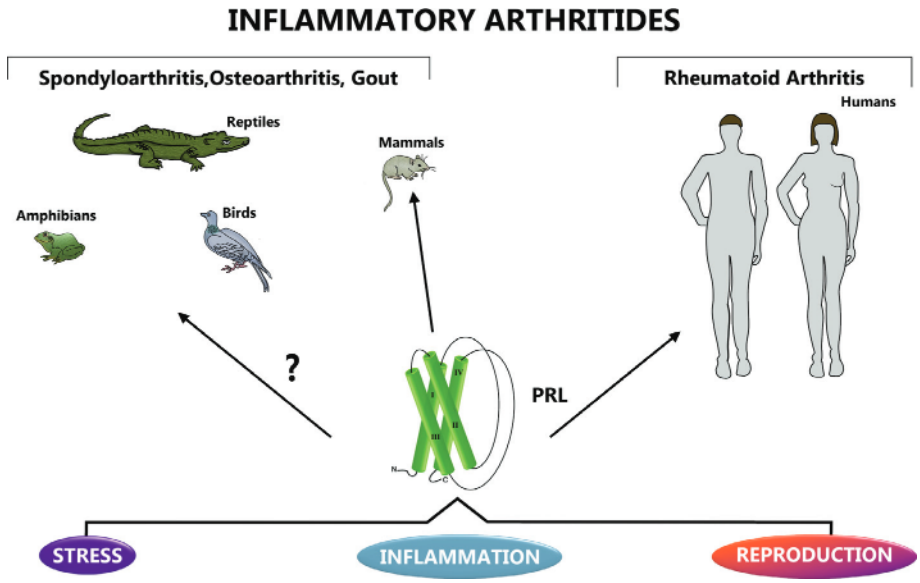

Fig. 1. Schematic representation illustrating the hypothesis that PRL levels influence the development and progression of inflammatory arthritides under conditions of stress, inflammation, and reproduction. Evidence supports these effects of PRL on rheumatoid arthritis in humans and other inflammatory arthritides in mammals, while its role remains speculative in non-mammalian vertebrates.

and Wilson, 2013). Likewise, PRL induces the growth of the mucosal epithelium lining the crop-sac (a pouch in the esophagus of birds) and clumps of cells are then shed into the lumen to feed the squabs as crop milk (Angelier and Chastel, 2009; Clapp et al., 2012). No form of lactation has been reported in contemporary reptiles, but it may have existed in their ancestral past (Else, 2013). Another phylogenetically conserved, reproductive effect of PRL is the stimulation of parental behavior, an action found in fish, birds, and mammals (Angelier and Chastel, 2009; Bole-Feysot et al., 1998; Whittington and Wilson, 2013).

Due to the increased metabolic demand related to feeding and tending the young, wild animals are especially susceptible to aversive situations (deleterious climatic events, starvation, predator attack) during the parental phase of the breeding cycle. Stressors and energetic constraints threaten parental survival, and diverse protective responses to stress have evolved. A well-known effect of stressors on parental birds is the interference with parental behavior, an effect that involves the stress-mediated downregulation of PRL levels (Angelier and Chastel, 2009). In mammals, however, there is an attenuation of neuroendocrine and emotional stress responses during pregnancy and lactation that may be an adaption that ensures maintenance of parental care although it is detrimental for parent survival (Torner and Neumann, 2002). Such attenuation can be counteracted by inhibiting the expression of PRL receptors in brain (Torner and Neumann, 2002; Torner et al., 2001). Thus, PRL has the ability to modify stress-related events either to the detriment or benefit of parental survival.

It has been proposed that arthritis developed as a survival adaptation for parents to conserve energy in conditions of severe environmental stressful conditions (Reser and Reser, 2010). Although insufficient information exists in non-mammalian species, the facts that reproductive effects of PRL and PRL stress-related interactions are phylogenetically conserved, and that PRL receptors are present in immune, bone, and muscle cells of fish and birds, prompt the speculation that PRL may act on non-mammalian vertebrates as an epigenetic, adaptive regulator of arthritis development, similar to its role in mammals (Fig. 1). Moreover, in these non-mammalian species PRL influence may extend to males and non-breeding females.

6. Concluding remarks

PRL is a regulatory hormone that can mediate stress–immune interactions in arthritic joints under reproductive and non-reproductive conditions. Arthritis and PRL have coexisted for millions of years, in a world populated by fish, amphibians, reptiles, birds, and only a few small mammals. Several functions of PRL have been conserved phylogenetically, including regulation of the stress and immune responses and parental care. The conservation of similar PRL effects throughout evolution reflects their high value and suggests they play a role in health and disease, warranting further investigation.

Acknowledgments

We thank Fernando López-Barrera and Francisco Javier Valles Valenzuela for their technical assistance, Guadalupe Calderón for artistic contribution, and Dorothy D. Pless for critically editing the manuscript. N. Adán and M.G. Ledesma-Colunga were supported by fellowships from the Council of Science and Technology of Mexico (CONACYT) and the Ph.D. Program in Biomedical Sciences of the National University of Mexico (UNAM). The study was supported by UNAM Grant (IN200312) and CONACYT Grant (161594) to C. Clapp.

References

Adan, N., Guzman-Morales, J., Ledesma-Colunga, M.G., Perales-Canales, S.I., Quintanar-Stephano, A., Lopez-Barrera, F., Mendez, I., Moreno-Carranza, B., Triebel, J., Binart, N., Martinez de la Escalera, G., Thebault, S., Clapp, C., 2013. Prolactin promotes cartilage survival and attenuates inflammation in inflammatory arthritis. J. Clin. Invest. 123, 3902–3913.
Angelier, F., Chastel, O., 2009. Stress, prolactin and parental investment in birds: a review. Gen. Comp. Endocrinol. 163, 142–148.
Barrett, J.H., Brennan, P., Fiddler, M., Silman, A., 2000. Breast-feeding and postpartum relapse in women with rheumatoid and inflammatory arthritis. Arthritis Rheum. 43, 1010–1015.
Ben-Jonathan, N., LaPensee, C.R., LaPensee, E.W., 2008. What can we learn from rodents about prolactin in humans? Endocr. Rev. 29, 1–41.
Berenbaum, F., 2013. Osteoarthritis as an inflammatory disease (osteoarthritis is not osteoarthrosis!). Osteoarthritis Cartilage/OARS Osteoarthritis Res. Soc. 21, 16–21.
Bole-Feysot, C., Goffin, V., Edery, M., Binart, N., Kelly, P.A., 1998. Prolactin (PRL) and its receptor: actions, signal transduction pathways and phenotypes observed in PRL receptor knockout mice. Endocr. Rev. 19, 225–268.
Braun, J., Sieper, J., 2007. Ankylosing spondylitis. Lancet 369, 1379–1390.
Brown, G.P., Shilton, C., Phillips, B.L., Shine, R., 2007. Invasion, stress, and spinal arthritis in cane toads. Proc. Natl. Acad. Sci. USA 104, 17698–17700.
Bu, G., Ying Wang, C., Cai, G., Leung, F.C., Xu, M., Wang, H., Huang, G., Li, J., Wang, Y., 2013. Molecular characterization of prolactin receptor (cPRLR) gene in chickens: gene structure, tissue expression, promoter analysis, and its interaction with chicken prolactin (cPRL) and prolactin-like protein (cPRL-L). Mol. Cell Endocrinol. 370, 149–162.
Cisneros, J.C., Gomes Cabral, U., de Beer, F., Damiani, R., Costa Fortier, D., 2010. Spondarthritis in the triassic. PLoS One 5, e13425.
Clapp, C., Martinez de la Escalera, L., Martinez de la Escalera, G., 2012. Prolactin and blood vessels: a comparative endocrinology perspective. Gen. Comp. Endocrinol. 176, 336–340.
Clement-Lacroix, P., Ormandy, C., Lepescheux, L., Ammann, P., Damotte, D., Goffin, V., Bouchard, B., Amling, M., Gaillard-Kelly, M., Binart, N., Baron, R., Kelly, P.A., 1999. Osteoblasts are a new target for prolactin: analysis of bone formation in prolactin receptor knockout mice. Endocrinology 140, 96–105.
Corbacho, A.M., Macotela, Y., Nava, G., Torner, L., Duenas, Z., Noris, G., Morales, M.A., Martinez De La Escalera, G., Clapp, C., 2000. Human umbilical vein endothelial cells express multiple prolactin isoforms. J. Endocrinol. 166, 53–62.
Chuang, E., Molitch, M.E., 2007. Prolactin and autoimmune diseases in humans. Acta Biomed. 78 (Suppl. 1), 255–261.
Da Silva, J.A., Spector, T.D., 1992. The role of pregnancy in the course and aetiology of rheumatoid arthritis. Clin. Rheumatol. 11, 189–194.
Degernes, L.A., Lynch, P.S., Shivaprasad, H.L., 2011. Degenerative joint disease in captive waterfowl. Avian Pathol. 40, 103–110.
Dorshkind, K., Horseman, N.D., 2001. Anterior pituitary hormones, stress, and immune system homeostasis. Bioessays 23, 288–294.
Dougados, M., Baeten, D., 2011. Spondyloarthritis. Lancet 377, 2127–2137.
Dugan, A.L., Thellin, O., Buckley, D.J., Buckley, A.R., Ogle, C.K., Horseman, N.D., 2002. Effects of prolactin deficiency on myelopoiesis and splenic T lymphocyte proliferation in thermally injured mice. Endocrinology 143, 4147–4151.
Else, P.L., 2013. Dinosaur lactation? J. Exp. Biol. 216, 347–351.
Firestein, G.S., 2009. Rheumatoid arthritis in a mouse? Nat. Clin. Pract. Rheumatol. 5, 1.
Forsyth, I.A., Wallis, M., 2002. Growth hormone and prolactin–molecular and functional evolution. J. Mammary Gland Biol. Neoplasia 7, 291–312.
Gala, R.R., 1990. The physiology and mechanisms of the stress-induced changes in prolactin secretion in the rat. Life Sci. 46, 1407–1420.
Golding, A., Haque, U.J., Giles, J.T., 2007. Rheumatoid arthritis and reproduction. Rheum. Dis. Clin. North Am. 33, 319–343, vi–vii.
Greer, L.L., Strandberg, J.D., Whitaker, B.R., 2003. *Mycobacterium chelonae* osteoarthritis in a Kemp's ridley sea turtle (*Lepidochelys kempii*). J. Wildl. Dis. 39, 736–741.
Haseeb, A., Haqqi, T.M., 2013. Immunopathogenesis of osteoarthritis. Clin. Immunol. 146, 185–196.
Huang, X., Hui, M.N., Liu, Y., Yuen, D.S., Zhang, Y., Chan, W.Y., Lin, H.R., Cheng, S.H., Cheng, C.H., 2009. Discovery of a novel prolactin in non-mammalian vertebrates: evolutionary perspectives and its involvement in teleost retina development. PLoS One 4, e6163.
Hull, K.L., Fathimani, K., Sharma, P., Harvey, S., 1998. Calcitropic peptides: neural perspectives. Comp. Biochem. Physiol. C Pharmacol. Toxicol. Endocrinol. 119, 389–410.
Huyser, B., Parker, J.C., 1998. Stress and rheumatoid arthritis: an integrative review. Arthritis Care Res. 11, 135–145.
Jacobi, A.M., Rohde, W., Volk, H.D., Dorner, T., Burmester, G.R., Hiepe, F., 2001. Prolactin enhances the in vitro production of IgG in peripheral blood mononuclear cells from patients with systemic lupus erythematosus but not from healthy controls. Ann. Rheum. Dis. 60, 242–247.
Jara, L.J., Medina, G., Saavedra, M.A., Vera-Lastra, O., Navarro, C., 2011. Prolactin and autoimmunity. Clin. Rev. Allergy Immunol. 40, 50–59.
Karlson, E., Mandl, L., Hankinson, S., Grodstein, F., 2004. Do breast-feeding and other reproductive factors influence future risk of rheumatoid arthritis? Results from the Nurses' Health Study. Arthritis Rheum. 50, 3458–3467.

Klepinger, L.L., 1978. Paleopathologic evidence for the evolution of rheumatoid arthritis. Am. J. Phys. Anthropol. 50, 119–122.
Kolmstetter, C., Munson, L., Ramsay, E.C., 2000. Degenerative spinal disease in large felids. J. Zoo Wildl. Med. 31, 15–19.
Kompanje, E., 1999. Considerations on the comparative pathology of the vertebrae in Mysticeti and Odontoceti; evidence for the occurrence of discarthrosis, zygarthrosis, infectious spondylitis and spondyloarthritis. Zoologische Mededeelingen 73, 99–130.
Krishnamra, N., Seemoung, J., 1996. Effects of acute and long-term administration of prolactin on bone ^{45}Ca uptake, calcium deposit, and calcium resorption in weaned, young, and mature rats. Can. J. Physiol. Pharmacol. 74, 1157–1165.
Kuiper, S., van Gestel, A.M., Swinkels, H.L., de Boo, T.M., da Silva, J.A., van Riel, P.L., 2001. Influence of sex, age, and menopausal state on the course of early rheumatoid arthritis. J. Rheumatol. 28, 1809–1816.
Langer-Gould, A., Beaber, B.E., 2013. Effects of pregnancy and breastfeeding on the multiple sclerosis disease course. Clin. Immunol. 149, 244–250.
Langer-Gould, A., Huang, S.M., Gupta, R., Leimpeter, A.D., Greenwood, E., Albers, K.B., Van Den Eeden, S.K., Nelson, L.M., 2009. Exclusive breastfeeding and the risk of postpartum relapses in women with multiple sclerosis. Arch. Neurol. 66, 958–963.
Manzon, L.A., 2002. The role of prolactin in fish osmoregulation: a review. Gen. Comp. Endocrinol. 125, 291–310.
Martin, L.B., 2009. Stress and immunity in wild vertebrates: timing is everything. Gen. Comp. Endocrinol. 163, 70–76.
Matera, L., Cesano, A., Bellone, G., Oberholtzer, E., 1992. Modulatory effect of prolactin on the resting and mitogen-induced activity of T, B, and NK lymphocytes. Brain Behav. Immun. 6, 409–417.
McCray, C.J., Agarwal, S.K., 2011. Stress and autoimmunity. Immunol. Allergy Clin. North Am. 31, 1–18.
McInnes, I.B., Schett, G., 2007. Cytokines in the pathogenesis of rheumatoid arthritis. Nat. Rev. Immunol. 7, 429–442.
Mok, C.C., Wong, R.W., Lau, C.S., 1998. Exacerbation of systemic lupus erythematosus by breast feeding. Lupus 7, 569–570.
Montgomery, D.W., 2001. Prolactin production by immune cells. Lupus 10, 665–675.
Nagafuchi, H., Suzuki, N., Kaneko, A., Asai, T., Sakane, T., 1999. Prolactin locally produced by synovium infiltrating T lymphocytes induces excessive synovial cell functions in patients with rheumatoid arthritis. J. Rheumatol. 26, 1890–1900.
Nunn, C., Rothschild, B., Gittleman, J., 2007. Why are some species more commonly afflicted by arthritis than others? A comparative study of spondyloarthropathy in primates and carnivores. J. Evol. Biol. 20, 460–470.
Oberbeck, R., Schmitz, D., Wilsenack, K., Schuler, M., Biskup, C., Schedlowski, M., Nast-Kolb, D., Exton, M.S., 2003. Prolactin modulates survival and cellular immune functions in septic mice. J. Surg. Res. 113, 248–256.
Ogueta, S., Munoz, J., Obregon, E., Delgado-Baeza, E., Garcia-Ruiz, J.P., 2002. Prolactin is a component of the human synovial liquid and modulates the growth and chondrogenic differentiation of bone marrow-derived mesenchymal stem cells. Mol. Cell Endocrinol. 190, 51–63.
Orbach, H., Shoenfeld, Y., 2007. Hyperprolactinemia and autoimmune diseases. Autoimmun. Rev. 6, 537–542.
Ostensen, M., 1992. The effect of pregnancy on ankylosing spondylitis, psoriatic arthritis, and juvenile rheumatoid arthritis. Am. J. Reprod. Immunol. 28, 235–237.
Ostensen, M., Villiger, P.M., 2007. The remission of rheumatoid arthritis during pregnancy. Semin. Immunopathol. 29, 185–191.
Quintanar, J.L., Salinas, E., Guerrero, R., Gomez, R., Vidal, S., Aranda, J., Clapp, C., 2007. Prolactin-like hormone in the nematode *Trichinella spiralis* larvae. Exp. Parasitol. 116, 137–141.
Ratkay, L.G., Weinberg, J., Waterfield, J.D., 2000. The effect of lactation in the post-partum arthritis of MRL-lpr/fasmice. Rheumatol. (Oxford) 39, 646–651.
Reichlin, S., 1988. Prolactin and growth hormone secretion in stress. Adv. Exp. Med. Biol. 245, 353–376.
Reser, J., Reser, W., 2010. Does rheumatoid arthritis represent an adaptive, thrifty condition? Med. Hypotheses 74, 189–194.
Rothschild, B., 2003. Osteoarthritis as a complication of artificial environment: the Cavia (Guinea pig) story. Ann. Rheum. Dis. 62, 1022–1023.
Rothschild, B., 2005. Primate spondyloarthropathy. Curr. Rheumatol Rep. 7, 173–181.
Rothschild, B., 2010. Macroscopic recognition of nontraumatic osseous pathology in the postcranial skeletons of crocodilians and lizards. J. Herpetol. 44, 13–20.
Rothschild, B., Hao-Wen, T., Tao, D., 2013. Arthritis through geologic time and its environmental implications. J. Anc. Dis. Prev. Rem. 1 (101). http://dx.doi.org/10.4172/jadpr1000101.
Rothschild, B., Panza, R., 2005. Epidemiologic assessment of trauma-independent skeletal pathology in non-passerine birds from museum collections. Avian Pathol. 34, 212–219.
Rothschild, B., Rothschild, C., Woods, R., 2001a. Inflammatory arthritis in canids: spondyloarthropathy. J. Zoo Wildl. Med. 32, 58–64.
Rothschild, B.M., 2001. Rheumatoid arthritis at a time of passage. J. Rheumatol. 28, 245–250.
Rothschild, B.M., Prothero, D.R., Rothschild, C., 2001b. Origins of spondyloarthropathy in *Perissodactyla*. Clin. Exp. Rheumatol. 19, 628–632.
Rothschild, B.M., Turner, K.R., DeLuca, M.A., 1988. Symmetrical erosive peripheral polyarthritis in the late Archaic period of Alabama. Science 241, 1498–1501.
Saag, K.G., Choi, H., 2006. Epidemiology, risk factors, and lifestyle modifications for gout. Arthritis Res Ther. 8 (Suppl. 1), S2.
Scott, D.L., Wolfe, F., Huizinga, T.W., 2010. Rheumatoid arthritis. Lancet 376, 1094–1108.
Sharkey, P.F., Paskin, D.L., Meade, T.D., Rothman, R.H., 2007. Diet, nutrition, obesity, and their roles in arthritis. Semin. Arthroplasty 18, 117–121.
Shelly, S., Boaz, M., Orbach, H., 2012. Prolactin and autoimmunity. Autoimmun. Rev. 11, A465–A470.
Shilton, C.M., Brown, G.P., Benedict, S., Shine, R., 2008. Spinal arthropathy associated with *Ochrobactrum anthropi* in free-ranging cane toads (*Chaunus* [*Bufo*] *marinus*) in Australia. Vet. Pathol. 45, 85–94.
Torner, L., Neumann, I.D., 2002. The brain prolactin system: involvement in stress response adaptations in lactation. Stress 5, 249–257.
Torner, L., Toschi, N., Pohlinger, A., Landgraf, R., Neumann, I.D., 2001. Anxiolytic and anti-stress effects of brain prolactin: improved efficacy of antisense targeting of the prolactin receptor by molecular modeling. J. Neurosci. 21, 3207–3214.
van Vollenhoven, R.F., 2009. Sex differences in rheumatoid arthritis: more than meets the eye. BMC Med. 7, 12.
Vidaller, A., Guadarrama, F., Llorente, L., Mendez, J.B., Larrea, F., Villa, A.R., Alarcon-Segovia, D., 1992. Hyperprolactinemia inhibits natural killer (NK) cell function in vivo and its bromocriptine treatment not only corrects it but makes it more efficient. J. Clin. Immunol. 12, 210–215.
Waites, G.T., Whyte, A., 1987. Effect of pregnancy on collagen-induced arthritis in mice. Clin. Exp. Immunol. 67, 467–476.
Warrell, D.A., Cox, T.M., Firth, J.D., 2010. Oxford Textbook of Medicine, fifth ed. Oxford University Press, New York.
Whittington, C.M., Wilson, A.B., 2013. The role of prolactin in fish reproduction. Gen. Comp. Endocrinol. 191, 123–136.
Wobeser, G., Runge, W., 1975. Arthropathy in white-tailed deer and a moose. J. Wildl. Dis. 11, 116–121.
Yu-Lee, L.Y., 2002. Prolactin modulation of immune and inflammatory responses. Recent Prog. Horm. Res. 57, 435–455.
Zermeno, C., Guzman-Morales, J., Macotela, Y., Nava, G., Lopez-Barrera, F., Kouri, J.B., Lavalle, C., de la Escalera, G.M., Clapp, C., 2006. Prolactin inhibits the apoptosis of chondrocytes induced by serum starvation. J. Endocrinol. 189, R1–R8.
Zhornitsky, S., Yong, V.W., Weiss, S., Metz, L.M., 2013. Prolactin in multiple sclerosis. Mult. Scler. 19, 15–23.
Zhou, J.F., Zadworny, D., Guemene, D., Kuhnlein, U., 1996. Molecular cloning, tissue distribution, and expression of the prolactin receptor during various reproductive states in *Meleagris gallopavo*. Biol. Reprod. 55, 1081–1090.

Chapter 4
Regulation of Blood Vessels by Prolactin and Vasoinhibins

Carmen Clapp, Stéphanie Thebault, Yazmín Macotela, Bibiana Moreno-Carranza, Jakob Triebel and Gonzalo Martínez de la Escalera

Abstract Prolactin (PRL) stimulates the growth of new blood vessels (angiogenesis) either directly through actions on endothelial cells or indirectly by upregulating pro-angiogenic factors like vascular endothelial growth factor (VEGF). Moreover, PRL acquires antiangiogenic properties after undergoing proteolytic cleavage to vasoinhibins, a family of PRL fragments (including 16 kDa PRL) with potent antiangiogenic, vasoconstrictive, and antivasopermeability effects. In view of the opposing actions of PRL and vasoinhibins, the regulation of the proteases responsible for specific PRL cleavage represents an efficient mechanism for controlling blood vessel growth and function. This review briefly describes the vascular actions of PRL and vasoinhibins, and addresses how their interplay could help drive biological effects of PRL in the context of health and disease.

4.1 Introduction

Prolactin (PRL) is remarkably versatile, as it regulates various events in reproduction, osmoregulation, growth, energy metabolism, immune response, brain function, and behavior [1–3]. Blood vessels are emerging as PRL targets contributing to these actions [4]. By transporting fluid, nutrients, oxygen, hormones, growth factors, cytokines, immune cells, and waste material, the vascular system helps regulate most if not all body functions including growth, energy homeostasis, inflammation, and brain activity. PRL stimulates or inhibits the proliferation, dilation, permeability, and regression of blood vessels. These opposing effects reside within the PRL molecule as the full-length protein promotes angiogenesis, but after proteolytic processing the resulting PRL fragments, vasoinhibins, exert antiangiogenic, vasoconstrictive, and antivasopermeability effects (Fig. 4.1). The combination of these stimulatory and inhibitory properties can lead to differences in the perfusion of target tissues, thereby influencing their growth and function. In this review, we

C. Clapp (✉) · S. Thebault · Y. Macotela · B. Moreno-Carranza
J. Triebel · G. Martínez de la Escalera
Instituto de Neurobiología, Universidad Nacional Autónoma de México,
Campus UNAM-Juriquilla, 76230 Querétaro, QRO, México
e-mail: clapp@unam.mx

M. Diakonova (ed.), *Recent Advances in Prolactin Research,* Advances in Experimental Medicine and Biology 846, DOI 10.1007/978-3-319-12114-7_4

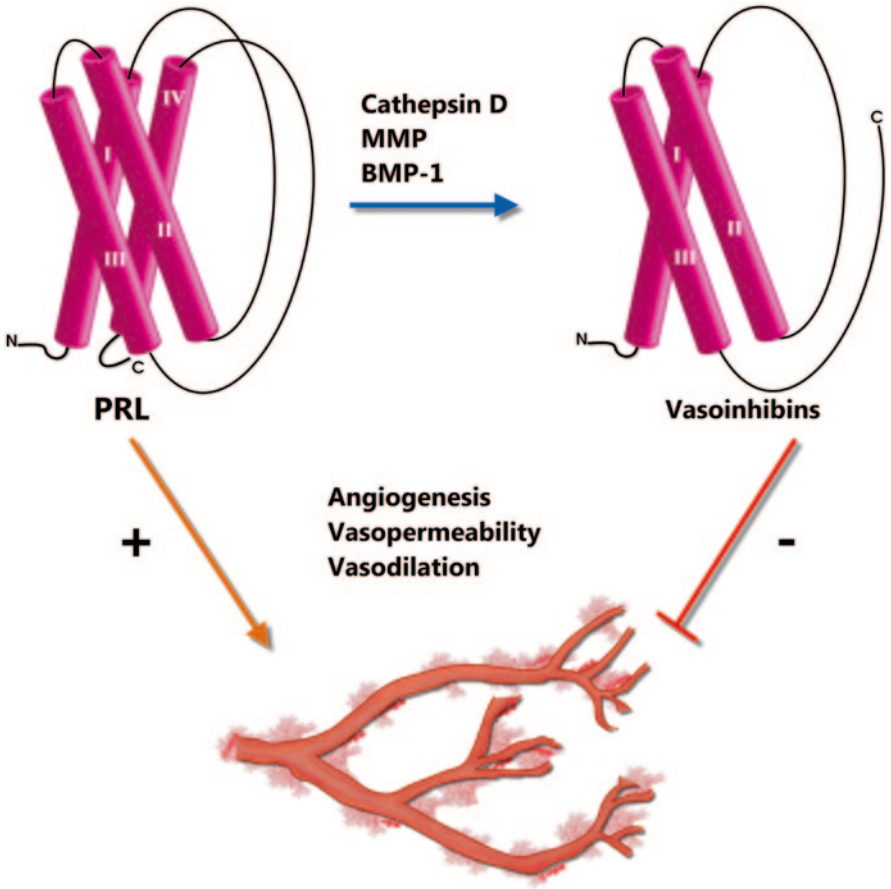

Fig. 4.1 *PRL* stimulates blood vessel growth and function and acquires vascular inhibitory properties after undergoing specific proteolytic cleavage to vasoinhibins by cathepsin D, matrix metalloproteases (MMP), and bone morphogenetic protein-1 (BMP-1)

clarify the advantage of the vasoinhibin nomenclature, and concisely address the generation of vasoinhibins, the effects of PRL and vasoinhibins on blood vessels, and how these vascular actions could affect tissue growth, function, and involution under normal and pathological conditions.

4.2 The Vasoinhibin Term

PRL fragments with inhibitory effects on blood vessels were originally termed "16 kDa PRL." The initial paper by Ferrara et al. [5] used a purified fraction of enzymatically cleaved rat PRL (having 145 amino acids and 16.3 kDa) that showed

an inhibitory effect on endothelial cell proliferation. However, follow-up studies, confirming and extending these vascular actions, used recombinant PRL fragments of different sizes that were still named 16 kDa PRL in an attempt to maintain the connection to the original preparation. Indeed, various laboratories used a recombinant fragment of 14 kDa containing the first 123 amino acids of human PRL [6–8], the same fragment but coupled to a polyhistidine tail [9, 10], a 15.6 kDa fragment containing the first 139 amino acids of human PRL [11–13], or a 17.2 kDa fragment containing the first 150 amino acids of human PRL [14]. The term 16 kDa PRL became even less accurate when studying the endogenous peptides generated by specific proteases. It then became evident that PRL fragments with inhibitory effects on blood vessels are not a single 16 kDa species, but rather a family of peptides with different molecular masses so far ranging from 14 to 18 kDa and all sharing the N-terminal region of PRL.

Different proteases generate the various fragments by cleaving at different sites near or within the long loop connecting the third and fourth α-helices of the PRL molecule (Fig. 4.1). Cathepsin D cleaves rat PRL and mouse PRL into a 16 kDa N-terminal fragment [15, 16], bovine PRL into 14 and 16 kDa N-terminal fragments [17], buffalo PRL into 11, 14, and 18 kDa antiangiogenic fragments [18], and human PRL into 11, 15, 16.5, and 17 kDa N-terminal fragments [19]. Matrix metalloproteases (MMP) predominantly cleave human and rat PRL at amino acids 155 and 153, respectively, to generate 17 kDa N-terminal fragments [20], and bone morphogenetic protein-1 (BMP-1) cleaves after the first 159 amino acids of human and mouse PRL, generating an 18 kDa fragment [21]. Since these peptides share blood vessel inhibitory properties, in 2006 we proposed the term “vasoinhibins” [20, 22] to refer to the whole family of PRL-derived N-terminal fragments that have inhibitory vascular effects. All PRL N-terminal fragments of 14 to 18 kDa that have been tested to date demonstrate blood vessel inhibitory properties, reinforcing the concept that this structure is responsible for the vasoinhibin identity.

4.3 Generation of Endogenous Vasoinhibins

The fact that vasoinhibins are produced by different proteases implies that their generation can occur under different conditions and tissue microenvironments. Cathepsin D is catalytically active at acidic pH (pH < 5.5), and recent findings showed that it is the main vasoinhibin-generating enzyme in anterior pituitary lactotrophs [23]. Cathepsin D is located in PRL secretory granules, which are acidic, and cathepsin-D null mice are devoid of vasoinhibins in the anterior pituitary gland [23]. Accordingly, vasoinhibins can be generated by cathepsin D during the pituitary PRL secretory process and thus, subjected to regulated release. Along this line, estradiol increases the synthesis and activity of cathepsin D [24], and the production of anterior pituitary vasoinhibins is higher in females [23], increases at proestrus with respect to diestrus, and estrogens stimulate their release [25].

Cathepsin D may also be released from secretory granules or lysosomes at anterior pituitary or extrapituitary locations to generate vasoinhibins outside cells. Cathepsin D cleaves PRL in the extracellular milieu of regressing corpus luteum [17] and mammary gland [16], and in cardiomyocytes under oxidative stress [13], conditions in which tissue remodelling and altered metabolic activity can acidify the pericellular pH. Cultured GH4C1 pituitary adenoma cells also secrete cathepsin D, and mimicking the tumor microenvironment by exposure to hypoxia reduces its release [26], suggesting that extracellular production of vasoinhibins could be decreased and favor the proangiogenic condition necessary for prolactinoma growth.

On the other hand, PRL may be physiologically cleaved outside cells by the extracellular matrix-degrading enzymes, MMP and BMP-1, which act at neutral pH and are secreted or anchored to the external cell surface. MMP and BMP-1 released by chondrocytes [20] and embryonic fibroblasts [21], respectively, generate vasoinhibins from PRL, a mechanism that may serve to maintain cartilage avascularity and to limit developmental angiogenesis. MMP and BMP-1 also produce other antiangiogenic factors by proteolytic processing [27, 28]; however, both types of proteases are upregulated in diseased states characterized by blood vessel growth and invasion [29, 30]. As high concentrations of MMP also lead to the degradation of both PRL and vasoinhibin [20], in some cases MMP upregulation may downregulate vasoinhibins to favor pathological angiogenesis.

Consistent with the ubiquitous nature of PRL-cleaving enzymes, endogenous vasoinhibins have been identified in the anterior [23] and posterior pituitary gland [31], hypothalamus [32], cartilage [20], retina [33], cardiomyocytes [13], corpus luteum [17], mammary gland [16], and in biological fluids (serum, amniotic fluid, and urine) [34, 35].

4.4 Vascular Effects of PRL and Vasoinhibins

The effects and signaling mechanisms of PRL and vasoinhibins on blood vessels have been extensively reviewed [4, 22, 36]. Here, we will briefly summarize previous findings with a focus on recent advances. PRL stimulates angiogenesis during development (chick chorioallantoic membrane, CAM) and in adult tissues (corpus luteum, testis, and heart). These observations were recently extended to include the angiogenesis of transplanted pancreatic islets [37] and the neovascularization associated with normal and regenerative liver growth, where inducing hyperprolactinemia increased hepatic endothelial cell proliferation and vascular endothelial growth factor (VEGF) expression [38, 39]. Moreover, in addition to the known effects of PRL on endothelial cell proliferation and VEGF expression, PRL was recently shown to stimulate the migration and tube formation of endothelial cells [40, 41], to reduce vasopermeability by upregulating the expression of tight-junction proteins between endothelial cells [42], and to promote intussusceptive angiogenesis in the CAM [40]. The latter differs from sprouting angiogenesis in that new blood vessels are formed by the splitting of an existing blood vessel in two, which is essentially independent of endothelial cell proliferation and thereby, less energy demanding [43].

PRL can promote angiogenesis by direct actions on endothelial cells. However, the effects of PRL on cultured endothelial cells are modest and not always observed [40, 41, 36]. PRL actions may be limited by underexpressed PRL receptors in endothelial cells. Exposure to ovarian follicular fluid stimulates the expression of the long and short PRL receptor isoforms in bovine umbilical vein endothelial cells (BUVEC), and PRL does not stimulate BUVEC proliferation unless the cells are pretreated with ovarian follicular fluid [44]. In addition, vascular endothelial cells produce and release PRL, so the locally produced hormone may limit the effects of exogenous PRL by occupying its receptors in endothelial cells. Yang and colleagues recently highlighted the role of PRL as an autocrine regulator of angiogenesis. They showed that PRL produced by endothelial cells is a downstream mediator of STAT5-induced endothelial cell migration, invasion, tube formation, and VEGF expression [41]. The fact that STAT5 mediates these angiogenesis events in response to fibroblast growth factor-2 (FGF-2) [45] places PRL in the signaling cascade of potent angiogenesis stimulators. Also, PRL itself activates STAT5 in endothelial cells [40, 41] and stimulates the expression of FGF-2 and VEGF by various nonendothelial cell types [4], suggesting that PRL acts as a positive autocrine and paracrine feedback regulator of angiogenesis.

The complexity of the vascular effects of PRL is further illustrated by conflicting data showing that PRL is unable to stimulate angiogenesis in the mouse cornea, that siRNA-targeting PRL results in angiogenesis in the rat retina, and that disruption of the PRL gene is associated with highly vascularized pituitary tumors in aged mice [4, 36]. Moreover, PRL has opposing effects on vascular resistance, blood volume, and blood flow that depend on the experimental model and conditions [36]. These inconsistencies may involve the proteolytic conversion of PRL to vasoinhibins.

Vasoinhibins inhibit angiogenesis, vasodilation, and vasopermeability, and promote vascular regression in the cornea, retina, heart, and xenografted tumors. They act directly on endothelial cells to inhibit the action of several vasoactive substances including: VEGF, FGF-2, interleukin 1-β, bradykinin, and acetylcholine. Vasoinhibins signal through a still-unidentified receptor distinct from the PRL receptor: (1) to cause cell cycle arrest by blocking activation of the MAPK pathway at the level of Ras, decreasing cyclin D1, and upregulating p21; (2) to inhibit endothelial cell migration by increasing type-1 plasminogen activator inhibitor and thus reducing urokinase activity, and by downregulating the Ras-Tiam1-Rac1-Pak1 pathway; and (3) to induce endothelial cell apoptosis by promoting NFκB-mediated caspase-8 and 9 activation, which in turn stimulate caspase-3 and DNA fragmentation. In addition, vasoinhibins were recently shown to induce the expression of microRNA-146a (miR-146a) in endothelial cells in an NFκB-dependent manner [46]. Silencing miR-146a expression prevented the inhibitory effects of vasoinhibins on endothelial cell proliferation and survival, but not on endothelial cell migration, revealing miR-146a as a mediator of a large fraction of vasoinhibins antiangiogenic effects.

Another key mechanism by which vasoinhibins regulate endothelial cell function, specifically causing vasoconstriction and reduced vasopermeability, is by blocking the activation of endothelial nitric oxide synthase (eNOS). They do so by promoting protein phosphatase 2 A-induced dephosphorylation and inactivation of eNOS, by blocking the activation of phospholipase C and the formation of inositol

1,4,5-triphosphate leading to a reduced release of Ca^{2+} from intracellular stores, and by interfering the expression of transient receptor potential canonical (TRPC) channels [47, 4]. Also, dephosphorylation-mediated inactivation of eNOS can contribute to vasoinhibin inhibition of endothelial cell proliferation and migration. Vasoinhibins block the increase in eNOS activity, migration, and proliferation of endothelial cells overexpressing wild type eNOS but did not affect these responses in cells overexpressing phosphomimetic or nonphosphorylatable eNOS mutants [48].

Besides inhibiting eNOS-mediated vasodilation, vasoinhibins can lower blood flow in developing blood vessels by reducing pericyte coverage of capillaries [49]. Vasoinhibins interfere with pericyte recruitment by disrupting the Notch signaling pathway in endothelial cells, and this action can lead to a dysfunctional vasculature in a murine melanoma tumor model [49]. Finally, vasoinhibins exert proinflammatory actions on blood vessels; they stimulate leukocyte adhesion to endothelial cells and leukocyte infiltration into tumors by activating NFκB and increasing the expression of adhesion molecules in endothelial cells [50]. These actions may also involve vasoinhibin-induced downregulation of eNOS, since VEGF stimulation of eNOS-mediated NO production promotes endothelial cell anergy [51].

In spite of the abundance of data concerning the vascular actions and signaling mechanisms of vasoinhibins, the nature of the vasoinhibin receptor remains unresolved. More than two decades ago, vasoinhibins were shown to bind to a single class of sites on endothelial cell membranes (Kd of 1–10 nM), associating with proteins of 52 and 32 kDa that were distinct from the PRL receptor [52]. Whether these represented receptors or regulatory binding proteins important for vasoinhibin functions is unknown. Difficulties in identifying the vasoinhibin receptor(s) may lie in that they could be forming a complex with other receptors and binding proteins. Similar receptor complexes have been proposed for angiostatin and endostatin, that are also families of antiangiogenic peptides derived by proteolysis from precursor proteins [53, 54].

4.5 Contribution of Blood Vessel Regulation to PRL Biological Effects

The influence of the vascular actions of PRL and vasoinhibins on the regulation of PRL target organs (crop-sac, mammary gland, corpus luteum, retina, cartilage, and heart) has been previously reviewed in a physiopathological [4, 36, 55, 56] and evolutionary [57] context. Here, we extend this discussion by addressing recent findings and promising new avenues.

4.5.1 Mammary Gland

The mammary gland stands as a major PRL target organ. PRL stimulates the growth, differentiation, milk production, and survival of mammary epithelium.

These events are dependent on the expansion and regression of the mammary gland vasculature [58], which may be influenced by PRL and vasoinhibins. PRL promotes the expression of VEGF in mammary epithelial cells [36], and weaning upregulates the expression and activity of the vasoinhibin-generating proteases, MMP, and cathepsin D [59]. Vasoinhibins were recently detected in mouse mammary glands, and their levels increased during involution together with those of the mature cathepsin D isoform [16]. Moreover, PRL stimulates the activation and polarized secretion of cathepsin D by mammary tissue [60]. This mechanism may help attenuate vascular expansion during lactation and promote blood vessel regression during involution since PRL expression and cathepsin D-mediated PRL cleavage increase in the lactating and regressing mammary gland [16, 36].

However, the mechanisms regulating the antiangiogenic effects of vasoinhibins may be altered in the malignant state. Neoplastic breast tissue shows diminished vasoinhibin-generating activity [61] and higher levels of PRL receptors in cells [62], including those of the microvasculature [40]. In contrast to the reduced growth observed in prostate, colon, and melanoma tumors expressing vasoinhibins, tumors derived from breast cancer cells induced to produce vasoinhibins exhibit decreased vascularization but no effect on tumor size [14]. This is surprising as vasoinhibins have the ability to inhibit and promote the growth [14] and apoptosis [16] of breast cancer cells, respectively.

4.5.2 Corpus Luteum

Similar to the mammary gland, the corpus luteum undergoes dramatic expansion and involution at the expense of the vasculature. In rodents, PRL is luteotrophic in pregnancy but luteolytic during nonfertile cycles. These opposing effects may reflect in part the vascular interplay between PRL and vasoinhibins. PRL stimulates the proliferation of endothelial cells in the corpus luteum, and lowering systemic PRL or disrupting the PRL receptor interferes with corpus luteum neovascularization. By using transgenic mice expressing only the long form of the PRL receptor, PRL-induced stimulation of VEGF production and neovascularization of the corpus luteum was specifically linked to the short form of the PRL receptor [63], which is the predominant form found in corpus luteum endothelial cells [64].

4.5.3 Retina

In contrast to reproductive organs, the vasculature is dormant throughout life in most adult tissues and is highly restricted in cases such as the retina. Vasoinhibins help maintain the quiescent state of retinal blood vessels and protect against aberrant vasopermeability and angiogenesis in retinopathy of prematurity and diabetic retinopathy. Retinal vasoinhibins may derive from PRL synthesized in the retina and from systemic PRL accessing the eye via its receptors in the ciliary body [65].

Hyperprolactinemia increases the levels of retinal vasoinhibins, which in turn reduce VEGF and diabetes-induced retinal vasopermeability [65]. Similarly, the transfer to the retina of the vasoinhibin gene via adenoassociated virus type 2 vectors prevents vascular alterations associated with nonproliferative diabetic retinopathy [66].

4.5.4 Heart

Accumulating evidence has linked vasoinhibin overproduction to the pathophysiology of peripartum cardiomyopathy. Increased oxidative stress causes cathepsin D-mediated PRL cleavage to vasoinhibins, which in turn interfere with the growth and function of coronary vasculature required for adequate performance of the maternal heart during pregnancy and lactation. MiR-146a, discovered as a major mediator of vasoinhibin antiangiogenic actions, is also responsible for vasoinhibin effects causing myocardial metabolic dysfunction [46]. Vasoinhibins stimulate the shedding from endothelial cells of exosomes loaded with mirR-146a that, when absorbed by cardiomyocytes, impairs their metabolic activity [46]. Altogether, these concepts have led to the development of promising combination therapies employing bromocriptine and to the evaluation of markers (cathepsin D activity and miR-146a serum levels) for diagnosis and disease monitoring [67].

4.5.5 Other

Other promising research directions relate to the liver, pancreas, and brain. Liver growth is angiogenesis-dependent and coincides with the hyperprolactinemia ocurring during pregnancy and lactation, cirrhosis [68], and after partial hepatectomy [69]. Absence of the PRL receptor confers reduced liver mass, and elevating systemic PRL promotes growth and neovascularization of the normal and regenerating adult liver [38]. During pregnancy, the need for insulin action results in pancreatic islet growth, which is angiogenesis dependent. PRL and placental lactogens stimulate the proliferation, survival, and insulin production by pancreatic β-cells [70], and PRL stimulates vascular density and downregulates the expression of the angiogenesis inhibitor thrombospondin-1 (TSP-1) in transplanted pancreatic islets [37]. Moreover, chronic exposure of isolated human islets to high glucose concentrations impairs angiogenesis, reduces PRL and MMP-9 expression, and increases TSP-1 synthesis [71]. These findings suggest that PRL mediates pancreatic islet neovascularization and growth during pregnancy, and that an altered production of PRL and vasoinhibins may impact abnormal islet angiogenesis in diabetes. PRL acts in the brain to stimulate neurogenesis and neuronal survival [3], which are effects frequently elicited by proangiogenic substances [72]. PRL also reduces the permeability of brain capillary endothelial cells in a NO-independent manner [42], and vasoinhibins inhibit NO-dependent vasopermeability in the retina, thus suggesting that the PRL-vasoinhibin system helps maintain the brain- and retinal-blood

barriers. Finally, exposure to stress reduces the conversion of PRL to vasoinhibins in the hypothalamus, and the intracerebroventricular administration of PRL and vasoinhibins attenuates and enhances stress-related behaviors (anxiety and depression) [32], respectively; these behaviors associate with altered cerebral blood flow and endothelial cell dysfunction [73].

Concluding Remarks

The vascular effects of PRL and vasoinhibins are emerging as novel mechanisms balancing growth, function, and involution. Further research is needed to clarify the regulation of the specific proteases, the receptors, and signaling pathways involved, and how PRL and vasoinhibins interact to affect blood vessel and organ function under health and disease.

Acknowledgements We thank Guadalupe Calderón for her artistic illustration, Fernando López-Barrera, Gabriel Nava, and Francisco Javier Valles Valenzuela for their technical assistance, and Dorothy D. Pless for critically editing the manuscript. This work was supported by grants from the National Council of Science and Technology of Mexico (161594 and 179496) and from UNAM (IN200312).

References

1. Bole-Feysot C, Goffin V, Edery M, Binart N, Kelly PA (1998) Prolactin (PRL) and its receptor: actions, signal transduction pathways and phenotypes observed in PRL receptor knockout mice. Endocr Rev 19(3):225–268
2. Ben-Jonathan N, Hugo ER, Brandebourg TD, LaPensee CR (2006) Focus on prolactin as a metabolic hormone. Trends Endocr Metab TEM 17(3):110–116
3. Grattan DR, Kokay IC (2008) Prolactin: a pleiotropic neuroendocrine hormone. J Neuroendocrinol 20(6):752–763
4. Clapp C, Thebault S, Jeziorski MC, Martinez De La Escalera G (2009) Peptide hormone regulation of angiogenesis. Physiol Rev 89(4):1177–1215
5. Ferrara N, Clapp C, Weiner R (1991) The 16 K fragment of prolactin specifically inhibits basal or fibroblast growth factor stimulated growth of capillary endothelial cells. Endocrinology 129(2):896–900
6. Clapp C, Martial JA, Guzman RC, Rentier-Delure F, Weiner RI (1993) The 16-kilodalton N-terminal fragment of human prolactin is a potent inhibitor of angiogenesis. Endocrinology 133(3):1292–1299
7. D'Angelo G, Struman I, Martial J, Weiner RI (1995) Activation of mitogen-activated protein kinases by vascular endothelial growth factor and basic fibroblast growth factor in capillary endothelial cells is inhibited by the antiangiogenic factor 16-kDa N-terminal fragment of prolactin. Proc Nat Acad Sci U S A 92(14):6374–6378
8. D'Angelo G, Martini JF, Iiri T, Fantl WJ, Martial J, Weiner RI (1999) 16 K human prolactin inhibits vascular endothelial growth factor-induced activation of Ras in capillary endothelial cells. Mol Endocrinol 13(5):692–704
9. Galfione M, Luo W, Kim J, Hawke D, Kobayashi R, Clapp C, Yu-Lee LY, Lin SH (2003) Expression and purification of the angiogenesis inhibitor 16-kDa prolactin fragment from insect cells. Protein Expr Purif 28(2):252–258

10. Garcia C, Aranda J, Arnold E, Thebault S, Macotela Y, Lopez-Casillas F, Mendoza V, Quiroz-Mercado H, Hernandez-Montiel HL, Lin SH, de la Escalera GM, Clapp C (2008) Vasoinhibins prevent retinal vasopermeability associated with diabetic retinopathy in rats via protein phosphatase 2 A-dependent eNOS inactivation. J Clin Invest 118(6):2291–2300
11. Tabruyn SP, Sorlet CM, Rentier-Delrue F, Bours V, Weiner RI, Martial JA, Struman I (2003) The antiangiogenic factor 16 K human prolactin induces caspase-dependent apoptosis by a mechanism that requires activation of nuclear factor-kappaB. Mol Endocrinol 17(9):1815–1823
12. Pan H, Nguyen NQ, Yoshida H, Bentzien F, Shaw LC, Rentier-Delrue F, Martial JA, Weiner R, Struman I, Grant MB (2004) Molecular targeting of antiangiogenic factor 16 K hPRL inhibits oxygen-induced retinopathy in mice. Investig Ophthalmol Visual Sci 45(7):2413–2419
13. Hilfiker-Kleiner D, Kaminski K, Podewski E, Bonda T, Schaefer A, Sliwa K, Forster O, Quint A, Landmesser U, Doerries C, Luchtefeld M, Poli V, Schneider MD, Balligand JL, Desjardins F, Ansari A, Struman I, Nguyen NQ, Zschemisch NH, Klein G, Heusch G, Schulz R, Hilfiker A, Drexler H (2007) A cathepsin D-cleaved 16 kDa form of prolactin mediates postpartum cardiomyopathy. Cell 128(3):589–600
14. Faupel-Badger JM, Ginsburg E, Fleming JM, Susser L, Doucet T, Vonderhaar BK (2010) 16 kDa prolactin reduces angiogenesis, but not growth of human breast cancer tumors in vivo. Horm Cancer 1(2):71–79
15. Baldocchi RA, Tan L, King DS, Nicoll CS (1993) Mass spectrometric analysis of the fragments produced by cleavage and reduction of rat prolactin: evidence that the cleaving enzyme is cathepsin D. Endocrinology 133(2):935–938.
16. Ishida M, Maehara M, Watanabe T, Yanagisawa Y, Takata Y, Nakajima R, Suzuki M, Harigaya T (2014) Vasoinhibins, N-terminal mouse prolactin fragments, participate in mammary gland involution. J Mol Endocrinol. 2014 52(3):279–87.
17. Erdmann S, Ricken A, Merkwitz C, Struman I, Castino R, Hummitzsch K, Gaunitz F, Isidoro C, Martial J, Spanel-Borowski K (2007) The expression of prolactin and its cathepsin D-mediated cleavage in the bovine corpus luteum vary with the estrous cycle. Am J Physiol Endocrinol Metab 293(5):E1365–E1377
18. Lee J, Majumder S, Chatterjee S, Muralidhar K (2011) Inhibitory activity of the peptides derived from buffalo prolactin on angiogenesis. J Biosci 36(2):341–354
19. Piwnica D, Touraine P, Struman I, Tabruyn S, Bolbach G, Clapp C, Martial JA, Kelly PA, Goffin V (2004) Cathepsin D processes human prolactin into multiple 16 K-like N-terminal fragments: study of their antiangiogenic properties and physiological relevance. Mol Endocr 18(10):2522–2542
20. Macotela Y, Aguilar MB, Guzman-Morales J, Rivera JC, Zermeno C, Lopez-Barrera F, Nava G, Lavalle C, Martinez de la Escalera G, Clapp C (2006) Matrix metalloproteases from chondrocytes generate an antiangiogenic 16 kDa prolactin. J Cell Sci 119(Pt 9):1790–1800
21. Ge G, Fernandez CA, Moses MA, Greenspan DS (2007) Bone morphogenetic protein 1 processes prolactin to a 17-kDa antiangiogenic factor. Proc Nat Acad Sci U S A 104 (24):10010–10015
22. Clapp C, Aranda J, Gonzalez C, Jeziorski MC, Martinez de la Escalera G (2006) Vasoinhibins: endogenous regulators of angiogenesis and vascular function. Trends Endocr Metab TEM 17(8):301–307
23. Cruz-Soto ME, Cosio G, Jeziorski MC, Vargas-Barroso V, Aguilar MB, Carabez A, Berger P, Saftig P, Arnold E, Thebault S, Martinez de la Escalera G, Clapp C (2009) Cathepsin D is the primary protease for the generation of adenohypophyseal vasoinhibins: cleavage occurs within the prolactin secretory granules. Endocrinology 150(12):5446–5454
24. Rochefort H, Chalbos D, Cunat S, Lucas A, Platet N, Garcia M (2001) Estrogen regulated proteases and antiproteases in ovarian and breast cancer cells. J Steroid Biochem Mol Biol 76(1–5):119–124
25. Ferraris J, Radl DB, Zarate S, Jaita G, Eijo G, Zaldivar V, Clapp C, Seilicovich A, Pisera D (2011) N-terminal prolactin-derived fragments, vasoinhibins, are proapoptoptic and antiproliferative in the anterior pituitary. PloS ONE 6(7):e21806

26. Cosio G, Jeziorski MC, Lopez-Barrera F, De La Escalera GM, Clapp C (2003) Hypoxia inhibits expression of prolactin and secretion of cathepsin-D by the GH4C1 pituitary adenoma cell line. Lab Invest 83(11):1627–1636
27. O'Reilly MS, Wiederschain D, Stetler-Stevenson WG, Folkman J, Moses MA (1999) Regulation of angiostatin production by matrix metalloproteinase-2 in a model of concomitant resistance. J Biol Chem 274(41):29568–29571
28. Gonzalez EM, Reed CC, Bix G, Fu J, Zhang Y, Gopalakrishnan B, Greenspan DS, Iozzo RV (2005) BMP-1/Tolloid-like metalloproteases process endorepellin, the angiostatic C-terminal fragment of perlecan. J Biol Chem 280(8):7080–7087
29. Shuman Moss LA, Jensen-Taubman S, Stetler-Stevenson WG (2012) Matrix metalloproteinases: changing roles in tumor progression and metastasis. Am J Pathol 181(6):1895–1899
30. St Croix B, Rago C, Velculescu V, Traverso G, Romans KE, Montgomery E, Lal A, Riggins GJ, Lengauer C, Vogelstein B, Kinzler KW (2000) Genes expressed in human tumor endothelium. Science 289(5482):1197–1202
31. Clapp C, Torner L, Gutierrez-Ospina G, Alcantara E, Lopez-Gomez FJ, Nagano M, Kelly PA, Mejia S, Morales MA, Martinez de la Escalera G (1994) The prolactin gene is expressed in the hypothalamic-neurohypophyseal system and the protein is processed into a 14-kDa fragment with activity like 16-kDa prolactin. Proc Nat Acad Sci U S A 91(22):10384–10388
32. Zamorano M, Ledesma-Colunga M, Adán N, Vera-Massieu C, Lemini M, Méndez I, Moreno-Carranza B, Neumann I, Thebault S, Martínez de la Escalera G, Torner L, Clapp C (2014) Vasoinhibin increases anxiety- and depression-related behaviors. Psychoneuroendocrinology Accepted (PNEC-D-13-00742). doi:10.1016/j.psyneuen.2014.03.006
33. Aranda J, Rivera JC, Jeziorski MC, Riesgo-Escovar J, Nava G, Lopez-Barrera F, Quiroz-Mercado H, Berger P, Martinez de la Escalera G, Clapp C (2005) Prolactins are natural inhibitors of angiogenesis in the retina. Invest Ophthalmol Visual Sci 46(8):2947–2953
34. Triebel J, Huefner M, Ramadori G (2009) Investigation of prolactin-related vasoinhibin in sera from patients with diabetic retinopathy. Eur J Endocrinol/Eur Federation End Soc 161(2):345–353
35. Gonzalez C, Parra A, Ramirez-Peredo J, Garcia C, Rivera JC, Macotela Y, Aranda J, Lemini M, Arias J, Ibarguengoitia F, de la Escalera GM, Clapp C (2007) Elevated vasoinhibins may contribute to endothelial cell dysfunction and low birth weight in preeclampsia. Lab Invest 87(10):1009–1017
36. Clapp C, Thebault S, Martinez de la Escalera G (2008) Role of prolactin and vasoinhibins in the regulation of vascular function in mammary gland. J Mammary Gland Biol Neoplasia 13(1):55–67
37. Johansson M, Olerud J, Jansson L, Carlsson PO (2009) Prolactin treatment improves engraftment and function of transplanted pancreatic islets. Endocrinology 150(4):1646–1653
38. Moreno-Carranza B, Goya-Arce M, Vega C, Adan N, Triebel J, Lopez-Barrera F, Quintanar-Stephano A, Binart N, Martinez de la Escalera G, Clapp C (2013) Prolactin promotes normal liver growth, survival, and regeneration in rodents: effects on hepatic IL-6, suppressor of cytokine signaling-3, and angiogenesis. Am J Physiol Regul Integr Comp Physiol 305(7):R720–R726
39. Olazabal IM, Munoz JA, Rodriguez-Navas C, Alvarez L, Delgado-Baeza E, Garcia-Ruiz JP (2009) Prolactin's role in the early stages of liver regeneration in rats. J Cell Physiol 219(3):626–633
40. Reuwer AQ, Nowak-Sliwinska P, Mans LA, van der Loos CM, von der Thusen JH, Twickler MT, Spek CA, Goffin V, Griffioen AW, Borensztajn KS (2012) Functional consequences of prolactin signalling in endothelial cells: a potential link with angiogenesis in pathophysiology? J Cell Mol Med 16(9):2035–2048
41. Yang X, Meyer K, Friedl A (2013) STAT5 and prolactin participate in a positive autocrine feedback loop that promotes angiogenesis. J Biol Chem 288(29):21184–21196
42. Rosas-Hernandez H, Cuevas E, Lantz SM, Hamilton WR, Ramirez-Lee MA, Ali SF, Gonzalez C (2013) Prolactin and blood-brain barrier permeability. Curr Neurovasc Res 10(4):278–286

43. De Spiegelaere W, Casteleyn C, Van den Broeck W, Plendl J, Bahramsoltani M, Simoens P, Djonov V, Cornillie P (2012) Intussusceptive angiogenesis: a biologically relevant form of angiogenesis. J Vascu Res 49(5):390–404
44. Castilla A, Garcia C, Cruz-Soto M, Martinez de la Escalera G, Thebault S, Clapp C (2010) Prolactin in ovarian follicular fluid stimulates endothelial cell proliferation. J Vasc Res 47(1):45–53
45. Yang X, Qiao D, Meyer K, Friedl A (2009) Signal transducers and activators of transcription mediate fibroblast growth factor-induced vascular endothelial morphogenesis. Cancer Res 69(4):1668–1677
46. Halkein J, Tabruyn SP, Ricke-Hoch M, Haghikia A, Nguyen NQ, Scherr M, Castermans K, Malvaux L, Lambert V, Thiry M, Sliwa K, Noel A, Martial JA, Hilfiker-Kleiner D, Struman I (2013) MicroRNA-146a is a therapeutic target and biomarker for peripartum cardiomyopathy. J Clin Invest 123(5):2143–2154
47. Thebault S, González C, García C, Arredondo Zamarripa D, Nava G, Vaca L, López-Casillas F, Martínez de la Escalera G, Clapp C (2011) Vasoinhibins prevent bradykinin-stimulated endothelial cell proliferation by inactivating eNOS via reduction of both intracellular Ca2+ levels and eNOS phosphorylation at Ser1179. Pharmaceuticals 4:1052–1069
48. Garcia C, Nunez-Anita RE, Thebault S, Arredondo Zamarripa D, Jeziorsky MC, Martínez de la Escalera G, Clapp C (2014) Requirement of phosphorylatable endothelial nitric oxide synthase at Ser-1177 for vasoinhibin-mediated inhibition of endothelial cell migration and proliferation in vitro. Endocrine 45(2):263–270
49. Nguyen NQ, Castermans K, Berndt S, Herkenne S, Tabruyn SP, Blacher S, Lion M, Noel A, Martial JA, Struman I (2011) The antiangiogenic 16 K prolactin impairs functional tumor neovascularization by inhibiting vessel maturation. PloS ONE 6(11):e27318
50. Tabruyn SP, Sabatel C, Nguyen NQ, Verhaeghe C, Castermans K, Malvaux L, Griffioen AW, Martial JA, Struman I (2007) The angiostatic 16 K human prolactin overcomes endothelial cell anergy and promotes leukocyte infiltration via nuclear factor-kappaB activation. Mol Endocrinol 21(6):1422–1429
51. Bouzin C, Brouet A, De Vriese J, Dewever J, Feron O (2007) Effects of vascular endothelial growth factor on the lymphocyte-endothelium interactions: identification of caveolin-1 and nitric oxide as control points of endothelial cell anergy. J Immunol 178(3):1505–1511
52. Clapp C, Weiner RI (1992) A specific, high affinity, saturable binding site for the 16-kilodalton fragment of prolactin on capillary endothelial cells. Endocrinology 130(3):1380–1386
53. Shi H, Huang Y, Zhou H, Song X, Yuan S, Fu Y, Luo Y (2007) Nucleolin is a receptor that mediates antiangiogenic and antitumor activity of endostatin. Blood 110(8):2899–2906
54. Takada Y (2012) Potential role of kringle-integrin interaction in plasmin and uPA actions (a hypothesis). J Biomed Biotechnol 2012:136302. doi:136310.131155/132012/136302
55. Clapp C, Thebault S, Arnold E, Garcia C, Rivera JC, de la Escalera GM (2008) Vasoinhibins: novel inhibitors of ocular angiogenesis. Am J Physiol Endocrinol Metab 295(4):E772–E778
56. Hilfiker-Kleiner D, Sliwa K (2014) Pathophysiology and epidemiology of peripartum cardiomyopathy. Nat Rev Cardiol. doi:10.1038/nrcardio.2014.37
57. Clapp C, Martinez de la Escalera L, Martinez de la Escalera G (2012) Prolactin and blood vessels: a comparative endocrinology perspective. Gen Comp Endocrinol 176(3):336–340
58. Andres AC, Djonov V (2010) The mammary gland vasculature revisited. J Mammary Gland Biol Neoplasia 15(3):319–328
59. Zaragoza R, Torres L, Garcia C, Eroles P, Corrales F, Bosch A, Lluch A, Garcia-Trevijano ER, Vina JR (2009) Nitration of cathepsin D enhances its proteolytic activity during mammary gland remodelling after lactation. Biochem J 419(2):279–288
60. Castino R, Delpal S, Bouguyon E, Demoz M, Isidoro C, Ollivier-Bousquet M (2008) Prolactin promotes the secretion of active cathepsin D at the basal side of rat mammary acini. Endocrinology 149(8):4095–4105
61. Baldocchi RA, Tan L, Hom YK, Nicoll CS (1995) Comparison of the ability of normal mouse mammary tissues and mammary adenocarcinoma to cleave rat prolactin. Proc Soc Exp Biol Med 208(3):283–287

62. Gill S, Peston D, Vonderhaar BK, Shousha S (2001) Expression of prolactin receptors in normal, benign, and malignant breast tissue: an immunohistological study. J Clin Pathol 54(12):956–960
63. Le JA, Wilson HM, Shehu A, Mao J, Devi YS, Halperin J, Aguilar T, Seibold A, Maizels E, Gibori G (2012) Generation of mice expressing only the long form of the prolactin receptor reveals that both isoforms of the receptor are required for normal ovarian function. Biol Reprod 86(3):86
64. Ricken AM, Traenkner A, Merkwitz C, Hummitzsch K, Grosche J, Spanel-Borowski K (2007) The short prolactin receptor predominates in endothelial cells of micro- and macrovascular origin. J Vasc Res 44(1):19–30
65. Arnold E, Rivera JC, Thebault S, Moreno-Paramo D, Quiroz-Mercado H, Quintanar-Stephano A, Binart N, Martinez de la Escalera G, Clapp C (2010) High levels of serum prolactin protect against diabetic retinopathy by increasing ocular vasoinhibins. Diabetes 59(12):3192–3197
66. Ramirez M, Wu Z, Moreno-Carranza B, Jeziorski MC, Arnold E, Diaz-Lezama N, Martinez de la Escalera G, Colosi P, Clapp C (2011) Vasoinhibin gene transfer by adenoassociated virus type 2 protects against VEGF- and diabetes-induced retinal vasopermeability. Invest Ophthalmol Visual Sci 52(12):8944–8950
67. Haghikia A, Podewski E, Libhaber E, Labidi S, Fischer D, Roentgen P, Tsikas D, Jordan J, Lichtinghagen R, von Kaisenberg CS, Struman I, Bovy N, Sliwa K, Bauersachs J, Hilfiker-Kleiner D (2013) Phenotyping and outcome on contemporary management in a German cohort of patients with peripartum cardiomyopathy. Basic Res Cardiol 108(4):366
68. Mukherjee S, Kar M, Dutta S (1991) Observation on serum prolactin in hepatic cirrhosis. J Indian Med Assoc 89(11):307–308
69. Buckley AR, Crowe PD, Bauman PA, Neumayer LA, Laird HE, 2nd, Russell DH, Putnam CW (1991) Prolactin-provoked alterations of cytosolic, membrane, and nuclear protein kinase C following partial hepatectomy. Dig Dis Sci 36(9):1313–1319
70. Sorenson RL, Brelje TC (1997) Adaptation of islets of Langerhans to pregnancy: beta-cell growth, enhanced insulin secretion and the role of lactogenic hormones. Horm Metab Res 29(6):301–307
71. Dubois S, Madec AM, Mesnier A, Armanet M, Chikh K, Berney T, Thivolet C (2010) Glucose inhibits angiogenesis of isolated human pancreatic islets. J Mol Endocrinol 45(2):99–105
72. Zeng L, He X, Wang Y, Tang Y, Zheng C, Cai H, Liu J, Wang Y, Fu Y, Yang GY (2014) MicroRNA-210 overexpression induces angiogenesis and neurogenesis in the normal adult mouse brain. Gene Ther 21(1):37–43
73. Park KE, Pepine CJ (2010) Pathophysiologic mechanisms linking impaired cardiovascular health and neurologic dysfunction: the year in review. Clevel Clin J Med 77(Suppl 3):S40–S45

Laboratory Investigation (2016) 96, 283–295

Diabetes enhances the efficacy of AAV2 vectors in the retina: therapeutic effect of AAV2 encoding vasoinhibin and soluble VEGF receptor 1

Nundehui Díaz-Lezama[1], Zhijian Wu[2], Elva Adán-Castro[1], Edith Arnold[1], Miguel Vázquez-Membrillo[1], David Arredondo-Zamarripa[1], Maria G Ledesma-Colunga[1], Bibiana Moreno-Carranza[1], Gonzalo Martinez de la Escalera[1], Peter Colosi[3] and Carmen Clapp[1]

Adeno-associated virus (AAV) vector-mediated delivery of inhibitors of blood–retinal barrier breakdown (BRBB) offers promise for the treatment of diabetic macular edema. Here, we demonstrated a reversal of blood–retinal barrier pathology mediated by AAV type 2 (AAV2) vectors encoding vasoinhibin or soluble VEGF receptor 1 (sFlt-1) when administered intravitreally to diabetic rats. Efficacy and safety of the AAV2 vasoinhibin vector were tested by monitoring its effect on diabetes-induced changes in the retinal vascular bed and thickness, and in the electroretinogram (ERG). Also, the transduction of AAV2 vectors and expression of AAV2 receptors and co-receptors were compared between the diabetic and the non-diabetic rat retinas. AAV2 vasoinhibin or AAV2 sFlt-1 vectors were injected intravitreally before or after enhanced BRBB due to diabetes induced by streptozotocin. The BRBB was examined by the Evans blue method, the vascular bed by fluorescein angiography, expression of the AAV2 EGFP reporter vector by confocal microscopy, and the AAV2 genome, expression of transgenes, receptors, and co-receptors by quantitative PCR. AAV2 vasoinhibin and sFlt-1 vectors inhibited the diabetes-mediated increase in BRBB when injected after, but not before, diabetes was induced. The AAV2 vasoinhibin vector decreased retinal microvascular abnormalities and the diabetes-induced reduction of the B-wave of the ERG, but it had no effect in non-diabetic controls. Also, retinal thickness was not altered by diabetes or by the AAV2 vasoinhibin vector. The AAV2 genome, vasoinhibin and sFlt-1 transgenes, and EGFP levels were higher in the retinas from diabetic rats and were associated with an elevated expression of AAV2 receptors (syndecan, glypican, and perlecan) and co-receptors (fibroblast growth factor receptor 1, αvβ5 integrin, and hepatocyte growth factor receptor). We conclude that retinal transduction and efficacy of AAV2 vectors are enhanced in diabetes, possibly due to their elevated cell entry. AAV2 vectors encoding vasoinhibin and sFlt-1 may be desirable gene therapeutics to target diabetic retinopathy and macular edema.

Laboratory Investigation (2016) **96,** 283–295; doi:10.1038/labinvest.2015.135; published online 16 November 2015

Blood–retinal barrier breakdown (BRBB) occurs in diabetic macular edema (DME), a complication of diabetic retinopathy (DR) where swelling of the central retina causes visual impairment.[1] The intravitreal delivery of anti-angiogenic and anti-vasopermeability factors can be an effective therapy to control DR and DME but often requires repeated treatments, which raise the risk of infection or other ocular complications.[1] By producing a more sustained therapy, viral vector-mediated gene transfer could avoid repeated intraocular administration and provide a permanent solution.

The most promising ocular gene therapy for DR is based on the intravitreal delivery of recombinant adeno-associated virus (AAV) vectors. They are generally safe, and the best characterized type 2 serotype (AAV2) produces long-term transgene expression in retinal ganglion cells after intravitreal delivery.[2] AAV2 vectors encoding inhibitors of vasopermeability such as soluble VEGF receptor 1 (sFlt-1),[3] vasoinhibin,[3] angiostatin,[4] and angiotensin-(1–7)[5] reduce retinal vascular leakage in diabetic rats after intravitreal injection. In these studies the vectors were supplied before, not after, inducing diabetes. However, testing the efficacy of

[1]Instituto de Neurobiología, Universidad Nacional Autónoma de México, Querétaro, Mexico; [2]Ocular Gene Therapy Core, National Eye Institute, NIH, Bethesda, MD, USA and [3]BioMarin Pharmaceutical, Novato, CA, USA
Correspondence: Professor C Clapp, PhD, Instituto de Neurobiología, Universidad Nacional Autónoma de México, Campus UNAM-Juriquilla, Querétaro 76230, México.
E-mail: clapp@unam.mx

Received 2 April 2015; revised 16 October 2015; accepted 20 October 2015

gene therapeutics after diabetes is well-established seems more medically relevant than developing prophylactic strategies. Recent studies have also emphasized the risk of systemic vector dissemination and immune activation following high doses of intravitreally delivered vectors,[2] so enhancing transduction efficiency is a primary goal.

In this study, we evaluated the inhibitory effect of AAV2 vectors encoding vasoinhibins and sFlt-1 on diabetes-induced BRBB when injected after BRBB is well-established. We found that the AAV2 vectors reverse BRB pathology and protect against retinal microvascular abnormalities and electrophysiological dysfunction; moreover, their retinal transduction is enhanced in the diabetic state by mechanisms that may include the upregulation of AAV2 primary receptors and co-receptors.

MATERIALS AND METHODS

Production of AAV2 Vectors

cDNAs encoding vasoinhibins (codons 1–142 of human prolactin), sFlt-1, and enhanced green fluorescent protein (EGFP) were obtained and cloned into AAV2 vectors downstream of a cytomegalovirus (CMV) immediate early promoter as previously described.[3] AAV2 preparations were produced using a three-plasmid cotransfection system and purified by polyethylene glycol precipitation and cesium chloride density gradient fractionation using a previously described method.[6] The purified vectors were formulated in 10 mM Tris-HCl and 180 mM NaCl (pH 7.4) and stored at − 70 °C before use. Quantification of vectors was done by real-time PCR using linearized plasmid standards. The titers of the vector preparations were 1.4×10^{12} vector genomes (vg) per ml for AAV2 vasoinhibin and AAV2 sFlt-1, and 1.4×10^{13} vg per ml for AAV2 EGFP. Two microliters of vector or vehicle was injected into the vitreous.

Animals

Male Wistar rats (250 to 300 g) were cared for in accordance with the US National Research Council's Guide for the Care and Use of Laboratory Animals (8th edn, National Academy Press, Washington, DC, USA). The Bioethics Committee of the Institute of Neurobiology of the National University of Mexico (UNAM) approved all animal experiments.

Groups without gene therapy

Animals were injected with a single intraperitoneal (i.p.) dose of streptozotocin (STZ; 60 mg/kg in 10 mM citrate buffer, pH 4.5) (Sigma-Aldrich, St Louis, MO) or vehicle after overnight fasting. Rats with a blood glucose concentration $\geq$ 250 mg/dl at 48 h were considered diabetic. Two, 4, and 6 weeks after STZ, rats were anesthetized with 70% ketamine and 30% xylazine (1 μl/g body weight, i.p.), and the BRBB was examined by the Evans blue method.

Groups with gene therapy after diabetes

Animals were injected with STZ or vehicle following the above procedures; 2 weeks later the diabetic and non-diabetic rats were anesthetized, and AAV2 vector (2.8×10^9 vg per eye) or vehicle was injected into the vitreous as previously described.[7] Four weeks after vector administration, some of the animals were anesthetized as above, and the BRBB was examined by the Evans blue method; other animals were subjected to fluorescein angiography, or to electroretinogram (ERG) examination and killed by decapitation to analyze retinal thickness. In addition, other rats were exposed to a CO_2-saturated inhalation chamber and killed by decapitation; their retinas were analyzed by quantitative PCR (qPCR) or flat-mounted for confocal microscopy evaluation.

Groups with gene therapy before diabetes

Animals were injected intravitreally with AAV2 vector (2.8×10^9 vg per eye) or vehicle, and 4 weeks later diabetes was induced with STZ. Four weeks post-STZ, retinas were evaluated by the Evans blue method.

In other experiments, retinas from non-diabetic and six-week diabetic rats were processed for qPCR, immunohistochemistry, or dissected, weighed, and homogenized in 150 μl lysis buffer (0.5% Igepal, 0.1% SDS, 50 mM Tris, 150 mM NaCl, 1μg/ml aprotinin, and 100 μg/ml PMSF, pH 7.4). Retinal homogenates were centrifuged (13 000 r.p.m. for 5 min), and the protein in the supernatant was evaluated by the Bradford method.[8]

Evans Blue Method

The BRBB was evaluated by the Evans blue method, as previously reported.[9] Briefly, anesthetized rats were injected (intrajugularly) with the Evans blue tracer (45 mg/kg, Sigma-Aldrich). Two hours later, 1 ml of blood was drawn from the heart to measure the Evans blue concentration in plasma, and the rats were perfused for 2 min via the left ventricle with PBS (pH 3.5 at 37 °C) at a pressure that allowed a flow rate of 70 ml/min before insertion of catheter and start of perfusion. The retina was dissected and vacuum-dried (SPD 1010 SpeedVac System, ThermoSavant, USA) for 5 h. After weighing the tissue, the Evans blue tracer was extracted by incubating each retina in 100 μl formamide (Mallinckrodt Baker, Phillipsburg, NJ) for 18 h at 72 °C. The extract was centrifuged at 300 000 *g* for 60 min at 4 °C. Absorbance was measured in the supernatant at 620 nm using the NanoDrop 1000 spectrophotometer (Thermo Fisher Scientific, Wilmington, DE). The tracer concentration in the extracts was calculated from a standard curve of Evans blue in formamide and normalized to the retina and body weight and to the Evans blue concentration in plasma.

Fluorescein Angiography

Anesthetized rats were injected intrajugularly with 100 mg/kg of fluorescein isothiocyanate-labeled dextran (50 mg/ml, FITC-dextran: MW 2×10^6 Da; Sigma-Aldrich). One hour

later, the rats were killed, and their retinas were flat-mounted, fixed for 4 h in freshly prepared 4% paraformaldehyde in 0.1 M PBS at room temperature, washed with PBS, mounted on glass slides with Vectashield (Vector Laboratories (Burlingame, CA), and coverslipped. Retinal flat-mounts were observed and digitalized with a ×4 objective under a fluorescence microscope (Olympus BX60 with a DP70 Olympus camera). Images were tiled to create a picture of the entire retina. The density of the capillary network was analyzed using the AngioTool image analysis sofware[10] having fixed settings for vessel diameter (1–5) and intensity (15–22).

Electroretinogram

Rats were anesthetized after dark adaptation overnight, and pupils were fully dilated with a 0.5% tropicamide and 0.5% phenylephrin solution. Flash ERG responses were recorded from both eyes by a silver chloride ring electrode placed on the cornea. Two reference electrodes were positioned subcutaneously near the eyes. The light stimulation included a 1-ms flash with an intensity of 0.9 log cd.s/m^2 (PS33 Plus PhotoStimulator, GRASS Technologies, Warwick, RI). The bandpass was set at 3 Hz to 0.3 kHz (P511AC Amplifier, GRASS Technologies). Sixteen responses were averaged. The A-wave amplitude was measured from baseline to the trough of the A-wave, and the B-wave amplitude from the trough of the A-wave to the peak of the B-wave.

Retinal Thickness

Eyes fixed in 4% paraformaldehyde for 24 h at room temperature were then dehydrated and embedded in paraffin. Orientation of the serial sections (8 μm) was assured by controlling that the cuttings passed through the optic nerve head and the cutting marker. Sections were stained with hematoxilin and eosin, and the total thickness of the retina and of both the inner and outer nuclear layers were measured at ×20 magnification using the ScanScope Digital Scanner and the Image Scope software (Aperio Technologies, Vista, CA). Images were taken at equivalent retinal eccentricities from the optic nerve head, and three measurements were taken on each retina within 1 mm of the optic nerve.

Quantitative PCR

AAV transgene expression

Total RNA was isolated from frozen retinas using TRIzol reagent (Life Technologies, Carlsbad, CA), and cDNA was synthesized with the High-Capacity cDNA Reverse Transcription Kit (Applied Biosystems, Warrington, UK). PCR products were separated on a 1.2% agarose gel and visualized using ethidium bromide, or detected and quantified with Maxima SYBR Green/ROX qPCR Master Mix (Thermo Scientific, Auburn, AL) in a 10-μl final reaction volume containing template and 0.5 mM of each of the following primer pairs for human *vasoinhibin*: 5′-CTGCCCGATGC CAGGTGA-3′ (sense) and 5′-GAAAGTCTTTTTGATTC ATCTGT-3′ (antisense); human *sFlt-1*: 5′-GACCTGGAGT TACCCTGATGA-3′ (sense) and 5′-ATGGTCCACTCCTTAC ACGAC-3′ (antisense); *glypican 1:* 5′-TGGCGCCTACGGTG GAAATGATGT-3′ (sense) and 5′-GAGTGGCGGCCGAGG TCTTCTGTC-3′ (antisense); *syndecan 4*: 5′-GAACCATGG CGCCTGTCTGC-3′ (sense) and 5′-CCTGGGCTCCTCCGT GTCATCT-3′ (antisense); *perlecan 1*: 5′-CTGCCACCTGA CAGTCGC-3′ (sense) and 5′-GCTCTGGCACCTGCAG-3′ (antisense); *hepatocyte growth factor receptor c-Met (hgfr c-Met)*: 5′-TCGTTCCTTGGGATTATTGC-3′ (sense) and 5′-TGTTTTGTTTTGGCACAGGA-3′ (antisense); *αvβ5 integrin*: 5′-CACCTGAATGAAGCCAATGA-3′(sense) and 5′-TCCATGCAAAATCTCCACAG-3′ (antisense); *fibroblast growth factor receptor 1* (*fgfr 1)*: 5′-CAACACCAAACCAA ACCGTA-3′ (sense) and 5′-GTTTTTCAACCAGCGCAAAG -3′ (antisense) and *hypoxanthine-guanine phosphoribosyltransferase (hprt)*: 5′-GACCGGTTCTGTCATGTCG-3′ (sense) and 5′-ACCTGGTTCATCATCACTAATCAC-3′ (antisense). The amplification conditions were 10 s at 95 °C, 30 s at each primer pair-specific annealing temperature, and 30 s at 72 °C for 40 cycles. The PCR data were analyzed by the 2–ΔΔCT method, and cycle thresholds were normalized to the housekeeping gene *hprt* to calculate mRNA expression levels.

AAV genome copy number

Total genomic DNA was isolated from frozen, AAV2-injected control and diabetic rat retinas. A 100-ng sample of genomic DNA was tested for the presence of AAV2 DNA by qPCR using primers binding to the CMV promoter. qPCR for the 28S ribosomal DNA was used as loading control for normalization purposes. PCR products were detected and quantified with Maxima SYBR Green /ROX qPCR Master Mix using the following primer pairs for CMV: 5′-TGCC CAGTACATGACCTTAT-3′ (sense) and 5′-AATGGGGCGG AGTTGTTAC-3′ (antisense); and rat 28S ribosomal DNA: 5′-CAGTACGAATACAGACCG-3′ (sense) and 5′-GGCAAC AACACATCATCAG-3′ (antisense). The amplification conditions for the CMV were 30 s at 94 °C, 30 s at 60.5 °C, and 30 s at 72 °C for 40 cycles, whereas for 28S ribosomal DNA the annealing temperature was 56.5 °C. For absolute quantification, standard curves for the two plasmids were performed using concentrations ranging from 10^7–10 molecules per μl as determined by spectrophotometry.

Histological Evaluation of EGFP

Eyes, without the lens, were fixed in 4% paraformaldehyde for 30 min at room temperature and washed with PBS. The entire retinas were carefully dissected from the eyecups, flat-mounted on glass slides by making four radial cuts from the edges to the equator, and coverslipped with mounting media (Vectashield) to directly detect EGFP fluorescence by confocal microscopy (LSM 780, Carl Zeiss MicroImaging GmbH, Göttingen, Germany). An observer blind to the experiment captured and evaluated serial optical z-sections from three different areas throughout the retinal ganglion cell layer neighboring the optic nerve. EGFP fluorescence per area

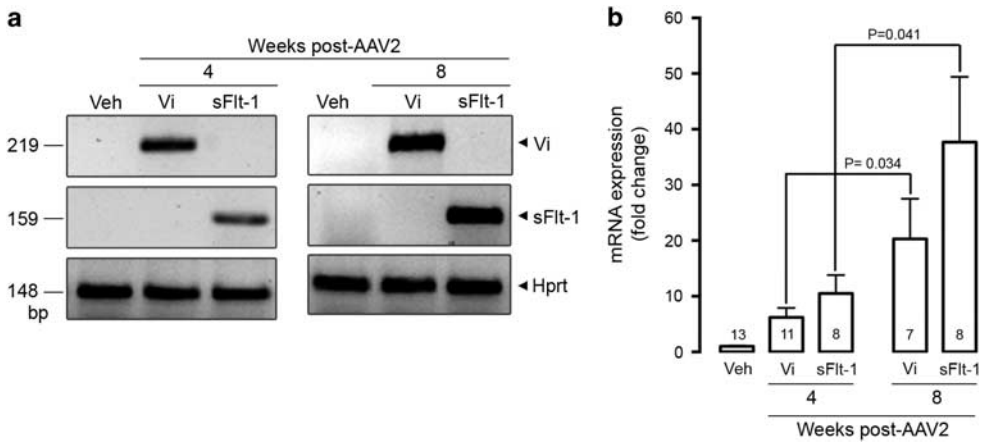

Figure 1 Verification of AAV2-mediated retinal transgene expression. (**a**) RT–PCR analysis of vasoinhibin (Vi) and sFlt-1 mRNA in retinas obtained from rats 4 and 8 weeks after they had been intravitreally injected with vehicle (Veh), AAV2 Vi, or AAV2 sFlt-1 vectors. The sizes of RT–PCR products are given in bp. Amplification of hypoxanthine-guanine phosphoribosyl transferase (Hprt) was used as an internal standard. (**b**) qRT–PCR-based quantification of Vi and sFlt-1 mRNA levels in retinas from rats 4 and 8 weeks after they had been intravitreally injected with Veh, AAV2 Vi, or AAV2 sFlt-1 vectors. Bars represent mean ± s.e.m. Numbers inside bars indicate the number of retinas evaluated. AAV2, adeno-associated virus type 2; qRT–PCR, quantitative reverse transcription PCR.

was quantified using the Pro-Plus image analysis software (Media Cybernetics, Silver Spring, MD).

Immunohistochemistry for FGFR1

Eyes were fixed in 4% paraformaldehyde for 4 h at room temperature and then cryo-protected with 15% sucrose for 1 day. Subsequently, eyes were frozen in optimal cutting temperature (OCT) compound (Tissue-Tek; Sakura Finetech Torrance, CA), and 12-μm-thick cryostat sections were mounted on gelatin-coated slides. Sections were washed with PBS to remove OCT, blocked with PBS containing 3% bovine serum albumin, 5% normal goat serum, and 0.1% Triton X-100 for 2 h at room temperature, and immunostained overnight at 4 °C with a 1:50 dilution of the anti-FGFR1 monoclonal antibody (ab823 from Abcam PLC, Cambridge, UK). After incubation, samples were washed three times with PBS for 15 min, labeled for 4 h with a 1:500 dilution of Alexa Fluor 488 goat anti-mouse secondary antibody (Invitrogen, Thermo Fisher Scientific, Waltham, MA), washed three times with PBS, coverslipped using DAPI Vectashield, and imaged by confocal microscopy.

Statistical Analysis

The statistical analyses were performed using the Sigma Stat 7.0 software (Systat Software, San Jose, CA). Statistical differences between two and more than three groups were determined by the unpaired two-tailed Student's *t*-test and one-way ANOVA followed by Bonferroni's or Tukey's *post hoc* comparison tests, respectively. The threshold for significance was set at $P<0.05$.

RESULTS

Verification of Vasoinhibin and sFlt-1 Transgene Expression in the Retina

Total retinal RNA from eyes injected with vehicle or with each one of the AAV2 vectors was treated with DNase to eliminate genomic DNA contamination. Amplification of DNase-treated RNA without reverse transcriptase generated no products for vasoinhibin or sFlt-1 (not shown). No human vasoinhibin or human sFlt-1 transcript was present in normal, vehicle-injected eyes (Figure 1a), confirming that the primers do not amplify endogenous vasoinhibin or sFlt-1 in the rat. Products of the expected size for human vasoinhibin and sFlt-1 were amplified in normal retinas 4 and 8 weeks after being transduced with the respective vectors (Figure 1a), and the expression of both transgenes was significantly higher at 8 weeks post transduction (Figure 1b).

The AAV2 Vasoinhibin and AAV2 sFlt-1 Vectors Reverse Diabetes-Induced Blood–Retinal Barrier Pathology

Table 1 shows the body weight and blood glucose levels for diabetic rats and their matched non-diabetic controls. Diabetic rats showed a reduced weight from 4 to 8 weeks post-STZ treatment, and their blood glucose levels were significantly higher compared with non-diabetic controls at all times.

The STZ rat model of diabetes mimics some of the early changes of human DR, including BRBB. When evaluated using the retinal accumulation of Evans blue or other plasma tracers, BRBB was reported as early as 5 days and up to 10 weeks post-STZ treatment.[3,4,9,11–14] Here, we confirmed the early and sustained damage of the BRB in this diabetes model by showing that a significant increase in the retinal accumulation of Evans blue-stained albumin occurs at 2 weeks

Table 1 Body weight and blood glucose concentrations of non-diabetic and diabetic rats

Duration of diabetes (week)	Treatment	*n*	Weight (g)	Blood glucose (mg/dl)
2	ND (NI)	4	334.5 ± 8.9	100.0 ± 3.3
	D (NI)	4	325.9 ± 6.9	478.6 ± 30.8*
4	ND (NI)	20	363.1 ± 6.3	98.6 ± 2.5
	D (NI)	20	274.4 ± 9.6*	469.7 ± 17.9*
	ND (Veh)	28	341.6 ± 5.8	103.9 ± 2.8
	D (Veh)	20	263.5 ± 4.5*	486.6 ± 15.3*
	ND (Vi)	9	348.9 ± 7.7	100.6 ± 5.12
	D (Vi)	3	275.9 ± 6.8*	496.0 ± 8.5*
	ND (sFlt-1)	3	359.4 ± 5.9	99.0 ± 4.8
	D (sFlt-1)	4	285.8 ± 7.2*	491.3 ± 19.5*
6	ND (NI)	5	442.9 ± 6.3	105.1 ± 4.81
	D (NI)	4	345.2 ± 10.4*	464.4 ± 16.3*
	ND (Veh)	16	449.9 ± 6.9	103.8 ± 3.5
	D (Veh)	14	327.0 ± 10.6*	463.3 ± 11.7*
	ND (Vi)	25	463.2 ± 12.9	101.8 ± 3.3
	D (Vi)	25	341.1 ± 11.2*	505.5 ± 10.4*
	ND (sFlt-1)	6	430.6 ± 14.6	102.3 ± 3.5
	D (sFlt-1)	6	319.4 ± 13.4*	469.2 ± 18.5*
	ND (EGFP)	10	460.7 ± 9.7	110.5 ± 4.5
	D (EGFP)	11	321.0 ± 21.2*	468.1 ± 24.9*
8	ND (Vi)	7	507.2 ± 8.8	108.9 ± 4.9
	D (Vi)	8	370.1 ± 7.8*	482.2 ± 16.7*

Rats treated (D) or not (ND) with streptozotocin (STZ), were non-injected (NI) or injected intravitreally with vehicle (Veh), AAV2 vasoinhibin (Vi), AAV2 sFlt-1 (sFlt-1), or AAV2 EGFP (EGFP) and evaluated at 2, 4, 6, and 8 weeks after STZ. *$P<0.001$ *vs* respective ND controls. Body weight and blood glucose values were similar within all ND and D groups at the same week period. Values represent mean ± s.e.m. Number of rats (*n*).

after STZ injection and is maintained at a similar level during the following 4 and 6 weeks (Figure 2a). To investigate the restoration of the BRB function, vehicle or 2.8×10^9 vg of the AAV2 vasoinhibin vector or the AAV2 sFlt-1 vector was injected intravitreally into non-diabetic or diabetic rats 2 weeks after treatment with STZ, and the BRBB was quantified 4 weeks after vector administration by the retinal accumulation of Evans blue. As expected, diabetes induced a significant increase in tracer accumulation in vehicle-injected rats (Figure 2b). Treatment with either the AAV2 vasoinhibin vector or the AAV2 sFlt-1 vector reversed the diabetes-induced increase in BRBB. Evans blue accumulation was significantly lower in the diabetic rat retinas transduced with the AAV2 vasoinhibin vector or the AAV2 sFlt-1 vector than in vehicle-injected diabetic rat retinas (Figure 2b). Moreover, diabetic rat retinas transduced with either one of these two vectors showed a level of Evans blue leakage similar to that in vehicle-injected, non-diabetic rats (Figure 2b). The reversal effect is specific to the vasoinhibin and the sFlt-1 transgenes, because the AAV2 EGFP vector had no effect, and none of the vectors modified Evans blue-stained albumin accumulation in non-diabetic rats (Figure 2b). These findings support the therapeutic potential of the AAV2 vasoinhibin and sFlt-1 vectors.

The AAV2 Vasoinhibin Vector Reduces Diabetes-Induced Retinal Microvessel Abnormalities and Electrophysiological Dysfunction

The therapeutic and safety properties of the AAV2 vasoinhibin vector were further investigated by evaluating the retinal vascular bed, electrophysiological function, and thickness of the retina in rats that had been diabetic for 6 weeks and injected with the vector or with vehicle 2 weeks after diabetes onset (as indicated in Figure 2b). Figure 3a shows representative images of the retinal vasculature of non-diabetic and diabetic rats obtained by fluorescein angiography. Consistent with previous findings using this technique,[15,16] the retinas of STZ-treated rats showed an intact vascular bed. However, the intensity of the fluorescein signal within the capillary vessels (arrow heads) was reduced in the vehicle-injected diabetic rat compared with the vehicle-injected non-diabetic control (Figure 3a). The fainter capillary vessels in the diabetic condition allowed better visualization of the short vertical capillary segments (indicated by arrows) connecting the superficial and the deep microvascular layers of the inner retina.[17] Accordingly, the microvessel fluorescein signal per area was significantly reduced in the diabetic rat compared with the non-diabetic control injected with vehicle (Figure 3b). No significant differences were observed in non-diabetic and diabetic rats injected with the AAV2 vasoinhibin vector with respect to the vehicle-injected non-diabetic control.

Next, we used the ERG to evaluate the functional status of the retina. Figure 4a shows representative ERG recordings under scotopic conditions of non-diabetic and diabetic rats injected with vehicle or with the AAV2 vasoinhibin vector. Quantitative analysis showed that the amplitude of the A-wave was similar among all groups (Figure 4b). However, the amplitude of the B-wave decreased significantly in vehicle-injected diabetic rats compared with the vehicle-injected non-diabetic controls (Figure 4c). The reduction of the B-wave was not statistically significant in diabetic rats treated with the AAV2 vasoinhibin vector, and this vector did not modify the B-wave amplitude of non-injected diabetic animals.

Finally, morphological examination of hematoxylin and eosin-stained retinal paraffin sections showed no difference in the thickness of the total retina, the inner nuclear layer, or the outer nuclear layer among groups (Figure 4d and e).

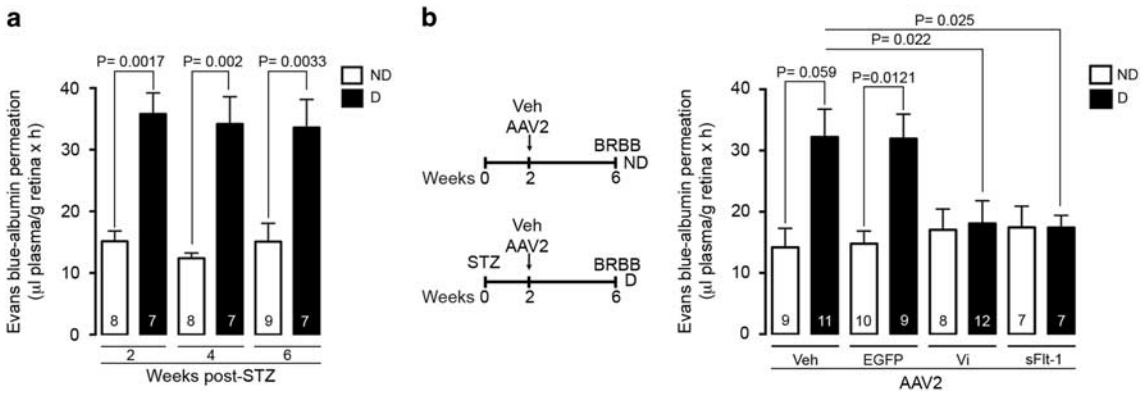

Figure 2 The AAV2 vasoinhibin and AAV2 sFlt-1 vectors reverse diabetes-induced blood–retinal barrier pathology. (**a**) BRBB evaluated by the retinal accumulation of Evans blue-stained albumin in non-diabetic (ND) control rats and in diabetic (D) rats 2, 4, and 6 weeks after treatment with STZ. (**b**) Post-diabetes design diagram: vehicle (Veh), or AAV2 vasoinhibin (Vi), AAV2 sFlt-1, or AAV2-enhanced green fluorescent protein (EGFP) vectors were injected intravitreally into ND or into D rats 2 weeks after treatment with STZ, and BRBB was evaluated 4 weeks after vector administration. Values represent mean ± s.e.m. Numbers inside bars indicate the number of retinas evaluated. AAV2, adeno-associated virus type 2; BRBB, blood-retinal barrier breakdown; STZ, streptozotocin.

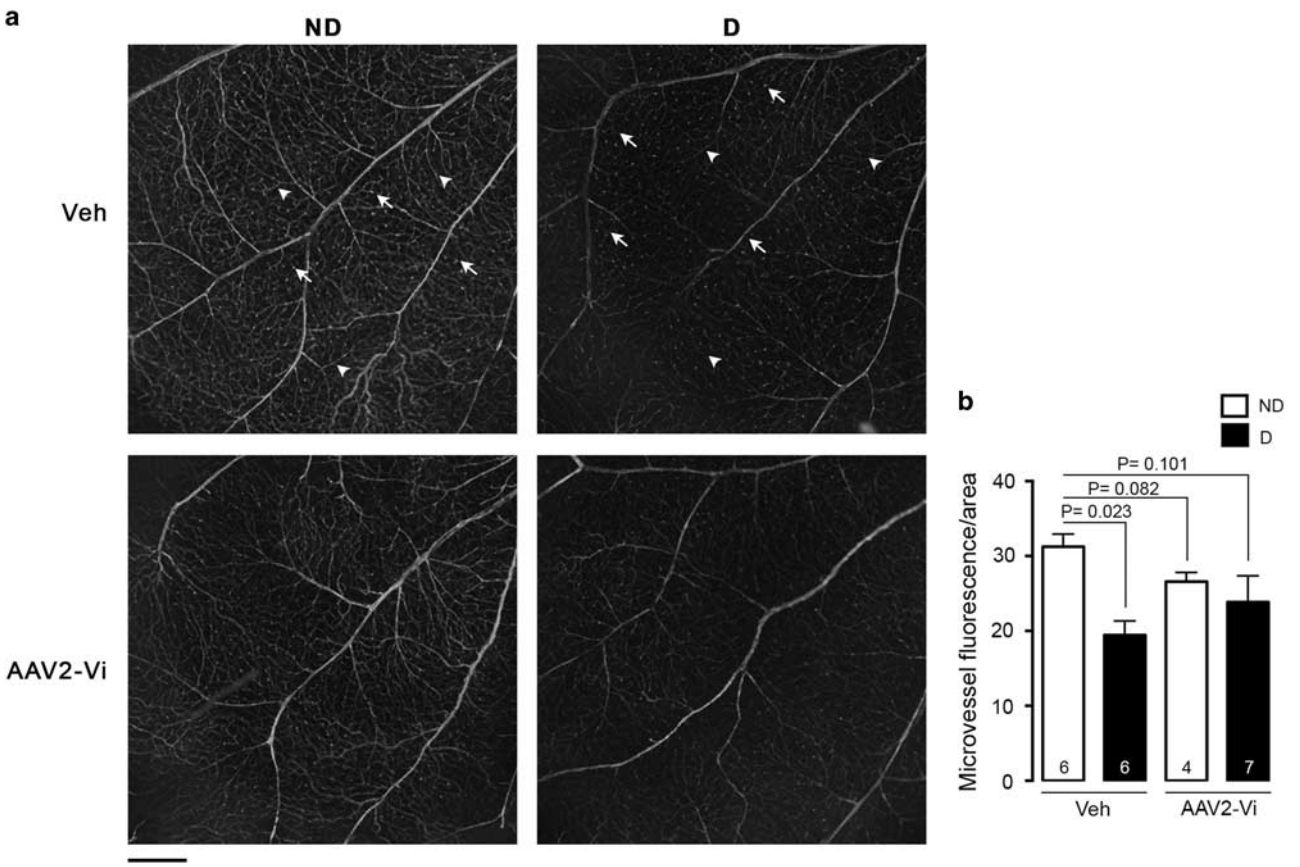

Figure 3 The AAV2 vasoinhibin vector reduces diabetes-induced microvessel abnormalities. (**a**) Representative images of fluorescein-labeled retinas from non-diabetic (ND) control rats and diabetic (D) rats injected intravitreally with vehicle (Veh) or the AAV2 vasoinhibin (Vi) vector 2 weeks after treatment with STZ and subjected to fluorescein angiography 4 weeks after vector administration. Arrow heads indicate microvessels. Arrows indicate the short vertical capillary segments that connect the superficial and deep microvascular layers of the inner retina. Scale bar, 200 μm. (**b**) Quantification of microvessel fluorescein signal per retinal area. Values represent mean ± s.e.m. Numbers inside bars indicate the number of retinas evaluated. AAV2, adeno-associated virus type 2; STZ, streptozotocin.

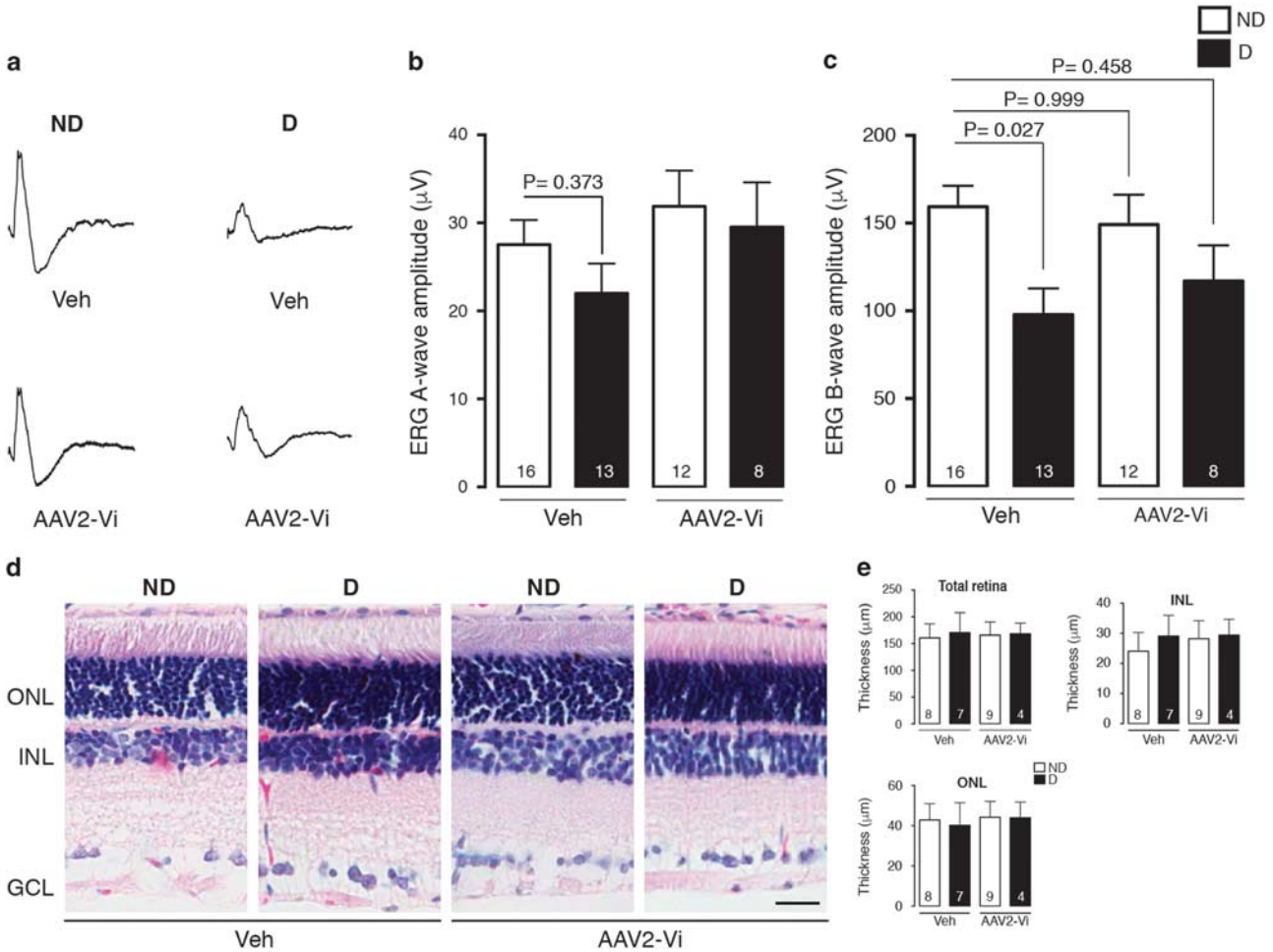

Figure 4 The AAV2 vasoinhibin vector reduces diabetes-induced retinal electrophysiological dysfunction. (**a**) Representative ERG responses under scotopic conditions of non-diabetic (ND) control rats and diabetic (D) rats injected intravitreally with vehicle (Veh) or the AAV2 vasoinhibin (Vi) vector 2 weeks after treatment with STZ and subjected to ERG evaluation 4 weeks after vector administration. Average amplitudes of A-wave (**b**) and B-wave (**c**). (**d**) Representative paraffin retinal cross-sections stained with hematoxilin and eosin subjected to morphogenic examination of the thickness of total retina and of both the inner nuclear layer (INL) and outer nuclear layer (ONL) (**e**) of retinas from ND and D rats injected intravitreally with the Veh or the AAV2 Vi 2 weeks after treatment with STZ and subjected to morphometric evaluation 4 weeks after vector administration. Values represent mean ± s.e.m. Numbers inside bars indicate the number of retinas evaluated. AAV2, adeno-associated virus type 2; ERG, electroretinogram; STZ, streptozotocin.

Diabetes Enhances the Efficacy, Transgene Expression, and Transduction of AAV2 Vectors in the Retina

The protection against BRBB was reduced or absent when either vector were injected prior to inducing diabetes (Figure 5). In this experiment, vectors were injected intravitreally 4 weeks before inducing diabetes, and BRBB was evaluated 4 weeks thereafter. The increase in BRBB due to diabetes was no longer significant in retinas transduced with the AAV2 vasoinhibin vector, suggesting that vasoinhibins may have a small protective effect. However, the AAV2 sFlt-1 vector did not inhibit diabetes-induced BRBB, and the level of tracer in the vasoinhibin and the sFlt-1-transduced retinas was similar to that observed in the diabetic, vehicle-injected control (Figure 5).

Differences in the experimental design between the before- and after-diabetes groups do not interfere with the proper evaluation of vector efficacy. The dissimilar times (6 and 4 weeks) following STZ injection result in BRBB of similar magnitudes (Figure 2a). Also, the shorter time post-AAV2 delivery (4 *vs* 8 weeks) in the after-diabetes group resulted in higher vector efficacy (Figure 2c) even though transgene expression increases over time (Figure 1b). These findings suggest that the diabetic state enhances the efficacy of AAV2 vasoinhibin and AAV2 sFlt-1 vectors to reduce blood–retinal barrier leakage.

To investigate whether increased AAV2 vector efficacy could be due to enhanced transgene expression in the retina of diabetic rats, we compared the expression levels of the vasoinhibin and sFlt-1 mRNAs encoded by the AAV2 vectors, 4 weeks after they had been injected intravitreally into non-diabetic and diabetic rats (Figure 6a). qPCR showed that the retinal expression of the vasoinhibin and sFlt-1 transgenes

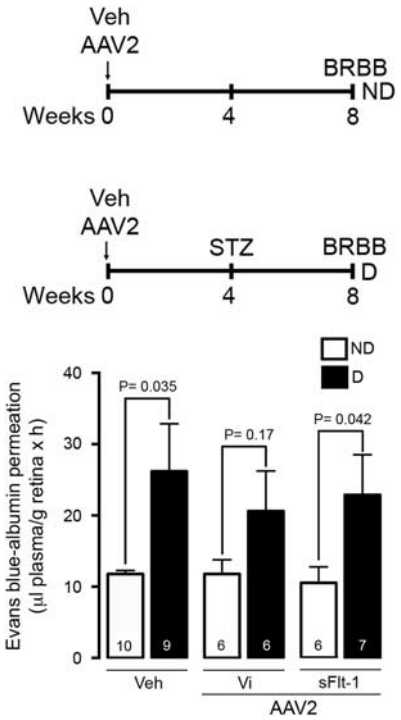

Figure 5 The AAV2 vasoinhibin and AAV2 sFlt-1 vectors fail to reduce diabetes-induced blood–retinal barrier pathology when injected prior to inducing diabetes. Pre-diabetes design diagram: vehicle (Veh), or AAV2 Vi, or AAV2 sFlt-1 vectors were injected intravitreally in non-diabetic rats (ND) or into rats (D) 4 weeks before treatment with STZ, and the retinal permeation of Evans blue-stained albumin was evaluated 8 weeks after vector administration. Values represent mean ± s.e.m. Numbers inside bars indicate the number of retinas evaluated. AAV2, adeno-associated virus type 2; STZ, streptozotocin.

was nearly fourfold greater in the retinas from diabetic rats than from the non-diabetic controls (Figure 6b). Transgene expression was further investigated by using an AAV2 EGFP reporter vector. The AAV2 EGFP vector was injected intravitreally into non-diabetic rats or into diabetic rats 2 weeks after treatment with STZ, and the levels of EGFP were evaluated by direct fluorescence on flat-mounted retinas 4 weeks after vector delivery. Scattered positive cells and cell fibers were visualized throughout the ganglion cell layer of retinas from non-diabetic rats (Figure 6c). In the diabetic rat retina there was a fivefold enhancement of EGFP fluorescence associated with both somas and projections, and many of the latter corresponded to fibers that make up the optic nerve (Figure 6c).

To investigate whether increased transgene expression involved an enhanced transduction of AAV2 vectors in the retina, we quantified the viral genome copy number by qPCR at 4 weeks after vectors had been injected intravitreally in non-diabetic and diabetic rats (Figure 6d). The AAV2 genome levels increased significantly in the retina of diabetic rats compared with the non-diabetic controls.

The Expression of Primary Receptors and Co-Receptors of AAV2 Is Elevated in the Retinas from Diabetic Rats

Transduction efficiency is influenced by receptor- and co-receptor-mediated AAV2 attachment.[18] To investigate whether a different abundance of AAV2 receptors and co-receptors between the normal and diabetic rat retina might account for the greater recruitment of viral particles in the diabetic state, we evaluated the mRNA levels of AAV2 primary receptors (glypican, syndecan, and perlecan)[20] and co-receptors (FGFR1,[21] αvβ5 integrin,[22] and HGFR[23]) by qPCR in retinas from non-diabetic and 4-week diabetic rats. The expression of all three primary receptors (Figure 7a) and all three co-receptors (Figure 7b) was significantly enhanced in the diabetic rat retina compared with non-diabetic controls. Consistent with these findings, FGFR1 immunoreactivity was faint and diffuse in the photoreceptors outer segments of the retina of non-diabetic rats, whereas it increased dramatically throughout the retina of diabetic rats (Figure 7c). Anti-FGFR1 staining was intense throughout the inner retina (inner nuclear layer, inner plexiform layer, and ganglion cell layer), and less intense and discrete in the outer retina (outer nuclear layer and outer segments) and choroid of diabetic rats. Omission of the primary antibody resulted in no labeling (not shown). Enhanced expression of AAV2 receptors and co-receptors does not reflect a general increase in protein synthesis, since total protein levels were similar in the retinas from diabetic and non-diabetic rats (Figure 7d).

DISCUSSION

Increased transport through the BRB occurs in DR and DME and is responsible for much of the vision loss due to diabetes.[1] By producing a sustained expression of antiangiogenic molecules, the AAV vectors eliminate the risks associated with repeated intraocular pharmacotherapy and offer considerable promise for the treatment of DR and DME. Here, we show that diabetes-induced BRB pathology is reversed by the intravitreal delivery of AAV2 vectors encoding the antiangiogenic and anti-vasopermeability factors sFlt-1 and vasoinhibin, and that the AAV2 vasoinhibin vector is a safe procedure for reducing retinal microvessel abnormalities and electrophysiological dysfunction due to diabetes. Moreover, we found that the diabetic state substantially enhances the retinal transduction, transgene expression, and efficacy of AAV2 vectors.

VEGF is a major promoter of BRBB in DR and DME. The levels of VEGF increase in the vitreous of patients with DR and DME[24,25] and the clinical use of anti-VEGF molecules improves DME.[26,27] One such anti-VEGF agent is sFlt-1, which corresponds to the secreted extracellular domain of VEGF receptor 1 and blocks VEGF action by sequestering VEGF.[28] Vasoinhibins comprise a family of peptides that are generated by the specific proteolytic cleavage of prolactin and they exert potent antiangiogenic and anti-vasopermeability effects.[29] Vasoinhibins are found in the retina,[7] and their systemic concentration is reduced in patients with DR.[30]

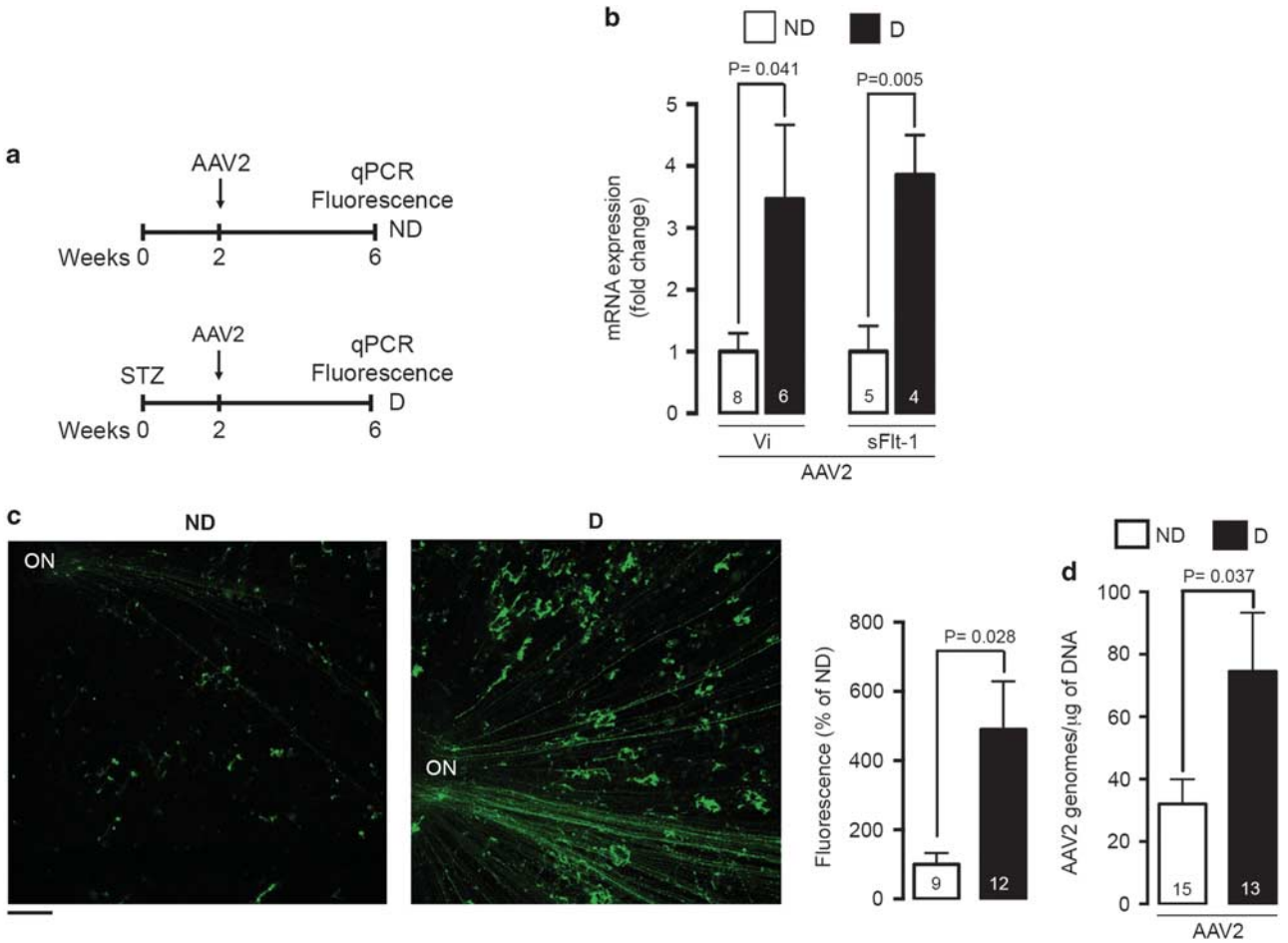

Figure 6 Diabetes enhances the retinal transgene expression and transduction of AAV2 vectors. (**a**) Post-diabetes design diagram: AAV2 vasoinhibin (Vi), AAV2 sFlt-1, or AAV2 EGFP vectors were injected intravitreally into non-diabetic (ND) or into diabetic (D) rats 2 weeks after treatment with STZ, and the expression of Vi and sFlt-1 mRNA and the levels of the EGFP were evaluated by qPCR and direct fluorescence on flat-mounted retinas, respectively. (**b**) qRT–PCR-based quantification of Vi and sFlt-1 mRNA levels in retinas from ND and D rats transduced with the AAV2 Vi and AAV2 sFlt-1 vectors. (**c**) Representative confocal microscope visualization of direct EGFP fluorescence in the ganglion cell layer of a flat-mounted retinal preparation from ND and D rats transduced with the AAV2 EGFP vector. Scale bar, 100 μm. (**d**) qPCR-based quantification of AAV genome copy number in retinas from ND and D rats transduced with AAV2 vectors. Values represent mean ± s.e.m. Numbers inside bars indicate the number of retinas evaluated. AAV2, adeno-associated virus type 2; ON, optic nerve; qRT–PCR, quantitative reverse transcription PCR; STZ, streptozotocin.

Vasoinhibins inhibit ischemia-induced retinal angiogenesis[31] and reduce diabetes-induced BRBB by targeting both the inner (vascular endothelial cells) and the outer (retinal pigment epithelium) components of the BRB.[32,33] The effects of vasoinhibins[3,32,33] and sFlt-1[34,35] against BRBB have been well-documented using Evans blue and a variety of other *in vivo* and *in vitro* techniques that have revealed signaling mechanisms mediating their action. For example, VEGF antagonists and vasoinhibins block calcium influx through transient receptor potential channels; they also inhibit the activation of phospholipase C gamma and phosphatidylinositol-3-kinase-Akt mechanisms, thereby leading to downstream blockage of eNOS activation and the reinforcement of junctional proteins linked to the actin cytoskeleton.[32,33,36–38]

AAV-mediated gene transfer of sFlt-1 successfully reduces BRBB when the vector is delivered before diabetes manifests in the spontaneously diabetic Torii rat.[34] AAV2 vectors encoding sFlt-1 or vasoinhibin also reduce BRBB in rats when injected before inducing diabetes with STZ.[3] While these findings demonstrate the preventive effect of these vectors against diabetes-mediated BRBB, the important question of whether BRBB can be reversed by AAV2 vectors had not been addressed. Here, we show that the AAV2 vasoinhibin and sFlt-1 vectors restored the BRB when injected after BRB damage is fully manifest. These findings demonstrate that both vectors reverse a retinal alteration that causes visual impairment in DR and DME.

Furthermore, the AAV2 vasoinhibin vector reduced other aspects of the retinal disease occurring in STZ-treated

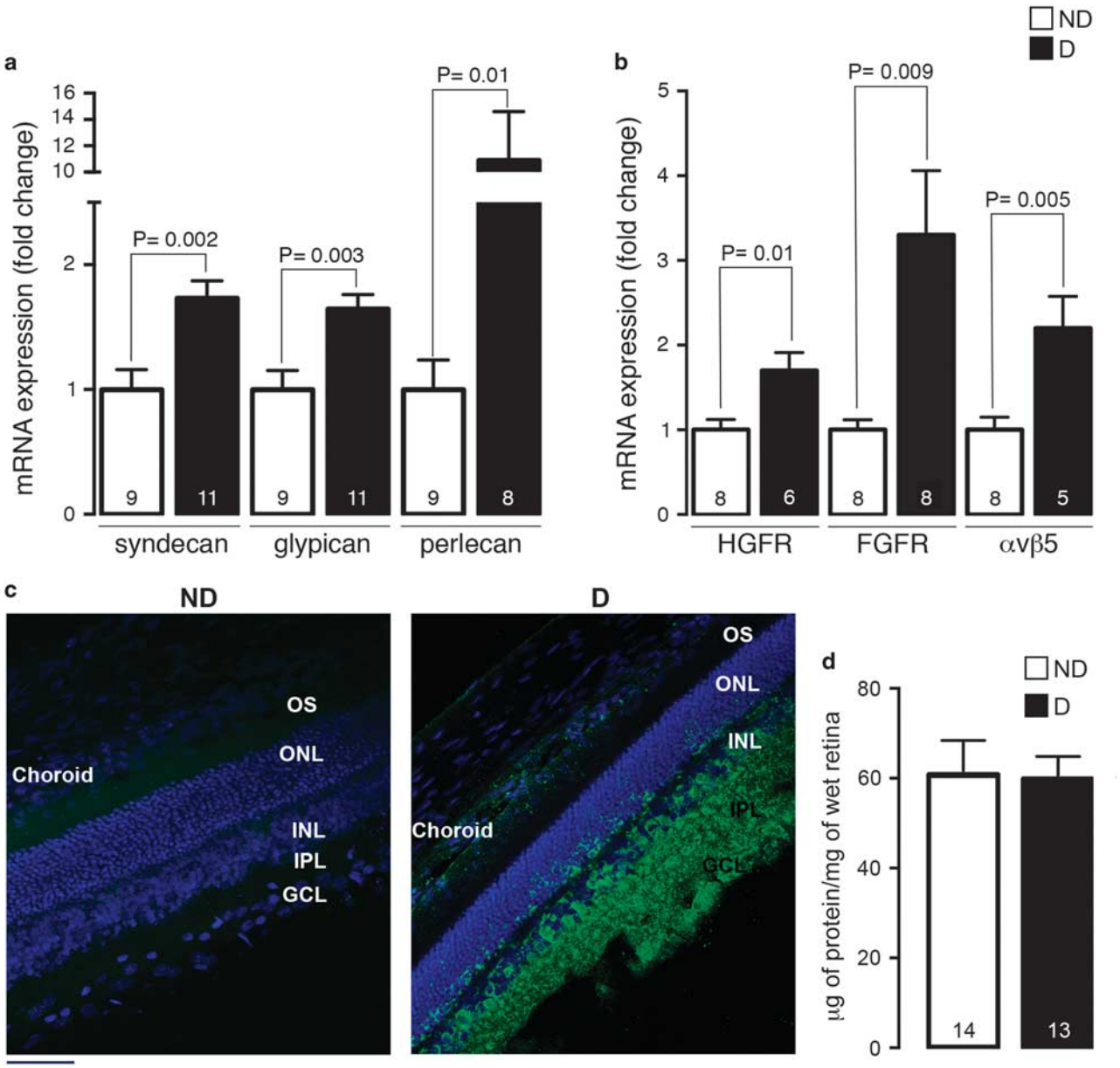

Figure 7 The expression of primary receptors and co-receptors of AAV2 is elevated in the retina from diabetic rats. qRT–PCR-based quantification of AAV2 receptors (glypican, syndecan, and perlecan) (**a**) and co-receptors (fibroblast growth factor receptor 1 (FGFR), αvβ5 integrin, and hepatocyte growth factor receptor (HGFR)) (**b**) in retinas from non-diabetic (ND) and 6-week diabetic (D) rats. (**c**) Immunolocalization and comparison of FGFR1 immunoreactivity between retinal sections of ND and six-week D rats. Scale bar, 50 μm. (**d**) Total protein levels in retinas from ND and six-week D rats. Values represent mean ± s.e.m. Numbers inside bars indicate the number of retinas evaluated. AAV2, adeno-associated virus type 2; GCL, ganglion cell layer; IPL, inner plexiform layer; ONL, outer nuclear layer; OS, outer segments; qRT–PCR, quantitative reverse transcription PCR.

rodents. It inhibited the reduction in fluorescein intensity within capillary vessels that may be caused by factors associated with perfusion abnormalities, such as decreased retinal blood flow,[15] subnormal retinal oxygenation,[39] and disruption of the BRB[15] (present results). Also, the amplitude of the B-wave, but not that of the A-wave of the ERG, commonly reduced in the STZ rodent model of DR,[16,40,41] was ameliorated by the AAV2 vasoinhibin vector. Supporting its safety, the vector did not modify the retinal vascular bed and the ERG in non-diabetic rats. Finally, we explored the thinning of the retina which, owing to the neurodegeneration of the inner retina, occurs in diabetic humans,[42–45] and in some,[46–49] but not all,[50] diabetic rodent studies. We confirmed that retinal thinning does not occur at 6 weeks post-STZ-treatment,[47,49] and showed that the AAV2 vasoinhibin vector did not modify it. These observations suggest that the expression of vasoinhibins by AAV2 vectors, as reported for sFlt-1,[51,52] is a safe procedure, causing no gross

retinal changes and protecting against retinal microvascular alterations and loss of retinal electrophysiological function in diabetes.

Reversal of BRB damage by the AAV2 vasoinhibin and sFlt-1 vectors occurred at a dose 10 times smaller than the one used in our previous study (2.8×10^9 vg *vs* 2.8×10^{10} vg).[3] However, using this smaller dose and the same experimental parameters of our previous report,[3] neither of the two vectors clearly prevented BRBB. The absence of effect may relate to the lower dose and/or to the smaller number of animals in our current study. Nonetheless, the vasoinhibin and the sFlt-1 vectors totally reversed the BRBB when delivered after inducing diabetes. Thus, it seemed likely that the efficacy of AAV2 vectors was being potentiated by the diabetic state.

Indeed, transgene expression is enhanced in the diabetic rat retina. The mRNA levels of the vasoinhibin and sFlt-1 transgenes were fourfold higher and the EGFP levels increased fivefold in the retinas from diabetic *vs* non-diabetic rats. Consistent with the reported tropism of intravitreally delivered AAV2 vectors,[53] the elevated AAV2 transgene expression occurred in the inner retina, particularly in ganglion cell somas and in their projections that make up the optic nerve. These findings suggest that the diabetic condition potentiates the action of AAV2 vectors by increasing their transduction in permissive cells. Supporting this possibility, we found that AAV2 genome levels were enhanced in the diabetic rat retina compared with the non-diabetic control. Transduction may be facilitated by a higher abundance of AAV2 receptors and co-receptors favoring cell entry.

Heparan sulfate proteoglycans (HSPG) are glycoproteins containing one or more HS chains, and structural determinants of HS interact with AAV2 capsid proteins.[54] HSPG associated with cell membranes (syndecans and glypicans) serve as primary receptors, enabling vector docking and the subsequent interactions with AAV2 co-receptors (FGFR1, αvβ5, and HGFR) required for endosomal entry. Also, HSPG associated with the extracellular matrix (perlecans) help store and concentrate AAV2, thus enabling their presentation to attachment and entry receptors.[55] We found that the mRNA levels of the core proteins in syndecan 4, glypican 1, and perlecan 1, and of all three co-receptors (FGFR1, αvβ5, and HGFR) increased in the diabetic rat retina. Furthermore, FGFR1 immunoreactivity, normally concentrated in photoreceptor cell bodies,[56] dramatically increased throughout the retina of diabetic rats, mainly in the inner retina, a localization pattern consistent with its reported presence in activated Müller cells.[57]

Increased levels of HSPG and of AAV2 co-receptors are not unexpected in DR and may contribute to its progression. High glucose levels upregulate cell-associated proteoglycans in retinal pericytes[58] and promote the secretion of HS chains by endothelial cells,[59] and VEGF increases the retinal expression of the HS side chains of HSPGs.[60] Perlecan binds FGFs,[61,62] and the intraretinal stores of immunoreactive bFGF and HSPG increase in patients with DR.[63] Of note, abnormal HSPG expression and structure can contribute to vascular leakage and to the release of pro-angiogenic factors in DR,[64] whereas bFGF, αvβ5 integrin, and HGF can signal to promote angiogenesis in DR.[65] However, contrary to what is expected from our findings using rats after 6 weeks of STZ, the mRNA levels of perlecan, the [^{35}S] sulfate incorporation into HSPG,[66] and the immunolocalization of HSPG[67] decrease in the retina of diabetic rats at 5 and 11 months after STZ treatment, respectively. These findings suggest that the synthesis of HSPG may change as diabetes progresses and emphasize the need to examine the long-term differential efficacy of AAV2 vectors.

Although the abundance of AAV2 receptors and co-receptors directly correlates with the efficacy of AAV2 vectors,[68–70] other major events can favor vector entry and transduction in diabetes. Diabetes alters the function and structure of all retinal cell types,[71] and loss of integrity and changes in retinal architecture are known to increase AAV vector transduction. Disruption of the inner limiting membrane caused by mild proteolytic digestion,[72] by structural changes of the Müller cell endfeet,[73] by laser pretreatment,[74] or by retinal degeneration[72] allow for enhanced AAV transduction of outer retinal cells after their intravitreal delivery. Moreover, nuclear uptake, capsid uncoating, and second-strand DNA synthesis following receptor binding are major rate-limiting steps in AAV transduction[75–78] that need to be investigated.

In conclusion, we have demonstrated the therapeutic potential of two AAV2 vectors encoding anti-vasopermeability and anti-angiogenic factors in DR and DME by delivering them after BRBB is well-established. While intravitreal delivery is a safe treatment, the transduction efficiency of AAV2 vectors can fall short of requirements for adequate retinal transgene expression,[68] and higher vector doses increase the risk of systemic dissemination and immune activation.[2] Our demonstration that vector efficacy and transduction after intravitreal delivery are enhanced by the diabetic state provides a way to conquer these problems and emphasizes the advantages of the AAV2 gene transfer approach to treat DR and DME. Non-invasive techniques such as fluorescein angiography, ocular coherence tomography, and magnetic resonance imaging are used increasingly to evaluate BRBB in a wide range of species including mice and rats.[79] These techniques will help stage AAV2 therapy and follow its efficacy, additional treatment benefits, and side effects over the time period relevant for translational research.

ACKNOWLEDGMENTS

We thank Fernando López-Barrera, Gabriel Nava, Nydia Hernández-Rios, Estela Albino Sánchez, Michael C Jeziorski, Daniel Mondragón, Antonio Prado, Martín García, and Alejandra Castilla for their technical assistance; and Dorothy D Pless for critically editing the manuscript. Nundehui Diaz-Lezama is a doctoral student from Programa de Doctorado en Ciencias Biomédicas, Universidad Nacional Autónoma de México (UNAM) and received fellowship 245224 from the National Council of Science and Technology of Mexico

(CONACYT). Research was supported by CONACYT grants SALUD-2011-1-161594 and 247164 to CC.

DISCLOSURE/CONFLICT OF INTEREST

The authors declare no conflict of interest.

1. Boyer DS, Hopkins JJ, Sorof J *et al.* Anti-vascular endothelial growth factor therapy for diabetic macular edema. Ther Adv Endocrinol Metab 2013;4:151–169.
2. Vandenberghe LH, Auricchio A. Novel adeno-associated viral vectors for retinal gene therapy. Gene Ther 2012;19:162–168.
3. Ramirez M, Wu Z, Moreno-Carranza B *et al.* Vasoinhibin gene transfer by adenoassociated virus type 2 protects against Vegf- and diabetes-induced retinal vasopermeability. Invest Ophthalmol Vis Sci 2011;52:8944–8950.
4. Shyong MP, Lee FL, Kuo PC *et al.* Reduction of experimental diabetic vascular leakage by delivery of angiostatin with a recombinant adeno-associated virus vector. Mol Vis 2007;13:133–141.
5. Verma A, Shan Z, Lei B *et al.* Ace2 and Ang-(1-7) confer protection against development of diabetic retinopathy. Mol Ther 2012;20:28–36.
6. Grimm D, Zhou S, Nakai H *et al.* Preclinical *in vivo* evaluation of pseudotyped adeno-associated virus vectors for liver gene therapy. Blood 2003;102:2412–2419.
7. Aranda J, Rivera JC, Jeziorski MC *et al.* Prolactins are natural inhibitors of angiogenesis in the retina. Invest Ophthalmol Vis Sci 2005;46:2947–2953.
8. Bradford MM. A rapid and sensitive method for the quantitation of microgram quantities of protein utilizing the principle of protein-dye binding. Anal Biochem 1976;72:248–254.
9. Xu Q, Qaum T, Adamis AP. Sensitive blood-retinal barrier breakdown quantitation using evans blue. Invest Ophthalmol Vis Sci 2001;42:789–794.
10. Zudaire E, Gambardella L, Kurcz C *et al.* A Computational tool for quantitative analysis of vascular networks. PLoS One 2011;6:e27385.
11. Shi X, Liao S, Mi H *et al.* Hesperidin prevents retinal and plasma abnormalities in streptozotocin-induced diabetic rats. Molecules 2012;17:12868–12881.
12. Zhang J, Wu Y, Jin Y *et al.* Intravitreal injection of erythropoietin protects both retinal vascular and neuronal cells in early diabetes. Invest Ophthalmol Vis Sci 2008;49:732–742.
13. Kusari J, Zhou SX, Padillo E *et al.* Inhibition of vitreoretinal vegf elevation and blood-retinal barrier breakdown in streptozotocin-induced diabetic rats by brimonidine. Invest Ophthalmol Vis Sci 2010;51:1044–1051.
14. Arnold E, Rivera JC, Thebault S *et al.* High levels of serum prolactin protect against diabetic retinopathy by increasing ocular vasoinhibins. Diabetes 2010;59:3192–3197.
15. Clermont A, Chilcote TJ, Kita T *et al.* Plasma kallikrein mediates retinal vascular dysfunction and induces retinal thickening in diabetic rats. Diabetes 2011;60:1590–1598.
16. Kern TS, Tang J, Berkowitz BA. Validation of structural and functional lesions of diabetic retinopathy in mice. Mol Vis 2010;16:2121–2131.
17. Paques M, Tadayoni R, Sercombe R *et al.* Structural and hemodynamic analysis of the mouse retinal microcirculation. Invest Ophthalmol Vis Sci 2003;44:4960–4967.
18. Schultz BR, Chamberlain JS. Recombinant adeno-associated virus transduction and integration. Mol Ther 2008;16:1189–1199.
19. Harbison CE, Chiorini JA, Parrish CR. The parvovirus capsid odyssey: from the cell surface to the nucleus. Trends Microbiol 2008;16:208–214.
20. Summerford C, Samulski RJ. Membrane-associated heparan sulfate proteoglycan is a receptor for adeno-associated virus type 2 virions. J Virol 1998;72:1438–1445.
21. Qing K, Mah C, Hansen J *et al.* Human fibroblast growth factor receptor 1 is a co-receptor for infection by adeno-associated virus 2. Nat Med 1999;5:71–77.
22. Summerford C, Bartlett JS, Samulski RJ. Alphavbeta5 integrin: a co-receptor for adeno-associated virus type 2 infection. Nat Med 1999;5:78–82.
23. Kashiwakura Y, Tamayose K, Iwabuchi K *et al.* Hepatocyte growth factor receptor is a coreceptor for adeno-associated virus type 2 infection. J Virol 2005;79:609–614.
24. Aiello LP, Avery RL, Arrigg PG *et al.* Vascular endothelial growth factor in ocular fluid of patients with diabetic retinopathy and other retinal disorders. N Engl J Med 1994;331:1480–1487.
25. Funatsu H, Yamashita H, Nakamura S *et al.* Vitreous levels of pigment epithelium-derived factor and vascular endothelial growth factor are related to diabetic macular edema. Ophthalmology 2006;113:294–301.
26. Stewart MW. Anti-Vegf therapy for diabetic macular edema. Curr Diab Rep 2014;14:510.
27. Stefanini FR, Badaro E, Falabella P *et al.* Anti-Vegf for the management of diabetic macular edema. J Immunol Res 2014;2014:632307.
28. Shibuya M. Vascular endothelial growth factor receptor-1 (Vegfr-1/Flt-1): a dual regulator for angiogenesis. Angiogenesis 2006;9:225–230.
29. Clapp C, Thebault S, Jeziorski MC *et al.* Peptide hormone regulation of angiogenesis. Physiol Rev 2009;89:1177–1215.
30. Triebel J, Huefner M, Ramadori G. Investigation of prolactin-related vasoinhibin in sera from patients with diabetic retinopathy. Eur J Endocrinol 2009;161:345–353.
31. Pan H, Nguyen NQ, Yoshida H *et al.* Molecular targeting of antiangiogenic factor 16k Hprl inhibits oxygen-induced retinopathy in mice. Invest Ophthalmol Vis Sci 2004;45:2413–2419.
32. Garcia C, Aranda J, Arnold E *et al.* Vasoinhibins prevent retinal vasopermeability associated with diabetic retinopathy in rats via protein phosphatase 2a-dependent Enos inactivation. J Clin Invest 2008;118:2291–2300.
33. Arredondo Zamarripa D, Diaz-Lezama N, Melendez Garcia R *et al.* Vasoinhibins regulate the inner and outer blood-retinal barrier and limit retinal oxidative stress. Front Cell Neurosci 2014;8:333.
34. Ideno J, Mizukami H, Kakehashi A *et al.* Prevention of diabetic retinopathy by intraocular soluble Flt-1 gene transfer in a spontaneously diabetic rat model. Int J Mol Med 2007;19:75–79.
35. Gehlbach P, Demetriades AM, Yamamoto S *et al.* Periocular gene transfer of sflt-1 suppresses ocular neovascularization and vascular endothelial growth factor-induced breakdown of the blood-retinal barrier. Hum Gene Ther 2003;14:129–141.
36. Bates DO. Vascular endothelial growth factors and vascular permeability. Cardiovasc Res 2010;87:262–271.
37. Gonzalez C, Corbacho AM, Eiserich JP *et al.* 16k-prolactin inhibits activation of endothelial nitric oxide synthase, intracellular calcium mobilization, and endothelium-dependent vasorelaxation. Endocrinology 2004;145:5714–5722.
38. Thebault S. Vasoinhibins prevent bradykinin-stimulated endothelial cell proliferation by inactivating Enos via reduction of both intracellular Ca2+ levels and enos phosphorylation at Ser1179. Pharmaceuticals 2011;4:1052–1069.
39. Luan H, Roberts R, Sniegowski M *et al.* Retinal thickness and subnormal retinal oxygenation response in experimental diabetic retinopathy. Invest Ophthalmol Vis Sci 2006;47:320–328.
40. Zhang Y, Zhang J, Wang Q *et al.* Intravitreal injection of exendin-4 analogue protects retinal cells in early diabetic rats. Invest Ophthalmol Vis Sci 2011;52:278–285.
41. Bhatt LK, Addepalli V. Attenuation of diabetic retinopathy by enhanced inhibition of Mmp-2 and Mmp-9 using aspirin and minocycline in streptozotocin-diabetic rats. Am J Transl Res 2010;2:181–189.
42. Biallosterski C, van Velthoven ME, Michels RP *et al.* Decreased optical coherence tomography-measured pericentral retinal thickness in patients with diabetes mellitus Type 1 with minimal diabetic retinopathy. Br J Ophthalmol 2007;91:1135–1138.
43. van Dijk HW, Kok PH, Garvin M *et al.* Selective loss of inner retinal layer thickness in type 1 diabetic patients with minimal diabetic retinopathy. Invest Ophthalmol Vis Sci 2009;50:3404–3409.
44. Oshitari T, Hanawa K, Adachi-Usami E. Changes of macular and Rnfl thicknesses measured by stratus Oct in patients with early stage diabetes. Eye (Lond) 2009;23:884–889.
45. van Dijk HW, Verbraak FD, Kok PH *et al.* Decreased retinal ganglion cell layer thickness in patients with type 1 diabetes. Invest Ophthalmol Vis Sci 2010;51:3660–3665.
46. Barber AJ, Lieth E, Khin SA *et al.* Neural apoptosis in the retina during experimental and human diabetes. early onset and effect of insulin. J Clin Invest 1998;102:783–791.
47. Park SH, Park JW, Park SJ *et al.* Apoptotic death of photoreceptors in the streptozotocin-induced diabetic rat retina. Diabetologia 2003;46:1260–1268.

48. Berkowitz BA, Roberts R, Stemmler A *et al.* Impaired apparent ion demand in experimental diabetic retinopathy: correction by lipoic acid. Invest Ophthalmol Vis Sci 2007;48:4753–4758.
49. Martin PM, Roon P, Van Ells TK *et al.* Death of retinal neurons in streptozotocin-induced diabetic mice. Invest Ophthalmol Vis Sci 2004;45:3330–3336.
50. Feit-Leichman RA, Kinouchi R, Takeda M *et al.* Vascular damage in a mouse model of diabetic retinopathy: relation to neuronal and glial changes. Invest Ophthalmol Vis Sci 2005;46:4281–4287.
51. Maclachlan TK, Lukason M, Collins M *et al.* Preclinical safety evaluation of Aav2-Sflt01- a gene therapy for age-related macular degeneration. Mol Ther 2011;19:326–334.
52. Lukason M, DuFresne E, Rubin H *et al.* Inhibition of choroidal neovascularization in a nonhuman primate model by intravitreal administration of an Aav2 vector expressing a novel Anti-Vegf molecule. Mol Ther 2011;19:260–265.
53. Auricchio A, Kobinger G, Anand V *et al.* Exchange of surface proteins impacts on viral vector cellular specificity and transduction characteristics: the retina as a model. Hum Mol Genet 2001;10: 3075–3081.
54. Kern A, Schmidt K, Leder C *et al.* Identification of a heparin-binding motif on adeno-associated virus type 2 capsids. J Virol 2003;77: 11072–11081.
55. Vives RR, Lortat-Jacob H, Fender P. Heparan sulphate proteoglycans and viral vectors: ally or foe? Curr Gene Ther 2006;6:35–44.
56. Ozaki S, Radeke MJ, Anderson DH. Rapid upregulation of fibroblast growth factor receptor 1 (Flg) by rat photoreceptor cells after injury. Invest Ophthalmol Vis Sci 2000;41:568–579.
57. Guillonneau X, Regnier-Ricard F, Laplace O *et al.* Fibroblast growth factor (Fgf) soluble receptor 1 acts as a natural inhibitor of Fgf2 neurotrophic activity during retinal degeneration. Mol Biol Cell 1998;9: 2785–2802.
58. Fisher EJ, McLennan SV, Yue DK *et al.* Cell-associated proteoglycans of retinal pericytes and endothelial cells: modulation by glucose and ascorbic acid. Microvasc Res 1994;48:179–189.
59. Han J, Zhang F, Xie J *et al.* Changes in cultured endothelial cell glycosaminoglycans under hyperglycemic conditions and the effect of insulin and heparin. Cardiovasc Diabetol 2009;8:46.
60. Witmer AN, van den Born J, Vrensen GF *et al.* Vascular localization of heparan sulfate proteoglycans in retinas of patients with diabetes mellitus and in vegf-induced retinopathy using domain-specific antibodies. Curr Eye Res 2001;22:190–197.
61. Joseph SJ, Ford MD, Barth C *et al.* A proteoglycan that activates fibroblast growth factors during early neuronal development is a perlecan variant. Development 1996;122:3443–3452.
62. Smith SM, West LA, Hassell JR. The core protein of growth plate perlecan binds Fgf-18 and alters its mitogenic effect on chondrocytes. Arch Biochem Biophys 2007;468:244–251.
63. Hanneken A, de Juan Jr. E , Lutty GA *et al.* Altered distribution of basic fibroblast growth factor in diabetic retinopathy. Arch Ophthalmol 1991;109:1005–1011.
64. Conde-Knape K. Heparan sulfate proteoglycans in experimental models of diabetes: a role for perlecan in diabetes complications. Diabetes Metab Res Rev 2001;17:412–421.
65. Friedlander M, Theesfeld CL, Sugita M *et al.* Involvement of integrins alpha V Beta 3 and alpha V beta 5 in ocular neovascular diseases. Proc Natl Acad Sci USA 1996;93:9764–9769.
66. Bollineni JS, Alluru I, Reddi AS. Heparan sulfate proteoglycan synthesis and its expression are decreased in the retina of diabetic rats. Curr Eye Res 1997;16:127–130.
67. Hammes HP, Weiss A, Hess S *et al.* Modification of vitronectin by advanced glycation alters functional properties in vitro and in the diabetic retina. Lab Invest 1996;75:325–338.
68. Coura Rdos S, Nardi NB. The state of the art of adeno-associated virus-based vectors in gene therapy. Virol J 2007;4:99.
69. Duan D, Li Q, Kao AW *et al.* Dynamin is required for recombinant adeno-associated virus type 2 infection. J Virol 1999;73:10371–10376.
70. Duan D, Yue Y, Yan Z *et al.* Endosomal processing limits gene transfer to polarized airway epithelia by adeno-associated virus. J Clin Invest 2000;105:1573–1587.
71. Antonetti DA, Barber AJ, Bronson SK *et al.* Diabetic retinopathy: seeing beyond glucose-induced microvascular disease. Diabetes 2006;55: 2401–2411.
72. Kolstad KD, Dalkara D, Guerin K *et al.* Changes in adeno-associated virus-mediated gene delivery in retinal degeneration. Hum Gene Ther 2010;21:571–578.
73. Vacca O, Darche M, Schaffer DV *et al.* AAV-mediated gene delivery in Dp71-null mouse model with compromised barriers. Glia 2014;62: 468–476.
74. Lee SH, Colosi P, Lee H *et al.* Laser photocoagulation enhances adeno-associated viral vector transduction of mouse retina. Hum Gene Ther Methods 2014;25:83–91.
75. Ding W, Zhang L, Yan Z *et al.* Intracellular trafficking of adeno-associated viral vectors. Gene Ther 2005;12:873–880.
76. Campbell EM, Hope TJ. Gene therapy progress and prospects: viral trafficking during infection. Gene Ther 2005;12:1353–1359.
77. Ferrari FK, Samulski T, Shenk T *et al.* Second-strand synthesis is a rate-limiting step for efficient transduction by recombinant adeno-associated virus vectors. J Virol 1996;70:3227–3234.
78. Thomas CE, Storm TA, Huang Z *et al.* Rapid uncoating of vector genomes is the key to efficient liver transduction with pseudotyped adeno-associated virus vectors. J Virol 2004;78:3110–3122.
79. Berkowitz B. MRI Studies of Blood-Retinal Barrier: New Potential for Translation of Animal Results to Human Application. In: Joussen AM, Gardner TW, Kirchhof B et al. (eds). *Retinal Vascular Disease*. Springer-Verlag: Berlin Heidelberg, 2007, pp 154–164.